Department of Chemical Engineering
Fuels and Energy Technology Institute

Changes in Char Structure and Reactivity during the Gasification of Low Rank Fuels

Tingting Li

This thesis is presented for the Degree of

Doctor of Philosophy

Of

Curtin University

May 2016

Declaration

To the best of my knowledge and belief this thesis contains no material previously published by any other person except where due acknowledgement has been made.

This thesis contains no material which has been accepted for the award of any other degree or diploma in any university.

Signature:……

Date: ……

Contents

Declaration ..... **II**
Contents ..... **III**
Abstract ..... **VII**
Acknowledgements ..... **IX**
List of Tables ..... **X**
List of Figures ..... **XI**

Chapter 1 Introduction **1**
1.1 Importance of coal in world energy demand 2
1.2 Importance of gasification technology for the utilisation of low-rank coals 3
1.3 Importance of the characterisation of char structure and its reactivity 4
1.4 Past efforts in understanding the char structure and its reactivity during the gasification of low-rank coals 5
1.5 Purpose of this study 8
1.6 Scope of this study 9
1.7 References 11

Chapter 2 Effects of gasification temperature on char structural evolution and AAEM retention during the gasification of Loy Yang brown coal **15**
2.1 Introduction 16
2.2 Experimental 17
2.2.1 Coal sample preparation 17
2.2.2 Gasification 17
2.2.3 Char characterisation 18
2.2.4 Quantification of AAEM species 19
2.2.5 Reactivity measurement 19
2.3 Results and discussion 20

2.3.1 Char yields 20
2.3.2 Changes in char structure during the gasification of Loy Yang coal 23
2.3.3 Retention of AAEM species in char during gasification at 900°C 31
2.3.4 Char-O_2 specific reactivity at low temperature 33
2.4 Conclusions 36
2.5 References 37

Chapter 3 Changes in char structure during low-temperature pyrolysis in N_2 and gasification in air of Loy Yang brown coal char 40
3.1 Introduction 41
3.2 Experimental 42
3.2.1 Char sample preparation and gasification experiments in a fluidised-bed/fixed-bed reactor 42
3.2.2 Pyrolysis and gasification of the chars in air in TGA 43
3.2.3 Characterisation of char structure 44
3.3 Results and discussion 44
3.3.1 Weight loss of the char during pysolysis 44
3.3.2 Changes in char structures during pyrolysis and gasification 45
3.3.3 Char-O_2 specific reactivity 52
3.4 Conclusions 54
3.5 References 55

Chapter 4 Effects of gasification atmosphere and temperature on char structural evolution during the gasification of Collie sub-bituminous coal 58
4.1 Introduction 59
4.2 Experimental 60
4.2.1 Coal sample preparation 60
4.2.2 Gasification 61
4.2.3 Char characterisation 61
4.3 Results and discussion 63
4.3.1 Char yields 63
4.3.2 Char structural changes 65

4.4 Conclusions 72
4.5 References 73

Chapter 5 Effects of char structure and AAEM retention in char during the gasification at 900°C on the changes in low-temperature char-O_2 reactivity for Collie sub-bituminous coal 76
5.1 Introduction 77
5.2 Experimental 78
5.2.1 Coal sample preparation and gasification experiments 78
5.2.2 Characterisation of char structure 79
5.2.3 Quantification of alkali and alkaline earth metallic (AAEM) species 79
5.2.4 Measurement of char-O_2 reactivity 80
5.3 Results and discussion 81
5.3.1 Changes in char structures 81
5.3.2 Retention of AAEM species in char during gasification 83
5.3.3 Char-O_2 reactivity at low temperature 85
5.4 Conclusions 92
5.5 References 93

Chapter 6 Insights into mechanisms of char-CO_2 and char-H_2O reactions by probing kinetic parameters 97
6.1 Introduction 98
6.2 Experimental 99
6.2.1 Coal sample preparation and gasification 99
6.2.2 Characterisation of char structure 100
6.2.3 Char conversion and char gasification reactivity 100
6.3 Results and discussion 102
6.3.1 Coal conversion 102
6.3.2 Isokinetic temperature 104
6.3.3 Changes in *Eapp* and *Aapp* during gasification 106
6.3.4 Effects of the char oxygenation on the changes in kinetic parameters 109

6.3.5 Effects of the relative ratio of small to large rings on the changes in kinetic parameters 111
6.4 Conclusions 114
6.5 References 115

Chapter 7 Conclusions and Recommendations for Future Work 119
7.1 Introduction 120
7.2 Conclusions 120
7.2.1 Effects of gasification temperature on char structural evolution and AAEM retention during the gasification of Loy Yang brown coal 120
7.2.2 Changes in char structure during low-temperature pyrolysis in N_2 and gasification in air of Loy Yang brown coal char 121
7.2.3 Effects of gasification atmosphere and temperature on char structural evolution during the gasification of Collie sub-bituminous coal 122
7.2.4 Effects of char structure and AAEM retention in char during the gasification at 900°C on the changes in low-temperature char-O_2 reactivity for Collie sub-bituminous coal 123
7.2.5 Insights into mechanisms of char-CO_2 and char-H_2O reactions by probing kinetic parameters 123
7.2.6. General concluding remarks 124
7.3 Future work 126

Appendix I Publications 127
Appendix II Permission of Reproduction from the Copyright Owner 129

Abstract

Gasification is one of the most promising technologies for the utilisation of low-rank fuels, due to their high gasification reactivities. The high efficiency of fuel utilisation and the excellent emission control by gasification-based technologies would greatly reduce the consumption rate of our limited fossil fuels and improve the environmental performance of energy processes. In comparison with the fast devolatilisation and the relatively quick reforming of volatiles, char gasification can be the rate-limiting step of the whole gasification process. Gaining high char reactivity is essential to improve the overall gasification efficiency.

Among many factors influencing the char reactivity, char structure and the properties of alkali and alkaline earth metallic (AAEM) species are among the most important factors for low-rank coals. Particularly, the char structure shows not only a direct effect to the char reactivity but also an indirect effect by influencing the catalytic activity. However, the quantitative analysis of char structure has not been extensively investigated due to the lack of suitable techniques. The recent advances in the FT-Raman spectroscopic methodology have provided a powerful technique to characterise the char structure semi-quantitatively.

The purpose of this study was to investigate the changes in char structure and its reactivity during the gasification of a Victorian brown coal and a Western Australian sub-bituminous coal under a wide range of experimental conditions. The gasification experiments were carried out in a novel fluidised-bed/fixed-bed reactor with the capability to provide fast heating rates and uniform temperature distribution. FT Raman spectroscopy was employed to characterise the char structure. The concentrations of AAEM species were determined by inductively coupled plasma – optical emission spectroscopy (ICP-OES). A thermogravimetric analyser (TGA) was used to measure the char reactivity in air at low temperature.

The results show that the reaction pathway does not change in a given gasification atmosphere within the temperature range investigated. While steam is a dominating factor for the evolution of char structure for the sub-bituminous coal, CO_2 plays an increasingly important role in char evolution and AAEM retention with increasing temperature for brown coal in the mixture of CO_2 and steam. The relative ratio of small to large aromatic ring systems in char greatly influences the char-O_2 reactivity for sub-bituminous coal. Furthermore, the condensation of aromatic ring systems in CO_2 tends to increase the apparent activation energy and pre-exponential factor that show kinetic compensation effects. For the gasification in steam that was accompanied with the formation of O-containing structures, these kinetic parameters, even though still showing kinetic compensation effects, tends to decrease during gasification.

Acknowledgements

I would like to express my sincere appreciation to my supervisor Prof. Chun-Zhu Li for his continuous guidance and support throughout my candidature. His strict attitude toward science would influence me all through my life. I would also like to thank all the postdoctoral researchers, postgraduate students, technical and administrative staffs at Fuels and Energy Technology Institute for various help I received.

My special thanks go to Prof. Penghua Qiu for the invaluable guidance and suggestions on my research work, Dr. Li Dong who taught me how to operate fluidised-bed reactor and Raman spectrometer. I would like to thank Dr Dimple Quyn and Dr. Lei Zhang for their help on assistance with the ash-digestion procedure and teaching me the operation of inorganic species detection.

I gratefully acknowledge the financial support of this study from the Australian Research Council (DP110105514), WA Department of Mines and Petroleum and the Commonwealth of Australia under the Australia-China Science and Research Fund. I would like to thank Dr Dimple Quyn for the preparation of Loy Yang brown coal samples. I would like to thank Muja power plant for providing Collie sub-bituminous raw coal.

Lastly, I would like to thank my parents, my parents-in-law, my husband and my dear son for their unconditional love and support.

List of Tables

Table 1-1 Summary of Raman peak/band assignment [27]. Copyright (2006), with permission from Elsevier. 7
Table 4-1 Properties of Collie coal in weight percentage (dry and ash free basis).... 60

List of Figures

Fig. 1-1 World primary energy demand by fuel. Bioenergy includes the traditional use of solid biomass and modern use of bioenergy (based on the data in Ref. 2)..... 3

Fig. 1-2 Simplified structure of the fluidised-bed/fixed-bed reactor used in this study [34]. Copyright (2002), with permission from Elsevier..... 10

Fig. 2-1 Char yields (dry basis) as a function of holding time for Loy Yang brown coal during gasification of in CO_2, 15% H_2O-Ar and 15% H_2O-CO_2 at (a) 800, (b) 850 and (c) 900°C. The char yields at 800°C were replotted from Ref. 4 and used for comparison purposes..... 22

Fig. 2-2 Total Raman area as a function of holding time for the char prepared from the gasification of Loy Yang brown coal at (a) 800, (b) 850 and (c) 900°C in CO_2, 15% H_2O-Ar and 15% H_2O-CO_2. The total Raman area data at 800°C were replotted from Ref. 4 and used for comparison purposes. 24

Fig. 2-3 Total Raman area as a function of holding time for the char prepared from the gasification of Loy Yang brown coal in (a) CO_2, (b) 15% H_2O-Ar and (c) 15% H_2O-CO_2 at 800, 850 and 900°C. The total Raman area data at 800°C were replotted from Ref. 4 and used for comparison purposes..... 25

Fig. 2-4 Ratio between small and large rings as a function of holding time during the gasification of Loy Yang brown coal in CO_2, 15% H_2O-Ar and 15% H_2O-CO_2 at (a) 800, (b) 850 and (c) 900°C. The ratio data at 800°C were replotted from Ref. 4 and used for comparison purposes..... 29

Fig. 2-5 Ratio between small and large ring as a function of holding time in (a) CO_2, (b) 15% H_2O-Ar and (c) 15% H_2O-CO_2 at 800, 850 and 900°C during the gasification of Loy Yang brown coal. The ratio data at 800°C were replotted from Ref. 4 and used for comparison purposes..... 30

Fig. 2-6 Concentrations of AAEM species in char as a function of char yield. The chars were produced from the gasification of Loy Yang brown coal in pure CO_2, 15% H_2O-Ar and 15% H_2O-CO_2 at 900°C. 32

Fig. 2-7 Specific char-O_2 reactivity measured in air in TGA at 420°C for the chars prepared from the gasification of Loy Yang brown coal in pure CO_2, 15% H_2O-Ar and 15% H_2O-CO_2 with different holding time (0, 3, 5 and 7 min as shown) at 900°C. 32

Fig. 3-1 Changes in the total Raman area during the pyrolysis and gasification in air in TGA at 420°C. The data for the gasified char were replotted from Ref. 26. 45

Fig. 3-2 Changes in (a) the band intensity ratio between small and large rings, (b) the percentage of small rings intensity in the total Raman area and (c) the percentage of large rings intensity in the total Raman area during the pyrolysis and gasification in air in TGA at 420°C. The data for the gasified char were plotted based on the results from Ref. 26. 49

Fig. 3-3 Changes in the fraction of S band intensity in the total Raman area during the pyrolysis and gasification in air in TGA at 420°C. The data for the gasified char were plotted based on the results from Ref. 26. 51

Fig. 3-4 Changes in the band intensity ratio of S band and D band during the pyrolysis and gasification in air in TGA at 420°C. The data for the gasified char were plotted based on the results from Ref. 26. 51

Fig. 3-5 Specific char-O_2 reactivity of the chars produced from the gasification of Loy Yang brown coal in 15% H_2O-CO_2 at 850°C [26]. The reactivity measurement was done at 420°C in air in TGA. 53

Fig. 4-1 A curve-fitted Raman spectrum of the char prepared from the gasification of Collie sub-bituminous coal in pure CO_2 at 800°C. 62

Fig. 4-2 Char yields (dry base) from the gasification of Collie sub-bituminous coal in pure CO_2, 15% H_2O balanced with Ar and 15% H_2O balanced with CO_2 as a function of holding time at (a) 800°C; (b) 850°C; (c) 900°C. The dashed lines show the predicted char yields based on those in 15% H_2O balanced with CO_2. 64

Fig. 4-3 Total Raman areas as a function of char yield for the chars produced in the gasification of Collie sub-bituminous coal in pure CO_2, 15% H_2O balanced with Ar and 15% H_2O balanced with CO_2 at (a) 800°C; (b) 850°C; (c) 900°C. 66

Fig. 4-4 Raman band ratios Gr+Vl+Vr/D as a function of char yield for the chars produced in the gasification of Collie sub-bituminous coal in pure CO_2, 15% H_2O balanced with Ar and 15% H_2O balanced with CO_2 at (a) 800°C; (b) 850°C; (c) 900°C. 70

Fig. 4-5 Raman band ratios Gr+Vl+Vr/D as a function of char yield for the chars produced in the gasification of Collie sub-bituminous coal at 800-900°C in (a) pure CO_2, (b) 15% H_2O balanced with Ar; (c) 15% H_2O balanced with CO_2. 71

Fig. 5-1 Total Raman area and Raman band ratio of (Gr+Vl+Vr)/D versus char yield for the chars obtained in pure CO_2, 15% H_2O-Ar and 15% H_2O-CO_2 during the gasification of Collie sub-bituminous coal at 900°C. (Replotted from the data in Ref. [11], with permission from Elsevier). 82

Fig. 5-2 Concentrations of AAEM species in char versus char yield for the chars obtained in pure CO_2, 15% H_2O balanced with Ar and 15% H_2O balanced with CO_2 at 900°C during the gasification of Collie sub-bituminous coal. 84

Fig. 5-3 Specific char-O_2 reactivity measured in air in TGA at 400°C/420°C for the chars prepared in pure CO_2, 15% H_2O balanced with Ar and 15% H_2O balanced with CO_2 during the gasification of Collie sub-bituminous coal at 900°C. 86

Fig. 5-4 Specific reactivity (measured in air in TGA at 420°C) of char versus the AAEM concentrations in char. The chars were produced in 15% H_2O balanced with Ar

during the gasification of Collie sub-bituminous coal at 900°C. The char conversion levels in TGA are labelled with numbers and dashed lines in the figure..... 88

Fig. 5-5 Specific reactivity (measured in air in TGA at 400/420°C) of char versus Na concentration in char. The chars were produced in pure CO_2, 15% H_2O balanced with Ar and 15% H_2O balanced with CO_2 during the gasification of Collie sub-bituminous coal at 900°C. The char conversion levels in TGA are labelled with numbers and dashed lines in the figure..... 90

Fig. 6-1 Coal conversion (daf) versus holding time in (a) CO_2, (b) 15% H_2O balanced with Ar and (c) 15% H_2O balanced with CO_2 at 800, 850 and 900°C during the gasification of Collie sub-bituminous coal in a fluidised-bed/fixed-bed reactor. (The experimental data are replotted based on the data in Ref. 11) 103

Fig. 6-2 Logarithm of char gasification reactivity as a function of reciprocal of absolute stemperature with different coal conversions (daf) for gasification in (a) pure CO_2, (b) 15% H_2O balanced with Ar and (c) 15% H_2O balanced with CO_2. 105

Fig. 6-3 The (a) activation energy and (b) logarithm of pre-exponential factor versus of coal conversion (daf) in pure CO_2, 15% H_2O-Ar and 15% H_2O-CO_2 during the gasification of Collie sub-bituminous coal. 107

Fig. 6-4 Logarithm of pre-exponential factor versus activation energy for the gasification of Collie sub-bituminous coal (a) in CO_2, 15% H_2O balanced with Ar and 15% H_2O balanced with CO_2 and (b) expansion of the plot for 15% H_2O-CO_2..... 108

Fig. 6-5 The (a) activation energy and (b) logarithm of pre-exponential factor versus total Raman area for the gasification of Collie sub-bituminous coal in CO_2, 15% H_2O balanced with Ar and 15% H_2O balanced with CO_2. (The total Raman area is plotted based on the data in Ref. [11]) 110

Fig. 6-6 The (a) activation energy and (b) logarithm of pre-exponential factor versus (Gr+Vl+Vr)/D for the gasification of Collie sub-bituminous coal in CO_2, 15% H_2O

balanced with Ar and 15% H_2O balanced with CO_2. (The ratio between small and large rings is plotted based on the data in Ref. [11]) 113

Chapter 1

Introduction

1.1 Importance of coal in world energy demand

With the rapid growth of world population and the improvements in productivity (such as GPD per person), the energy demand will grow comparatively [1]. In the latest World Energy Outlook 2015, it is predicted that the world population will increase from 7122 to 9036 million during the period of 2013 and 2040 with a compound average annual growth rate of 0.9% [2]. In the meantime, the global energy demand will significantly increase by 32% from 2013 to 2040 [2].

The world primary energy demand that consists of different fuels from 2000 to 2040 is illustrated in Fig. 1-1. It is clear to see that fossil fuels will remain the largest portions of energy sources in the next two decades [2]. As the most abundant fossil fuel, the proven global coal reserves (coal that is known to exist and with a possibility of economical exploitation with current technologies) will reach at around 970 billion tonnes, which would be sufficient to support current global production levels for about 120 years [2]. With the large amount of reserves and less energy security concerns (geographically dispersed), coal will still occupy 25% of the primary energy demand in 2040 despite the growth rate is expected to slow down over the prediction period.

Compared with high-rank coals, low-rank coals have not been widely exploited due to its high content of moisture, low heating value and weak coking property. At the end of 2014, the reserves of low-rank coals (brown coal and sub-bituminous coal) account approximately for 55% of the proven coal reserves [3]. Thus the utilisation of low-rank coals in an efficient and environmental-friendly way demands great efforts from coal scientists and technologists.

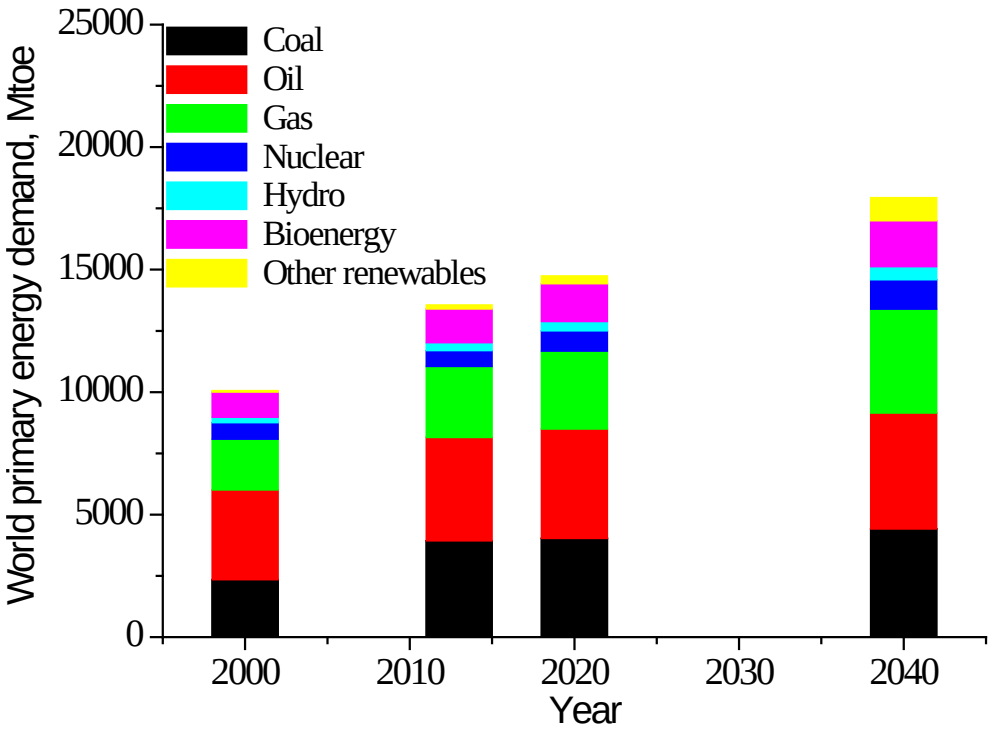

Fig. 1-1 World primary energy demand by fuel. Bioenergy includes the traditional use of solid biomass and modern use of bioenergy (based on the data in Ref. 2).

1.2 Importance of gasification technology for the utilisation of low-rank coals

Gasification converts a solid fuel into gaseous products, which can be a good resource of energy or be used for synthetising chemicals, liquid fuels or other gaseous fuels [4]. The high efficiency of fuel utilisation by gasification-based technologies would extensively reduce the consumption of our limited energy resource. Gasification has been used for a long time, but is still developing, to provide clean energy with the utilisation of a wide range of fuels [5]. In traditional energy technologies, such as pulverised fuel combustion, low-rank fuels (such as low-rank coals, biomass and solid wastes) are considered as low-grade fuels [5]. However, these low-rank fuels featuring high gasification reactivities are exclusively suitable for gasification-based technologies. Considering the large reserves and special features of low-rank coals, gasification-based technologies would make the utilisation of low-rank coals highly efficient in long term.

Apart from the high efficiency of low-rank fuel utilisation, gasification-based technologies have good environmental performance. With increasing concerns on the environmental pollution and the global climate change, more stringent policies have been set to reduce the emissions of the greenhouse gas (CO_2) and air pollutants (such as NO_x and SO_x). Thereby, seeking a clean way to utilise coal is imperative for continuous development. In the advanced gasification-based electricity generation technologies, such as advanced pressurised fluidised bed combustion (APFBC) and integrated gasification combined cycle (IGCC), most of the air pollutants can be significantly reduced [6-11]. Compared with the traditional pulverised coal fired technology, these advanced power generation technologies offer better emission controls. As one of the indispensible parts, coal gasification technology plays a key role in developing the advanced technologies for clean power utilisation.

1.3 Importance of the characterisation of char structure and its reactivity

In order to achieve constant and never ending progress of low-rank coal utilisation, great efforts have been made by coal scientists and technologists on understanding the coal gasification mechanisms in the past decades, including analysis based on experimental data and kinetic simulation based on gas-solid reaction models [4,12-26]. Overall, as char gasification is the rate-limiting step in the whole gasification process, thereby gaining insights into the char gasification mechanism and achieving high char reactivity is crucial to enhance the whole gasification rate and efficiency. Among many factors influencing the char reactivity, char structure and the properties of AAEM species are the most important [12-13].

Gasification is a relatively slow process compared with combustion, especially for fluidised-bed gasification. As the holding time is extended under gasification, drastic changes in char structure may take place within a lower conversion level during gasification than during combustion. It is even more important for low-rank coals (brown coal and sub-bituminous coal), as they are more sensitive to thermal treatment than high-rank coals. Moreover, the char structure can directly determine the preferential consumption of carbon atoms [13-16,19,21,27,29-31]. Thus it is important

to trace the char structural evolution to gain better understanding of the char gasification mechanism.

The existence of alkali and alkaline earth metallic (AAEM) species in low-rank coals produces both problems and benefits to coal utilisation. The AAEM species can react with other minerals and sulphur to form sulphates and other salts such as NaCl, resulting in the surface slagging and fouling. AAEM species can also cause corrosion and erosion damages to gas turbine blades. On the bright side, the AAEM species can serve as superior catalysts to promote the reactions between char and other reactants [4,12,17-20,28,32]. A catalyst must interact with the char, so as to stimulate its catalytic activity. Thus the structural features of the char is essential to the char-catalyst interaction.

In general, investigation on the changes in char structure and its reactivity during gasification plays a significantly positive role on the progress of coal gasification-based technologies.

1.4 Past efforts in understanding the char structure and its reactivity during the gasification of low-rank coals

Due to the significance of char characterisation in understanding gasification mechanisms, many studies have been carried out to gain information about the chemical structure of chars, particularly the structure of their carbon skeleton. Different from ordered graphitic structures, the chars produced from gasification at low temperature are highly disordered. The special features of the gasified chars make FT-Raman spectroscopy as one of the most suitable tools for char characterisation.

Li and co-workers have established a new methodology for char structural characterisation using FT-Raman spectroscopy [27]. It has shown to be applicable to a wide range of fuels. Briefly, the Raman spectra of the chars obtained from pyrolysis/gasification are deconvoluted using 10 Gaussian bands. The peak/band assignment is shown in Table. 1-1 [27]. The overlap between G and D bands, which is

thought to contain more structural information for highly disordered carbonaceous materials, is divided into 3 bands, Gr, Vl and Vr. In this study, the characterisation of char structures is mainly based on four bands (Gr, Vl, Vr, D and S). The intensities of Gr, Vl and Vr are combined to represent the aromatic ring systems with <6 rings that exist in amorphous carbon materials. The intensity of D band stands for large aromatic ring systems with no less than 6 rings. S band at 1185 cm^{-1} represents cross-linking structures, such as $C_{aromatic}$-C_{alkyl}.

The chars produced from the pyrolysis of Loy Yang brown coal in a fluidised-bed/fixed-bed reactor were firstly used for the demonstration of the new methodology by Li and co-workers [27]. Distinct difference has been shown in this work on the interpretation of Raman data of the char from that of highly ordered carbon materials (only G and D bands are considered). With increasing pyrolysis temperature, the total Raman area decreased, owing to the loss of O-containing species and the condensation of aromatic rings. The effects of ion-exchangeable Na and Ca on the char gasification were also discussed. Li and co-workers also studied on the changes in char structure during the gasification of brown coal in air in TGA (thermogravimetric analyser) at 400°C [35] and in steam in a fluidised-bed/fixed-bed reactor at 800 and 900°C [19]. The papers revealed that in the presence or absence of the catalysts, the preferential reaction sites on the char were different. The different char structure subsequently influenced its reactivity.

Table 1-1 Summary of Raman peak/band assignment [27]. Copyright (2006), with permission from Elsevier.

Band name	Band position, cm^{-1}	Description	Bond type
Gl	1700	Carbonyl group C=O	sp^2
G	1590	Graphite E^2_{2g}; aromatic ring quadrant breathing; alkene C=C	sp^2
Gr	1540	Aromatics with 3~5 rings; amorphous carbon structures	sp^2
Vl	1465	Methylene or methyl; semi-circle breathing of aromatic rings; amorphous carbon structures	sp^2, sp^3
Vr	1380	Methyl group; semi-circle breathing of aromatic rings; amorphous carbon structures	sp^2, sp^3
D	1300	D band on highly ordered carbonaceous materials; C-C between aromatic rings and aromatics with not less than 6 rings	sp^2
Sl	1230	Aryl-alkyl ether; para-aromatics	sp^2, sp^3
S	1185	$C_{aromatic}$-C_{alkyl}; aromatic (aliphatic) ethers; C-C on hydroaromatic rings; hexagonal diamond carbon sp^3; C-H on aromatic rings	sp^2, sp^3
Sr	1060	C-H on aromatic rings; benzene (ortho-di-substituted) ring	sp^2
R	960~800	C-C on alkanes and cyclic alkanes; C-H on aromatic rings	sp^2, sp^3

Tay and co-workers have studied the gasification mechanism of brown coal in a series of atmospheres, while some are oxidising and others are reducing atmospheres [14,36-38]. Tay took the Raman band ratio of $I_{(Gr+Vl+Vr)}/I_D$ as an indicator of reaction pathway for char gasification. According to Tay's finding, char-CO_2, char-H_2O and char-O_2 reactions follow different reaction pathways under the designed experimental conditions (using a fluidised-bed/fixed-bed reactor at 800°C). Meanwhile, it reveals that the Raman-sensitive O-containing functional groups are responsible for enhancing the char gasification reaction rate.

In general, with the employment of Raman spectroscopy, extensive studies have been carried out to gain additional information of highly disordered char structure. The structural evolution and its reactivity of the char produced from pyrolysis/gasification have been better understood.

1.5 Purpose of this study

Based on the above findings, it is believed that the acquisition of char structural evolution with the application of FT-Raman spectroscopy provides important information in understanding the gasification mechanisms. This study focuses on gaining insights into the mechanisms of low-rank coal gasification through tracing the changes in char structure and the retention of AAEM species during gasification and their effects on the subsequent char-O_2 reactivity at low temperature.

As steam is the most commonly used gasifying agent and coal/char-O_2 reaction is a major source of heat supply for a gasifier, char-H_2O and char-O_2 reactions will be investigated in this work. CO_2 is also abundant in a gasifier both as a product of carbon-oxygen reaction and water-gas-shift reaction [39]. Thus char-CO_2 reaction will be discussed as well. As the activation energy is higher for gasification in CO_2 than in H_2O [4], the gasification rate for the char-CO_2 reaction would change more rapidly with temperature than char-H_2O reaction. What will be the difference in the char structure and the retention of AAEM species at different temperature in individual atmosphere and their mixture will be explored in this study.

Same as one type of low-rank coals, a sub-bituminous coal would be different from a brown coal from the aspects of its organic structure (higher rank) and its inorganic species. Thus apart from a Victorian brown coal, a Western Australian sub-bituminous coal will be used in this work. Whether the effects of gasification temperature and atmosphere on the evolution of the char structure and the retention of AAEM species will be the same between these two low-rank coals will be studied.

1.6 Scope of this study

A fluidised-bed/fixed-bed reactor (shown in Fig. 1-2) will be employed in this fundamental research. It can provide heating rates as high as 10^3-10^5°C/s [34]. This study investigates the structural evolution and its reactivity of the char during the gasification of a Victorian brown coal and a Western Australian sub-bituminous coal. CO_2, H_2O, O_2 and the mixture of CO_2 and H_2O are used as gasifying agents. The kinetic parameters and the volatilisation of AAEM species are examined as well to provide further insights into the gasification mechanisms.

This thesis is composed of 7 chapters. Chapter 1 provides an overview of the importance of coal in the energy supply and its utilisation. Chapter 2-6 will present the experimental results and the interpretation of the results.

Chapters 2-3 will present the behaviour of Loy Yang brown coal during gasification over a wider range of temperature. Chapter 2 will show the effects of gasification temperature on the changes in char structure and the AAEM retention in char left after gasification. Chapter 3 will display the structural evolution of Loy Yang brown coal char during low-temperature pyrolysis and gasification in air.

Chapters 4-6 will focus on the gasification mechanisms of Collie sub-bituminous coal. Firstly, Chapter 4 will start with the effects of gasification atmosphere and temperature on the changes in char structure during the gasification of Collie sub-bituminous coal. Chapter 5 will explore the effects of char structure and AAEM retention in char during gasification at high temperature on the changes in char-O_2 reactivity at low

temperature for Collie sub-bituminous coal. Chapter 6 will present the kinetic parameters for the gasification of Collie sub-bituminous coal to provide additional information on investigating the gasification mechanisms.

Chapter 7 will summarise the thesis and give recommendations for future work.

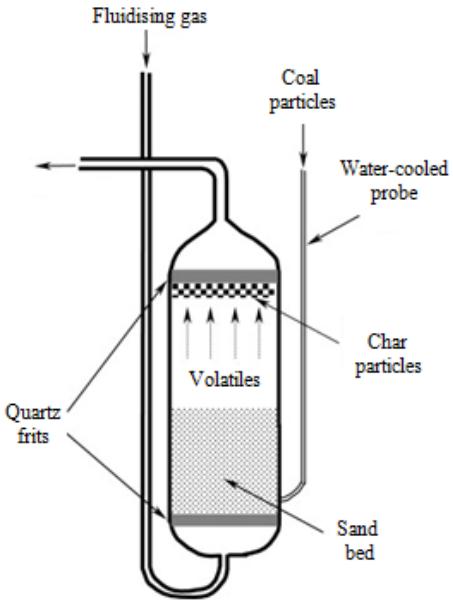

Fig. 1-2 Simplified structure of the fluidised-bed/fixed-bed reactor used in this study [34]. Copyright (2002), with permission from Elsevier.

1.7 References

[1] BP Global. BP Energy Outlook 2016. BP 2016.

[2] IEA. World Energy Outlook 2015, International Energy Agency 2015.

[3] BP Global. BP statistical review of world energy 2015. BP 2015.

[4] Tomita A, Ohtsuka Y. Chapter 5 Gasification and combustion of brown coal. In: Li C-Z, editor. Advances in the Science of Victorian Brown Coal: Elsevier; 2004, p. 223-85.

[5] Li C-Z. Special issue-gasification: a route to clean energy. Process Safety and Environmental Protection 2006;84:407-8.

[6] Miller BG. Clean coal technologies for advanced power generation. Clean Coal Energy Technology. Oxford: Butterworth Heinemann; 2011. P. 251-300 [Chapter 7].

[7] Kakaras E, Koumanakos AK, Doukelis A. Pressurized fluidized bed combustion (PFBC) combined cycle systems. In: Rao A, editor. Combined Cycle Systems for Near-Zero Emission Power Generation. Cambridge: Woodhead Publishing; 2012. P. 220-33 [Chapter 7].

[8] Promes EJO, Woudstra T, Schoenmakers L, Oldenbroek V, Thattai AT, Aravind PV. Thermodynamic evaluation and experimental validation of 253 MW Integrated Coal Gasification Combined Cycle power plant in Buggenum, Netherlands. Applied Energy 2015;155:282-94.

[9] Park SH, Chunga SW, Lee SK, Choi HK, Lee SH. Thermo-economic evaluation of 300 MW class integrated gasification combined cycle with ash free coal (AFC) process. Applied Thermal Engineering 2015;89:843-52.

[10] Asif M, Bak C, Saleem MW, Kim WS. Performance evaluation of integrated gasification combined cycle (IGCC) utilizing a blended solution of ammonia and 2-amino-2-methyl-1-propanol (AMP) for CO_2 capture. Fuel 2015;160:513-24.

[11] Esmaili E, Mostafavi E, Mahinpey N. Economic assessment of integrated coal gasification combined cycle with sorbent CO_2 capture. Applied Energy 2016;169:341-52.

[12] Li C-Z. Some recent advances in the understanding of the pyrolysis and gasification behaviour of Victorian brown coal. Fuel 2007;86:1664-83.

[13] Li C-Z. Importance of volatile-char interactions during the pyrolysis and gasification of low-rank fuels – A review. Fuel 2013;112:609-23.

[14] Tay HL, Kajitani S, Wang S, Li C-Z. A preliminary Raman spectroscopic perspective for the roles of catalysts during char gasification. Fuel 2014;121:165-72.

[15] Xu X, Wang Y, Chen Z, Chen X, Zhang H, Bai L, Zhang S. Variations in char structure and reactivity due to the pyrolysis and in-situ gasification using Shengli brown coal. Journal of Analytical and Applied Pyrolysis 2015;115:233-41.

[16] Zhang L, Kajitani S, Umemoto S, Wang S, Quyn DM, Song Y, Li T, Zhang S, Dong L, Li C-Z. Changes in nascent char structure during the gasification of low-rank coals in CO_2. Fuel 2015;158:711-8.

[17] Matsuoka K, Yamashita T, Kuramoto K, Suzuki Y, Takaya A, Tomita A. Transformation of alkali and alkaline earth metals in low rank coal during gasification. Fuel 2008;87:885-93.

[18] Rizkiana J, Guan G, Widayatno WB, Hao X, Li X, Huang W, Abudula A. Promoting effect of various biomass ashes on the steam gasification of low-rank coal. Applied Energy 2014;133:282-8.

[19] Li X, Li C-Z. Volatilisation and catalytic effects of alkali and alkaline earth metallic species during the pyrolysis and gasification of Victorian brown coal. Part VIII. Catalysis and changes in char structure during gasification in steam. Fuel 2006;85:1518-25.

[20] Quyn DM, Wu H, Hayashi Ji, Li C-Z. Volatilisation and catalytic effects of alkali and alkaline earth metallic species during the pyrolysis and gasification of Victorian brown coal. Part IV. Catalytic effects of NaCl and ion-exchangeable Na in coal on char reactivity. Fuel 2003;82:587-93.

[21] Wang S, Li T, Wu L, Zhang L, Dong L, Hu X, Li C-Z. Second-order Raman spectroscopy of char during gasification, Fuel Processing Technology 2015;135:105-11.

[22] Islam S, Kopyscinski J, Liew SC, Hill JM. Impact of K_2CO_3 catalyst loading on the CO_2-gasification of Genesse raw coal and low-ash product. Powder Technology 2016;290:141-7.

[23] Zhang F, Xu D, Wang Y, Argyle MD, Fan M. CO_2 gasification of Powder River Basin coal catalyzed by a cost-effective and environmentally friendly iron catalyst. Applied Energy 2015;145:295-305.

[24] Kim RG, Hwang CW, Jeon CH. Kinetics of coal char gasification with CO_2: Impact of internal/external diffusion at high temperature and elevated pressure. Applied Energy 2014;129:299-307.

[25] Kajitani S, Tay HL, Zhang S, Li C-Z. Mechanisms and kinetic modelling of steam gasification of brown coal in the presence of volatile-char interactions. Fuel 2013;103:7-13.

[26] Tanner J, Bhattacharya S. Kinetics of CO_2 and steam gasification of Victorian brown coal chars. Chemical Engineering Journal 2016;285:331-40.

[27] Li X, Hayashi Ji, Li C-Z. FT-Raman spectroscopic study of the evolution of char structure during the pyrolysis of a Victorian brown coal. Fuel 2006;85:1700-7.

[28] Li C-Z, Sathe C, Kershaw JR, Pang Y. Fates and roles of alkali and alkaline earth metals during the pyrolysis of a Victorian brown coal. Fuel 2000;79:427-38.

[29] Zhang L, Li T, Quyn DM, Dong L, Qiu P, Li C-Z. Structural transformation of nascent char during the fast pyrolysis of mallee wood and low-rank coals. Fuel Processing Technology 2015;138:390-6.

[30] Wang Y, Chen X, Yang S, He X, Chen Z, Zhang S. Effect of steam concentration on char reactivity and structure in the presence/absence of oxygen using Shengli brown coal. Fuel Processing Technology 2015;135:174-9.

[31] Zhang L, Li T, Quyn DM, Dong L, Qiu P, Li C-Z. Formation of nascent char structure during the fast pyrolysis of mallee wood and low-rank coals. Fuel 2015;150:486-92.

[32] Rizkiana J, Guan G, Widayatno WB, Hao X, Huang W, Tsutsumi A, Abudula A. Effect of biomass type on the performance of cogasification of low rank coal with biomass at relatively low temperatures. Fuel 2014;134:414-9.

[33] Frau C, Ferrara F, Orsini A, Pettinau A. Characterization of several kinds of coal and biomass for pyrolysis and gasification. Fuel 2015;152:138-45.

[34] Quyn DM, Wu H, Li C-Z. Volatilisation and catalytic effects of alkali and alkaline earth metallic species during the pyrolysis and gasification of Victorian brown coal. Part I. Volatilisation of Na and Cl from a set of NaCl-loaded samples.

Fuel 2002;81:143-9.

[35] Li X, Hayashi J-I, Li C-Z. Volatilisation and catalytic effects of alkali and alkaline earth metallic species during the pyrolysis and gasification of Victorian brown coal. Part VII. Raman spectroscopic study on the changes in char structure during the catalytic gasification in air. Fuel 2006;85:1509-17.

[36] Tay HL, Kajitani S, Zhang S, Li C-Z. Effects of gasifying agent on the evolution of char structure during the gasification of Victorian brown coal. Fuel 103 (2013) 22-28.

[37] Tay HL, Kajitani S, Zhang S, Li C-Z. Inhibiting and other effects of hydrogen during gasification: Further insights from FT-Raman spectroscopy. Fuel 2014;116:1-6.

[38] Tay HL, Li C-Z. Changes in char reactivity and structure during the gasification of a Victorian brown coal: Comparison between gasification in O_2 and CO_2. Fuel Processing Technology 2010;91:800-4.

[39] Walker PL, Rusinko FJ, Austin LG. Gas Reactions of Carbon. Advances in Catalysis and Related Subjects. 1959;11:133-221.

Chapter 2

Effects of gasification temperature on char structural evolution and AAEM retention during the gasification of Loy Yang brown coal

2.1 Introduction

Gasification is one of the most effective ways to utilise low-rank fuels, such as Loy Yang brown coal, owing to its high gasification reactivity [1-2]. One essential reason for the high gasification reactivity is the existence of highly dispersed alkali and alkaline earth metallic species (AAEM species) in Loy Yang brown coal, which act as good catalysts [3]. The AAEM species in Loy Yang brown coal have been shown to enhance the gasification rate by participating in the reaction between the char matrix and the radicals produced from the gasifying agent(s) [4]. The interaction between the char and the catalysts that can influence the activity of the catalysts was largely determined by the char structure [4]. Moreover, the char structure could directly determine the preferential consumption of carbon atoms in the char during gasification [5]. Thus the evolution of char structure is another significant factor that could affect the gasification reactivity.

Some researchers [4,6-9] have studied the evolution of char structure and the retention of AAEM species for Loy Yang brown coal during gasification in different gasifying agents. It has been concluded that the gasifying agents have strong impact on the char structure and the retention of catalytic species, subsequently leading to different reaction pathways of char gasification among different gasification atmospheres [4,7-9] and influencing the char-O_2 specific reactivity at low temperature [6-8].

Among many gasifying agents, steam is the most commonly used one in the gasifiers, producing the main products of CO and H_2 [10].CO_2 is also abundant in a gasifier as a product of carbon-oxygen reaction and water-gas-shift reaction, participating in the secondary reaction with carbon [11]. Generally, the reaction between char and a mixture of CO_2 and steam is inevitable in a gasifier. It is known that the activation energy is higher for char-CO_2 reaction than that for char-H_2O reaction [11-12], thus the gasification rate would change more rapidly for char-CO_2 reaction with varying gasification temperature. Whether an interaction between CO_2 and H_2O exists, and if so the effects of gasification temperature on the relative importance of CO_2 and H_2O

on char evolution and AAEM retention during the gasification of Loy Yang brown coal in the gas mixture are still unclear.

This study mainly focuses on the char structural evolution and AAEM retention during gasification at 800-900°C in different gasification atmospheres. With the employment of FT-Raman spectroscopy, the structural features were characterised for the chars collected at different gasification conversion levels. An inductively coupled plasma – optical emission spectroscopy (ICP-OES) was used to quantify the concentrations of AAEM species left after gasification. The char-O_2 specific reactivity was measured in a thermogravimetric analyser at low temperature. The results show that the competition exists between char-CO_2 and char-H_2O reactions, occurring on part of the active sites on the char. Different from a decisive role of H_2O at 800°C, CO_2 acts as an increasingly more decisive role in the char structural evolution and AAEM retention with temperature increasing to 900°C in the gas mixture.

2.2 Experimental

2.2.1 Coal sample preparation

A Loy Yang brown coal from Victoria was selected in this work. More details of the procedure for sample preparation can be found elsewhere [13]. After being dried at low temperatures (<35°C), the Loy Yang brown coal was ground and sieved to a required particle size range (between 106-150μm). The coal consisted of 70.4, 5.4, 0.62, 0.28 wt% (daf) of C, H, N and S individually, with an ash yield being of 1.1wt% (db) [13].

2.2.2 Gasification

A fluidised-bed/fixed-bed quartz reactor was used to conduct the gasification experiments for Loy Yang brown coal in pure CO_2, 15% H_2O (Ar acts as a balancing gas) and a mixture of 15% H_2O and CO_2 (serving as the balancing gas) between 800 and 900°C. More detailed information of the reactor has been stated in Ref. 14. The

data (at 800°C) for the chars prepared from the gasification of Loy Yang brown coal were replotted from Ref. 4 and used herein for comparison purposes only. In this fundamental study, a fluidised-bed/fixed-bed reactor has been chosen due to its ability to provide fast heating rates and uniform temperature distribution. The reactor consisted of a quartz tube with two quartz frits as well as inlets and outlets. The silica sand (with particle sizes of 300-350 μm) that placed on the lower frit was fluidised by the fluidising gas, acting as a fluidised bed during experiment. The reactor was heated up by an external electrical furnace. Two thermocouples were placed into the main reaction area of the reactor and the top of upper frit respectively to monitor the internal temperature distribution. After achieving the required temperature, about 1.5g coal was fed into the reactor with a feeding rate of 75 mg/min. In order to keep the coal samples at room temperature before arriving at the main reaction zone, the particles were fed through a water-cooled tube. After experiencing rapid pyrolysis and gasification, most of the char particles would be elutriated out of the sand bed and accumulate under the top frit in the reactor body, which then underwent in-situ gasification without exiting the reactor. For the gasification carried out in H_2O-containing atmospheres, deionised water was delivered into the reactor by a HPLC pump at 0.22 L/min. Once fed into the reactor, the water would turn into steam and be mixed and diluted by the carrier gas, accounting for 15% of the total carrier gas. At the end of feeding or a pre-set holding time in the gasification atmosphere was accomplished, the reactor was taken up from the furnace instantly to quench the reaction. The char collected from the experiment was sealed and stored in the fridge until required for further analysis. The oxidation of the samples has been minimised. Each of the char samples was well mixed before analysis, ensuring the reproducibility of the analysis results. The char yield was calculated by the weight difference of the fluidised-bed/fixed-bed reactor before and after every experiment at room temperature. TGA was used to measure the moisture in the coal/char, which will be considered in the char yield calculation.

2.2.3 Char characterisation

The structural features of the chars produced from gasification and further pyrolysis

were characterised with a Perkin-Elmer Spectrum GX FT-IR/Raman spectrometer [6]. The char sample was mixed with IR grade KBr to the same concentration of 0.25 wt% to facilitate the comparison of the total Raman area among different chars [6]. The KBr was used to dissipate the laser heat, preventing the char sample from being burned. The mixture of char sample and KBr was then finely ground to record the Raman spectrum of the char. A laser power of 150 mW was used in sample scanning. Afterwards, the Raman spectrum in the range of 800 and 1800 cm^{-1} was deconvoluted with 10 Gaussian bands following the procedures established in our previous work [6]. FT-Raman spectroscopy has been proved to be a powerful tool to study the highly disordered carbon materials [4,6-9,15-19]. The total Raman peak area and the aromatic ring systems are two primary variables that represent the extent of the oxygenation of char and the condensation of char, respectively.

2.2.4 Quantification of AAEM species

The AAEM species in char were quantified according to the procedure developed previously in our group [20]. Firstly, the char was ashed in air in a muffle furnace to remove the carbonaceous matter. After ashing, a mixture of concentrated HF and HNO_3 (1:1 in volume) acids was used to digest the ash. The ash was fully dissolved after 16 hours at 80°C and then the lid was removed to allow the acids to evaporate. This was carried out in a dedicated fume cupboard designed for work with HF acid. A dilute HNO_3 was used to wash the residue inside the beaker after evaporation and kept in a vial for further analysis. The AAEM species were quantified using a Perkin-Elmer Optima 7300 DV inductively coupled plasma – optical emission spectroscopy (ICP-OES).

2.2.5 Reactivity measurement

A Perkin-Elmer Pyris 1 TGA was selected to determine the char-O_2 reactivity by following the method set up previously [14]. Briefly, the char was initially heated to 105°C (at 20°C/min) in nitrogen (99.999%, ultra high purity). In order to completely dry the chars, it was kept for 20 min at 105°C followed by a temperature increase to

420°C. After holding for 2 min at 420°C, the gas was switched to air to initiate the measurement of char-O_2 reactivity. Eventually, after the weight loss remained unchanged, the temperature was further raised to 600°C to burn off all the carbonaceous material. The final weight was taken as the weight of ash. The char-O_2 reactivity was calculated by equation as follow:

$$\mathrm{R} = -\frac{1}{W}\frac{dW}{dt} \qquad (2-1)$$

where W is the char weight (the dry and ash free basis) at any given time t.

2.3 Results and discussion

2.3.1 Char yields

Figure 2-1 shows the char yield as a function of holding time during the gasification of Loy Yang brown coal in pure CO_2, 15% H_2O-Ar or the mixture of 15% H_2O and CO_2 (the data at 800°C were replotted from Ref. 4 and used herein for comparison purposes), apart from the three solid lines that represent the char yields obtained directly from the experiments, one dash line was marked in each figure. The dash line was drawn as a prediction of char yield in 15% H_2O-CO_2, assuming that there is no competition of active sites between H_2O and CO_2. It was calculated by the individual char conversion in 15% H_2O-Ar and 85% CO_2 alone. It is clear that the dash line was lower (which means the char yield dropped faster) than the actual char yield obtained from the gasification in 15% H_2O-CO_2 at each temperature, respectively. These data indicate that the competitions do exist between the reactions of char-H_2O and char-CO_2 within the temperature range of 800 to 900°C.

As shown in Figs. 2-1a and 1b, the gasification rate of char-H_2O reaction was apparently higher (the char yields dropped more rapid) than that of char-CO_2 reaction at 800 and 850°C. However, the gasification rates in these two atmospheres were getting closer (the char yields were almost overlapped and even lower for char-CO_2

gasification at 3 min holding) when the temperature increased to 900°C. This is because the activation energy is higher for the gasification of Loy Yang brown coal in CO_2 than that in H_2O [10,12], and therefore the gasification rate changes much quicker with temperature for the former reaction. This is in turn related to different evolution of char structure and/or transformation of AAEM species during the gasification in each atmosphere, which will be discussed in the following sections.

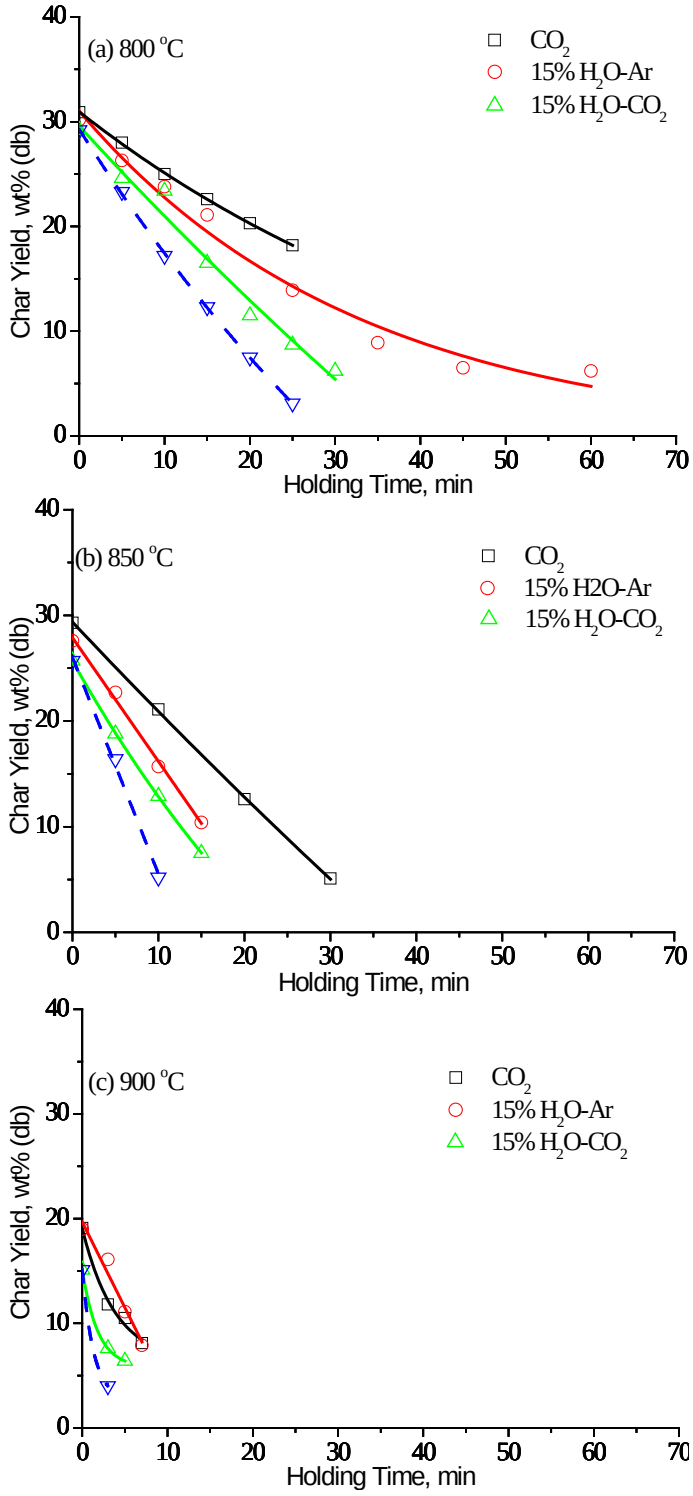

Fig. 2-1 Char yields (dry basis) as a function of holding time for Loy Yang brown coal during gasification of in CO_2, 15% H_2O-Ar and 15% H_2O-CO_2 at (a) 800, (b) 850 and (c) 900°C. The char yields at 800°C were replotted from Ref. 4 and used for comparison purposes.

2.3.2 Changes in char structure during the gasification of Loy Yang coal

2.3.2.1 Oxygenation of the char

The total Raman area is mainly affected by the extent of the graphitisation of the char structure and the amount of O-containing species formed in the char [6]. The enhanced graphitisation would enhance the light absorption of the char and subsequently reduce the total Raman area. While the formation of O-containing species would boost the Raman intensity, owing to the resonance effect between O and the connected aromatic rings.

Figure 2-2 displays the changes in the total Raman area of Loy Yang brown coal char as a function of char yield in three different atmospheres (CO_2, H_2O and the mixture of CO_2 and H_2O). As shown in Fig. 2-2a (data replotted from Ref. 4), the total Raman area of the chars obtained in 15% H_2O-Ar or 15% H_2O-CO_2 increased significantly from around 1500 to 3500 with increasing char conversion level (i.e. decreasing char yield). While only a slight increase from around 1100 to 1600 was observed in pure CO_2. In another word, more O-containing structures were formed in the presence of H_2O than in pure CO_2, thereby enhancing the Raman peak intensity [4,6]. At 850 and 900°C (Figs. 2-2b and 2-2c), the total Raman area were classified into two groups as well. A remarkable increase of total Raman area with decreasing char yield was observed in H_2O-containing atmospheres. While for the chars produced from pure CO_2, the total Raman area was almost constant as gasification proceeded. It is suspected that the formation and decomposition of O-containing species reached a dynamic balance in pure CO_2.

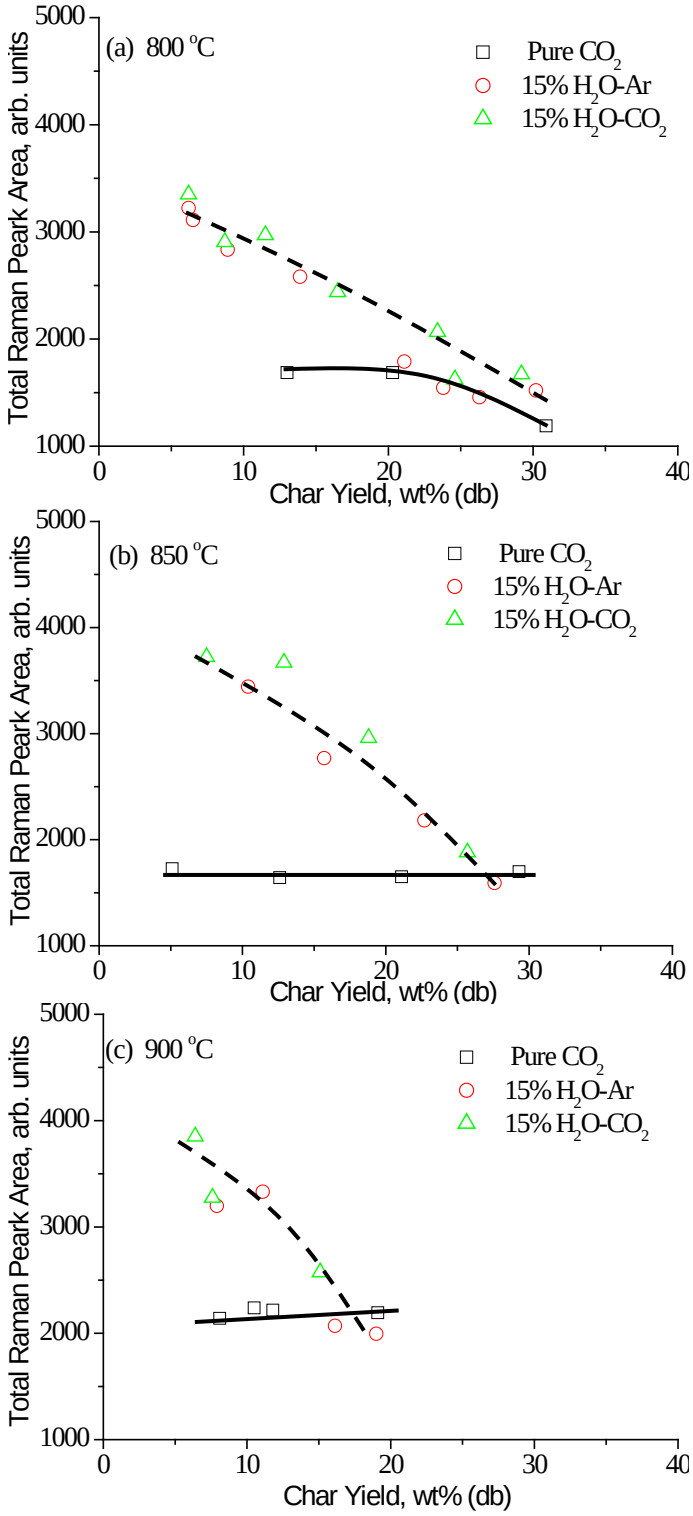

Fig. 2-2 Total Raman area as a function of holding time for the char prepared from the gasification of Loy Yang brown coal at (a) 800, (b) 850 and (c) 900°C in CO_2, 15% H_2O-Ar and 15% H_2O-CO_2. The total Raman area data at 800°C were replotted from Ref. 4 and used for comparison purposes.

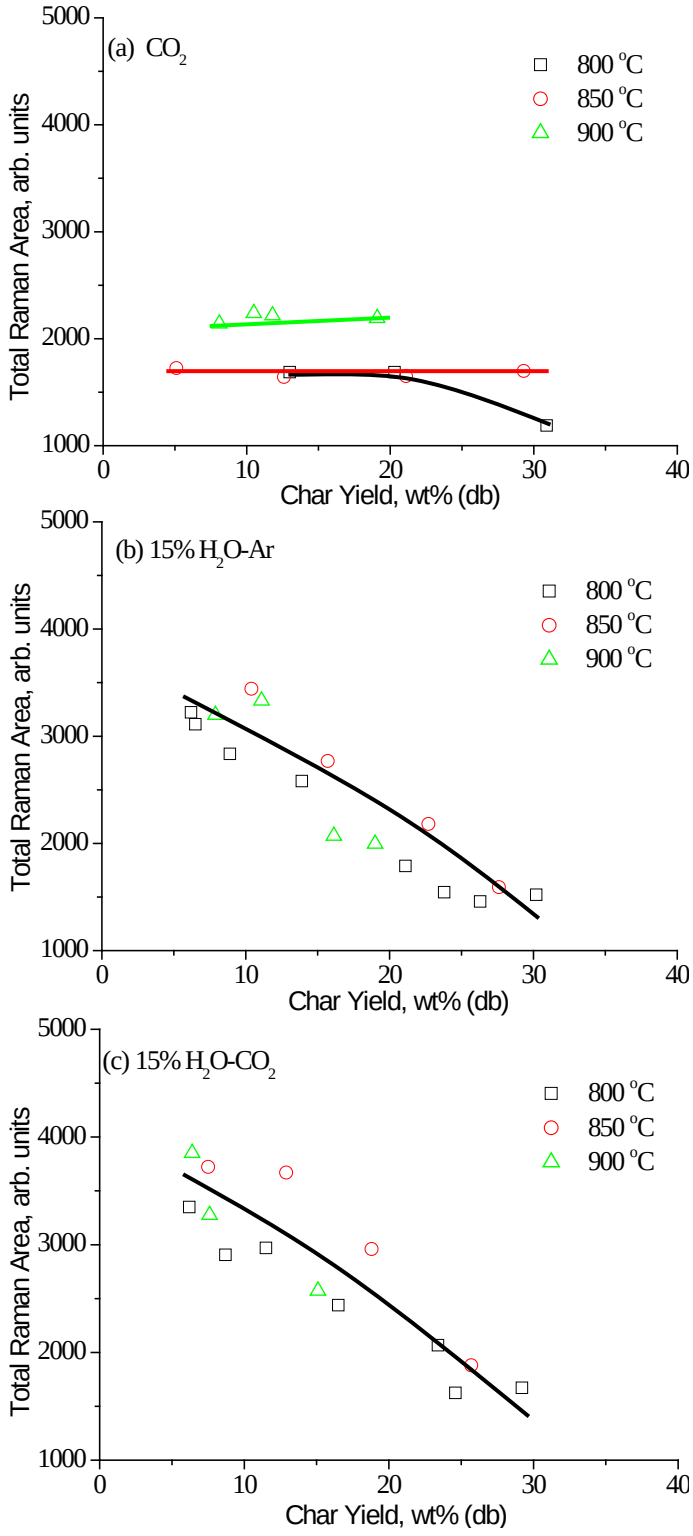

Fig. 2-3 Total Raman area as a function of holding time for the char prepared from the gasification of Loy Yang brown coal in (a) CO_2, (b) 15% H_2O-Ar and (c) 15% H_2O-CO_2 at 800, 850 and 900°C. The total Raman area data at 800°C were replotted from Ref. 4 and used for comparison purposes.

In order to gain better understanding of the effect of temperature on the oxygenation of the char structure, the total Raman area of the chars obtained at different temperature were replotted as a function of char yield for each gasification atmosphere, respectively. In Fig. 2-3a, the total Raman area of the chars prepared in pure CO_2 slightly increased from about 1100 (at 800°C) to around 1600 (at 850°C) and further increased to 2100 at 900°C. It is indicated that with temperature increasing from 800 to 900°C, more O-containing species were formed in pure CO_2. These data provide further evidence/agreement with our previous study [4] in that the increases in gasification rate with temperature in CO_2 are accompanied by (or due to) the increases in the total Raman area, the latter in turn reflect the oxygenation of the gasifying char. While for the chars prepared in H_2O-containing atmospheres, the total Raman area almost followed broadly the same increasing trend as a function of decreasing char yield (as shown in Figs. 2-3b and 2-3c). These data indicate that, while the char was continuously oxygenated (i.e. increasing total Raman area) in H_2O and the mixture of CO_2 and H_2O, the oxygenation does not appear to be the only factor determining the char gasification rate.

2.3.2.2 Changes in the aromatic ring systems in the char

10 Gaussian bands were used to curve fit the Raman spectrum (between 800 and 1800 cm^{-1}) [6]. The band assignment was developed by our group and more details can be found in Ref. 6. In this study, four major bands will be discussed to track the evolution of carbon skeletal structure of the char during gasification. As shown in Fig. 2-4, the band ratio $I_{(Gr+Vl+Vr)}/I_D$ was drawn as a function of char yield for Loy Yang brown coal during gasification in three atmospheres at 800, 850 and 900°C. The three bands of (Gr+Vl+Vr) together stand for aromatic rings with less than 6 rings (especially 3-5 rings), which typically found in amorphous carbon materials. The D band stands for the large aromatics with not less than six rings [6]. Thus, the band area ratio between (Gr+Vl+Vr) and D broadly reflects the relative amount of small and large rings in the char.

As displayed in Fig. 2-4, the band ratio $I_{(Gr+Vl+Vr)}/I_D$ decreased with decreasing char

yield as gasification proceeded in all three atmospheres at all temperatures investigated, implying that the relative amounts of smaller rings reduced with increasing holding time in the gasifying agents. With the same char yield (reaching the same conversion level), the relative ratio is higher for the chars prepared in pure CO_2 than that for the chars prepared in H_2O-containing atmospheres at each temperature. In the previous studies [4,8-9,21], it is known that the intermediates of char-H_2O reaction, such as H radicals, would penetrate into the char matrix and cause condensation of ring systems, resulting in the conversion of small to larger aromatic rings in the char (as reflected by the decreasing ratio). As Raman spectroscopy detects the bulk properties of the char structure, the different ratio of small to large aromatic rings at each conversion level indicated that the char-CO_2 and char-H_2O reactions take place in different reaction pathways at least for conditions investigated in this study.

As for the changes in the chars prepared in 15% H_2O-CO_2, the ratio between small and large aromatic rings was a little different at different gasification temperature. At 800°C, the ratio for the chars obtained from 15% H_2O-CO_2 was almost overlapped with that from 15% H_2O-Ar. Increasing the temperature to 850°C, the ratio for the chars obtained from 15% H_2O-CO_2 was close to, but slightly higher than, that from 15% H_2O-Ar. Furthermore, at 900°C, the ratio for the chars obtained from 15% H_2O-CO_2 was not close to that from either pure CO_2 or 15% H_2O-Ar. It is almost in between the ratios for the chars obtained in CO_2 and 15% H_2O-Ar individually. It is fair to say that H_2O plays a decisive role in the char structural evolution for Loy Yang brown coal during gasification in the gas mixture of 15% H_2O and CO_2 at 800°C [8]. With the temperature increasing from 800 to 900°C, CO_2 plays an increasingly more important role on the changes in char structure during gasification in the mixture.

In Fig. 2-5, the ratio of $I_{(Gr+Vl+Vr)}/I_D$ is replotted as functions of char yield and temperature for the chars prepared in different gasifying agents. Looking at the changes in the ratio of small to large aromatic rings in each gasification atmosphere, it is observed that the ratio dropped with decreasing char yield and followed the same trend for the chars obtained at different temperatures. In other word, at the same char conversion level, the structures of the chars obtained at different gasification

temperature were the same within one gasification atmosphere based on the probing into aromatic rings in the chars. The char-CO_2 or char-H_2O reaction pathways for the Loy Yang brown coal do not change from 800 to 900°C.

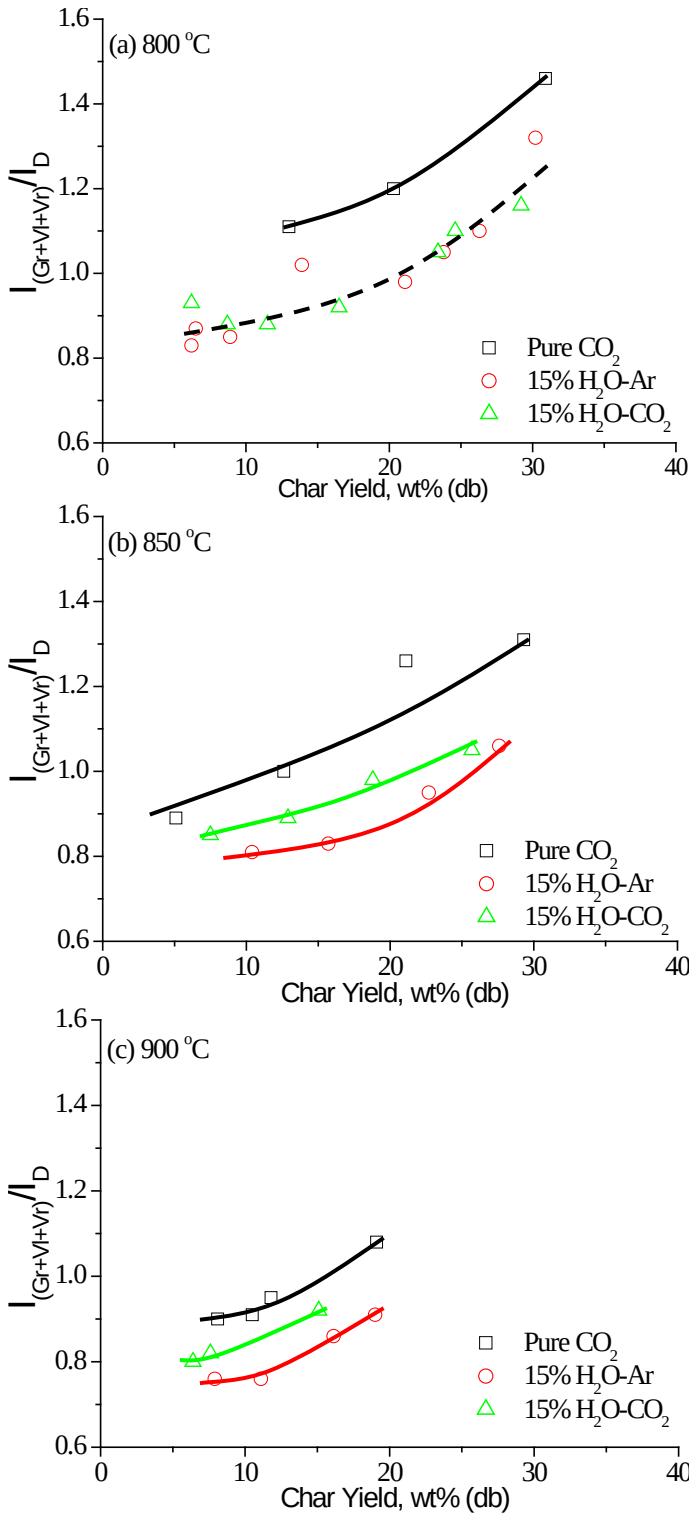

Fig. 2-4 Ratio between small and large rings as a function of holding time during the gasification of Loy Yang brown coal in CO_2, 15% H_2O-Ar and 15% H_2O-CO_2 at (a) 800, (b) 850 and (c) 900°C. The ratio data at 800°C were replotted from Ref. 4 and used for comparison purposes.

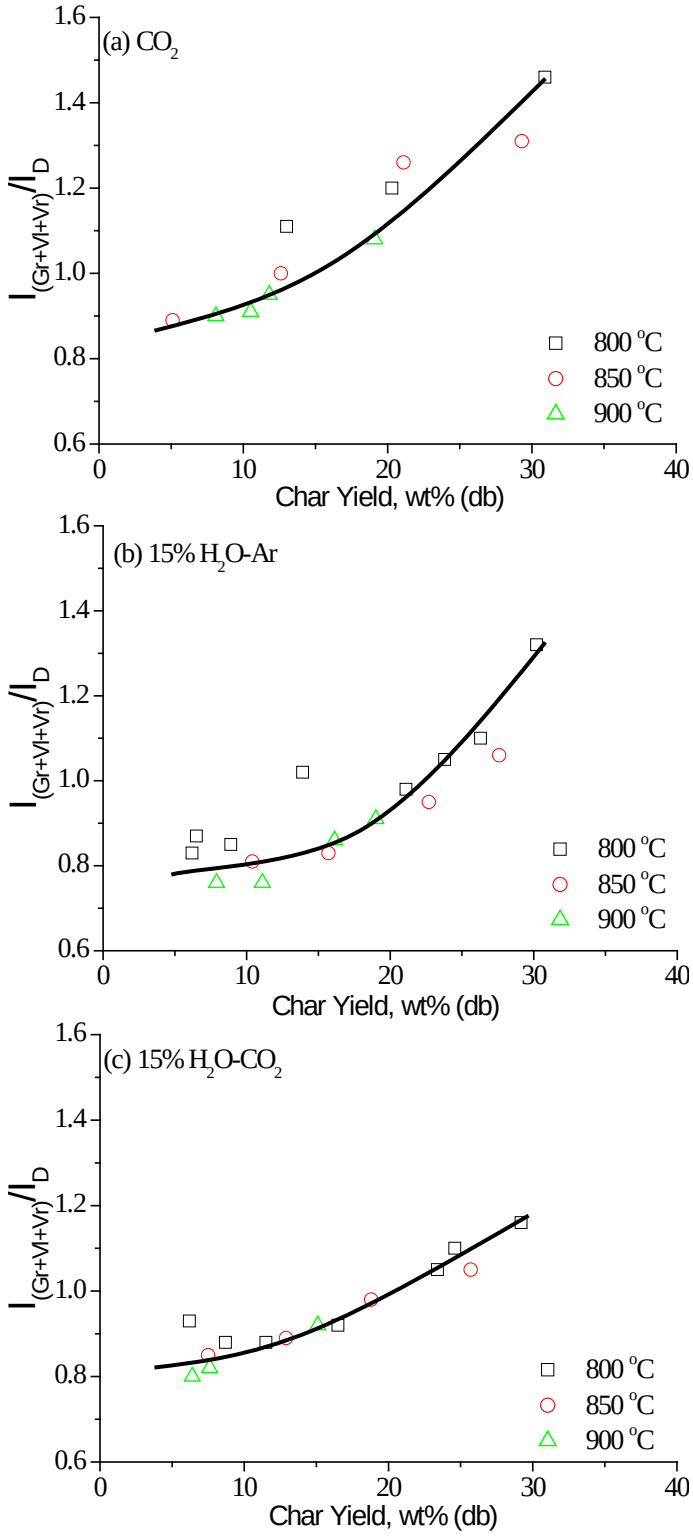

Fig. 2-5 Ratio between small and large ring as a function of holding time in (a) CO_2, (b) 15% H_2O-Ar and (c) 15% H_2O-CO_2 at 800, 850 and 900°C during the gasification of Loy Yang brown coal. The ratio data at 800°C were replotted from Ref. 4 and used for comparison purposes.

2.3.3 Retention of AAEM species in char during gasification at 900°C

Other than the char structure, the existence of AAEM species in the char matrix can influence the char reactivity as well [3]. Furthermore, these factors would affect each other. Thus the concentration of different AAEM species (Na, Mg and Ca) in the gasified chars produced at 900°C were quantified and plotted as a function of char yield in Fig. 2-6. For the chars obtained from the gasification of Loy Yang brown coal in three different atmospheres, the concentration of Na (Fig. 2-6a) almost followed the same trend. The concentration of Na increased with decreasing char yield as gasification proceeded, in agreement with previous measurement of the Na concentration for the 800°C char [4,8]. This is at least partly due to the relative enrichment of Na relative to other main elements (especially carbon) in char.

It is clear that the concentrations of Mg and Ca levelled off in pure CO_2, which means a remarkable volatilisation of Mg and Ca took place during gasification. For the gasification in 15% H_2O-Ar, the concentrations of Mg and Ca increased significantly with increasing holding time in gasifying agents. During the gasification in 15% H_2O-CO_2, they both increased slightly with decreasing char yield. It is known that Mg and Ca exist in the form of carbonates in O-containing atmospheres and the agglomeration could cause the loss of Mg and Ca [22]. In the presence of H_2O, the H radicals would prevent the formation of carbonate agglomeration. Thus the retention of Mg and Ca in char was higher in 15% H_2O-Ar and 15% H_2O-CO_2. Different from the same increasing trend of the Mg and Ca concentrations in H_2O-containing atmospheres at 800°C [4,8], the concentrations of Mg and Ca were slightly lower in 15% H_2O-CO_2 than those in 15% H_2O-Ar at 900°C. As mentioned earlier, CO_2 plays an increasingly crucial role in the char structural change from 800 to 900°C, which in turn affected the bonding of Ca and Mg to the char, thus their retention in the char.

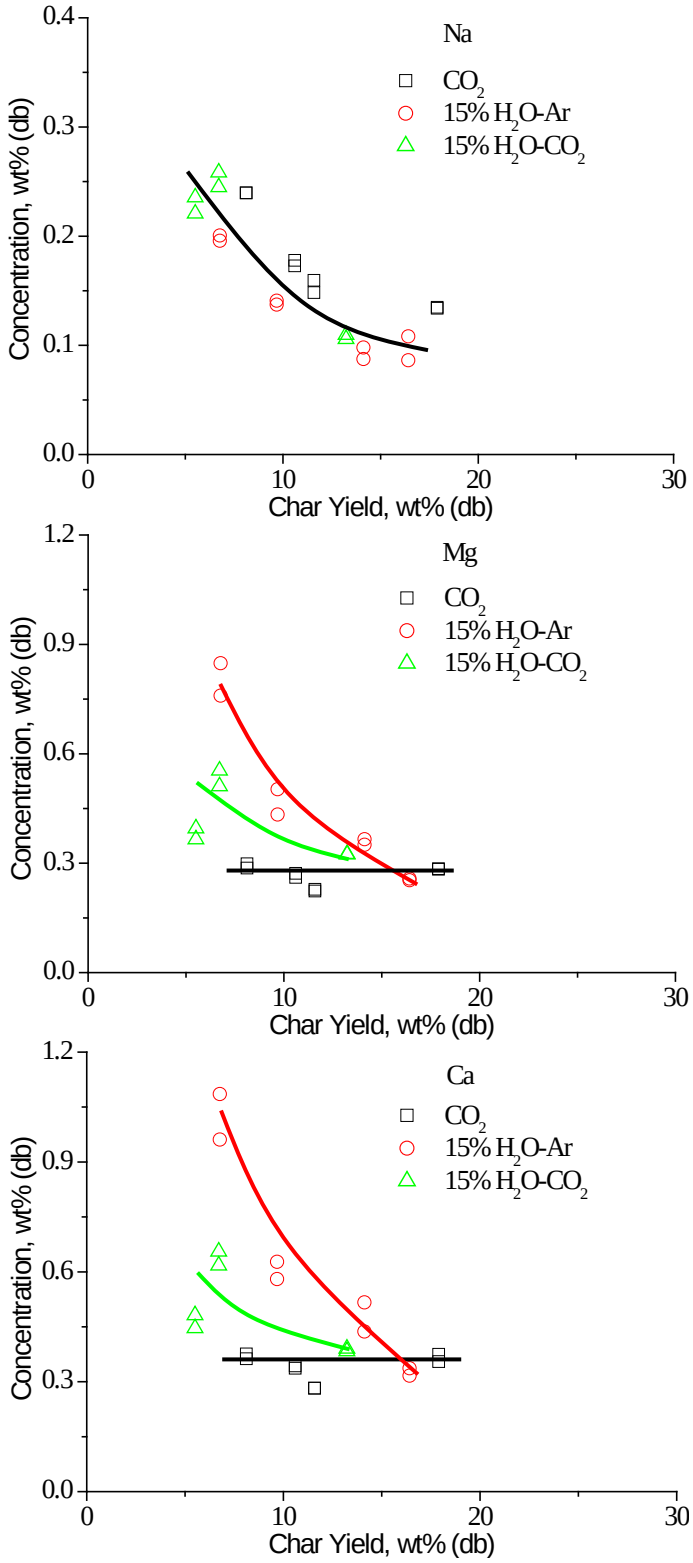

Fig. 2-6 Concentrations of AAEM species in char as a function of char yield. The chars were produced from the gasification of Loy Yang brown coal in pure CO_2, 15% H_2O-Ar and 15% H_2O-CO_2 at 900°C.

2.3.4 Char-O_2 specific reactivity at low temperature

Figure 2-7 illustrates the specific char-O_2 reactivity for the chars obtained from the gasification in three atmospheres with different holding time (0, 3, 5 and 7 min as shown) at 900°C. The measurement of char-O_2 reactivity was carried out in air in TGA at 420°C. It can be seen that the char-O_2 reactivities are broadly higher for the chars prepared in pure CO_2 (Fig. 2-7a) than those in 15% H_2O-Ar (Fig. 2-7b). The char-O_2 reactivity was affected by two main factors, including the char structure and AAEM retention. According to previous work on Loy Yang brown coal, it is known that the concentration of Na in char plays a more essential role than those of Mg and Ca species in affecting the char-O_2 reactivity at low temperature [14]. Thus only the concentration of Na was considered for the comparison in char-O_2 reactivity. As shown in Fig. 2-6, the concentration of Na (Fig. 2-6a) increased with decreasing char yield in the same trend for both chars produced in pure CO_2 and 15% H_2O-Ar. For the chars with similar char yield, the concentration of Na in char should be similar. However, the char-O_2 reactivities were not similar for the chars produced in pure CO_2 and in 15% H_2O-Ar respectively. Hence, it is concluded that the char structure should be the most responsible factor for the difference in char-O_2 reactivity. As mentioned earlier in Fig. 2-4c, the ratio of small and large aromatic rings was much higher for the chars produced in pure CO_2. In other word, the char structure was more condensed for the chars obtained in 15% H_2O-Ar at 900°C, thereby decreasing the subsequent char-O_2 reactivity at 420°C.

As for the chars prepared in the mixture of 15% H_2O and CO_2, the char-O_2 reactivity at low char conversions was much higher than those of the chars prepared in pure CO_2 or in 15% H_2O-Ar. It is clearly shown in Fig. 2-1c that the char yield decreased fastest in the gas mixture, which means the reaction took place most fiercely. More reactions took place simultaneously and the chars were more likely partially broken. In other words, the initial broad peak in char-O_2 specific reactivity (Fig. 2-7c, char conversion <70%) was due to some partially broken char structures formed during the gasification in 15% H_2O-CO_2 at 900°C. After their consumption, the subsequent increases in

char-O_2 reactivity (char conversion >70%) were due to the accumulation of AAEM species especially Na in char (shown in Fig. 2-6a).

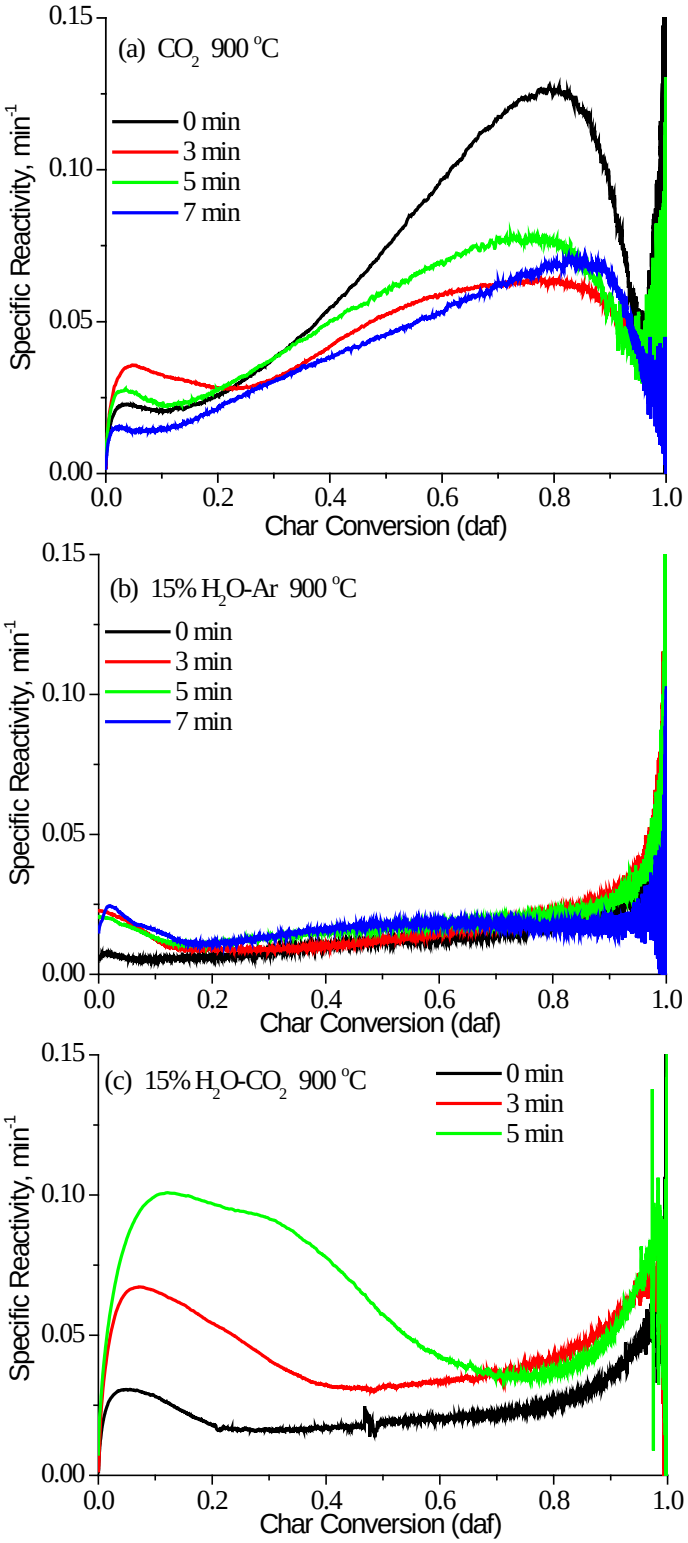

Fig. 2-7 Specific char-O_2 reactivity measured in air in TGA at 420°C for the chars prepared from the gasification of Loy Yang brown coal in pure CO_2, 15% H_2O-Ar and 15% H_2O-CO_2 with different holding time (0, 3, 5 and 7 min as shown) at 900°C.

2.4 Conclusions

The gasification of Loy Yang brown coal carried out from 800°C to 900°C in CO_2, H_2O and the gas mixture reveals that the competitions exist between the reactions of char-CO_2 and char-H_2O within temperature investigated. The increasing total Raman area caused by the formation of O-containing structures in char does not appear to be the only factor determining the char gasification rate in H_2O-containing atmospheres. Different from a decisive role of H_2O at 800°C, CO_2 plays an increasingly more crucial role in the char structural changes and the retention of Ca and Mg with temperature increasing to 900°C in 15% H_2O-CO_2.

2.5 References

[1] Li C-Z. Special issue-gasification: A route to clean energy. Process Safety and Environmental Protection2006;84:407-8.

[2] Hayashi J-i, Kudo S, Kim H-S, Norinaga K, Matsuoka K, Hosokai S. Low-temperature gasification of biomass and lignite: consideration of key thermochemical phenomena, rearrangement of reactions, and reactor configuration. Energy Fuels 2014;28:4-21.

[3] Li C-Z. Some recent advances in the understanding of the pyrolysis and gasification behaviour of Victorian brown coal. Fuel 2007;86:1664-83.

[4] Tay HL, Kajitani S, Wang S, Li C-Z. A preliminary Raman spectroscopic perspective for the roles of catalysts during char gasification. Fuel 2014;121:165-72.

[5] Takarada T, Tamai Y, Tomita A. Reactivities of 34 coals under steam gasification. Fuel 1985;64:1438-42.

[6] Li X, Hayashi J-i, Li C-Z. FT-Raman spectroscopic study of the evolution of char structure during the pyrolysis of a Victorian brown coal. Fuel 2006;85:1700-7.

[7] Tay HL, Li C-Z. Changes in char reactivity and structure during the gasification of a Victorian brown coal: Comparison between gasification in O_2 and CO_2. Fuel Processing Technology 2010;91:800-4.

[8] Tay HL, Kajitani S, Zhang S, Li C-Z. Effects of gasifying agent on the evolution of char structure during the gasification of Victorian brown coal. Fuel 2013;103:22-8.

[9] Tay HL, Kajitani S, Zhang S, Li C-Z. Inhibiting and other effects of hydrogen during gasification: Further insights from FT-Raman spectroscopy. Fuel 2014;116:1-6.

[10] Tomita A, Ohtsuka Y. Chapter 5 Gasification and combustion of brown coal. In: C.-Z. Li, editor. Advances in the Science of Victorian Brown Coal: Elsevier; 2004. p. 223-85.

[11] Walker PL, Rusinko FJ, Austin LG. Gas Reactions of Carbon. Advances in Catalysis and Related Subjects. 1959;11:133-221.

[12] Tanner J, Bhattacharya S. Kinetics of CO_2 and steam gasification of Victorian brown coal chars. Chemical Engineering Journal 2016;85:331-40.

[13] Quyn DM, Wu H, Li C-Z. Volatilisation and catalytic effects of alkali and alkaline earth metallic species during the pyrolysis and gasification of Victorian brown coal. Part I. Volatilisation of Na and Cl from a set of NaCl-loaded samples. Fuel 2002;81:143-9.

[14] Quyn DM, Wu H, Hayashi Ji, Li C-Z. Volatilisation and catalytic effects of alkali and alkaline earth metallic species during the pyrolysis and gasification of Victorian brown coal. Part IV. Catalytic effects of NaCl and ion-exchangeable Na in coal on char reactivity. Fuel 2003;82:587-93.

[15] Wang Y, Chen X, Yang S, He X, Chen Z, Zhang S. Effect of steam concentration on char reactivity and structure in the presence/absence of oxygen using Shengli brown coal. Fuel Processing Technology 2015;135:174-9.

[16] Sun J, Chen X, Wang F, Lin X, Wang Y. Effects of oxygen on the structure and reactivity of char during steam gasification of Shengli brown coal. Journal of Fuel Chemistry and Tchnology 2015;43:769-78.

[17] Zhang L, Kajitani S, Umemoto S, Wang S, Quyn DM, Song Y, Li T, Zhang S, Dong L, Li C-Z. Changes in nascent char structure during the gasification of low-rank coals in CO_2. Fuel 2015;158:711-8.

[18] Zhu X, Sheng C. Influences of carbon structure on the reactivities of lignite char reacting with CO_2 and NO. Fuel Processing Technology 2010;91:837-42.

[19] Zhang L, Li T, Quyn DM, Dong L, Qiu P, Li C-Z. Structural transformation of nascent char during the fast pyrolysis of mallee wood and low-rank coals. Fuel Processing Technology 2015;138:390-6.

[20] Li C-Z, Sathe C, Kershaw JR, Pang Y. Fates and roles of alkali and alkaline earth metals during the pyrolysis of a Victorian brown coal. Fuel 2000;79:427-38.

[21] Li X, Li C-Z. Volatilisation and catalytic effects of alkali and alkaline earth metallic species during the pyrolysis and gasification of Victorian brown coal. Part VIII. Catalysis and changes in char structure during gasification in steam. Fuel 2006;85:1518-25.

[22] Quyn DM, Hayashi Ji, Li C-Z. Volatilisation of alkali and alkaline earth metallic species during the gasification of a Victorian brown coal in CO_2. Fuel 2005;86:1241-51.

Every reasonable effort has been made to acknowledge the owners of copyright material. I would be pleased to hear from any copyright owner who has been omitted or incorrectly acknowledged.

Chapter 3

Changes in char structure during low-temperature pyrolysis in N_2 and gasification in air of Loy Yang brown coal char

3.1 Introduction

Owing to the high gasification kinetics of low-rank coals, gasification-based technologies can greatly improve the thermodynamics of their utilisation [1-2]. In a typical gasifier, a series of chemical reactions take place simultaneously. Among the basic chemical reactions that proceed in a gasifier, char-CO_2, char-H_2O and partial oxidation char-O_2 are the primary reactions to produce the syngas (CO and H_2) [3]. In the absence of the external thermal energy supply, the exothermic reaction of coal with oxygen is an essential source of thermal energy to satisfy the energy demand required for coal drying, heating up the reactants to the targeted reaction temperature and the breakage of chemical bonds [3].

Based on previous work, it is known that a significant factor influencing the achievement of high gasification rate is the high char reactivity [4]. The char reactivity for low-rank coals is primarily affected by the concentration of catalyst, the chemical form of catalyst, the distribution of catalyst and the char structure [5]. Among these factors, char structure is paramount as it could not only directly determine the preferential consumption of carbon atoms but also affect the char's holding capacity of the catalyst and the catalyst distribution in the char [4-7]. Due to the important role of char structure, investigation on the char structural evolution during gasification is indispensable for the study on char reactivity.

The mechanism of char-O_2 reaction has been extensively studied. In many past studies, pitch coke, graphite or other highly ordered carbons has been employed [8-10]. However, for the chars produced from the pyrolysis/gasification of low-rank fuels, the true graphitic structure does not exist [11-13]. Thus the findings based on the research on the highly ordered carbon materials are not suitable for the study on the char produced from low-rank fuels, which is mainly composed of highly disordered carbon materials. Moreover, the main focus on the char structure should be the reactive part of the char. FT-Raman spectroscopy has been approved to be suitable for this task [6-7,14-23]. In the past decade, Li and co-workers investigated on the char structural changes during the catalytic gasification of brown coal char in air with the

employment of FT-Raman spectroscopy [24]. The results show that, in the absence or presence of the catalysts, the gasification occurs on different preferred reaction sites of the char. Recently, Zhang and co-workers investigated the evolution of nascent char structure during the gasification of brown coal char and sub-bituminous coal char in air [25]. They find that the breakage of aromatic rings leads to the formation of dangling structures and smaller ring systems.

The structure of a char after partial gasification (gasified char) would differ from that of a pyrolysed char in the aromatic ring systems. There would be less small rings left in the gasified char than the pyrolysed char, as the smaller rings would be easily consumed during gasification. The reaction pathway in air for a gasified char that consists of relatively high amount of large rings would be the same as a pyrolysed char that is richer in small rings or not is still unclear, which arouses the incentive of this study as a continuation of our previous studies in this area. This study mainly focuses on the structural changes in the gasified char during the pyrolysis in N_2 and gasification in air at 420°C. The starting char samples were obtained from the gasification of Loy Yang brown coal in 15% H_2O-CO_2 at 850°C [26]. A low gasification temperature in air was selected so as to avoid ignition of char sample and to keep the reaction limited by chemical reactions. FT-Raman spectroscopy has been employed to characterise the char structural evolution during gasification. The results show that the original char structure determines the exact reaction pathway for the small/large rings during the pyrolysis in N_2 and gasification in air.

3.2 Experimental

3.2.1 Char sample preparation and gasification experiments in a fluidised-bed/fixed-bed reactor

The gasified chars used in this study were produced from the gasification of Victorian Loy Yang brown coal in 15% H_2O-CO_2 with 0, 10 or 15 min holding at 850°C in a fluidised-bed/fixed-bed reactor [26]. Briefly, around 1.5g coal (accurately weighed) with the particle size between 106 and 150 μm were delivered into the reactor by a

stream of feeding gas. At the end of feeding (which was also the starting point of holding time), the chars were gasified for different time to achieve different conversion levels. The deionised water was delivered by a HPLC pump at the desired rate. Once delivered into the reactor, which is heated up by an external furnace, the water would instantly turn into steam (accounts for 15% of total gas flow) and be mixed with CO_2 (99.999% purity, accounts for 85% of total gas flow). After achieving the pre-set holding time, the reactor was raised out of the furnace instantly and the char was gathered for analysis at a later date. In order to minimise the oxidation of the samples, the char was well sealed and stored in the fridge. The reproducibility of the analysis results was shown a good performance as each of the char samples was well mixed before analysis.

3.2.2 Pyrolysis and gasification of the chars in air in TGA

The char sample obtained from the gasification at 850°C was placed in a platinum crucible and heated up to 105°C in N_2 to remove the moisture content from the char in a Perkin-Elmer Pyris 1 thermogravimetric analyser (TGA).

Pyrolysis of the char. After holding for 20 min at 105°C, the temperature was further increased to 420°C (20 K/min). Once the peak temperature was reached, the TGA would stop heating and the char sample was cooled down by a stream of N_2 at 0.1 L/min. The TGA furnace would stay at the original position to ensure that the char would not contact with air until the temperature dropped to room temperature. The furnace was lowered down and the char sample was taken out and ground with KBr (serving as a heat-dissipating medium) for the analysis of char structural properties with FT-Raman spectroscopy.

Further gasification of the char in air. Following the pyrolysis of the char sample in N_2, the gas atmosphere was changed to air promptly to initiate gasification at 420°C. The char samples were held for different periods of time to obtain the chars with varying conversion levels. After the gasification in air reached the pre-set holding time, the char sample was mixed well with KBr for the analysis of char structure.

After holding for a certain time, the weight loss of the char in air would level off and the temperature was further went up to 600°C to burn out the carbonaceous material left in the char. The materials left in the crucible were ash and considered in the char specific reactivity calculation:

$$R = -\frac{1}{W}\frac{dW}{dt} \qquad (3-1)$$

w is the weight of char at any given time t on the dry and ash free basis.

3.2.3 Characterisation of char structure

The Raman spectrum of the char was obtained with a Perkin-Elmer Spectrum GX FT-IR/Raman spectrometer [13]. The method was stated in detail in Ref. 13. Briefly, 0.25 wt% for char in the finely ground char-KBr mixture was used to facilitate the comparison of total Raman area. 150 mW laser power was used to scan the mixture of char and KBr for 200 times to obtain the Raman spectrum. 10 Gaussian bands were used to curve-fit the spectrum between 800 and 1800 cm^{-1}, which was developed in our group [13]. The key focus is the bands of Gr, Vl, Vr, D and S, which could represent the key carbon skeletal structures of the chars investigated in this study.

3.3 Results and discussion

3.3.1 Weight loss of the char during pysolysis

Before the temperature reached 420°C to initiate the gasification in air, the char was firstly heated up in N_2, which is termed as pyrolysis. Around 3% weight loss occurred during the pyrolysis of the char from room temperature to 420°C in N_2 for all the selected char samples.

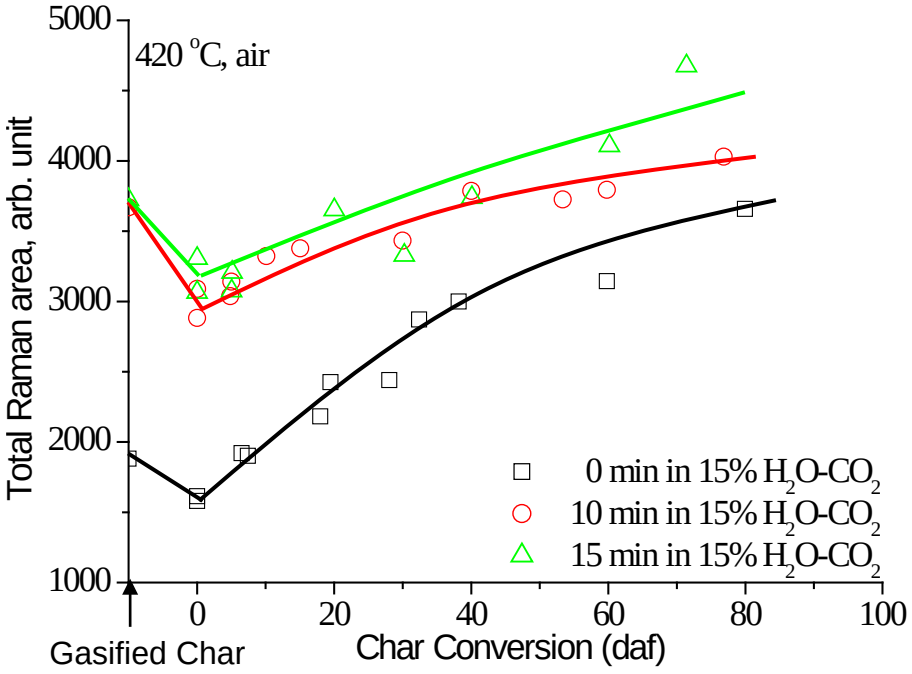

Fig. 3-1 Changes in the total Raman area during the pyrolysis and gasification in air in TGA at 420°C. The data for the gasified char were replotted from Ref. 26.

3.3.2 Changes in char structures during pyrolysis and gasification

3.3.2.1 Changes in the total Raman area

In Fig. 3-1, the data plotted at "Gasified Char" represent the values of the chars obtained directly from the gasification at 850°C [26]. Each point corresponds to one gasification experiment conducted in the fluidised-bed/fixed-bed reactor at 850°C. The data shown at 0 char conversion level stand for the values of the chars obtained after pyrolysis to 420°C. Afterwards, the data account for the chars obtained at varying conversion levels during the gasification in air. Each point starting from 0 conversion level represents one experiment carried out in TGA.

The total Raman peak intensity between 800 and 1800 cm^{-1} was integrated and expressed hereafter as the total Raman area of the char. It is known that the Raman intensity is mainly influenced by two factors, including Raman scattering ability and light absorptivity of char [13]. The O-containing structures connected to aromatic rings tend to give a resonance effect between the O and the aromatic ring that can

enhance the total Raman intensity. On the other side, the condensed aromatic ring systems in char have high light absorptivity, leading to decreasing total Raman intensity.

Figure 3-1 illustrates the changes in the total Raman area for the chars after pyrolysis to 420°C and/or further gasification in air at 420°C. After being gasified in 15% H_2O-CO_2 at 850°C, the total Raman area of the chars increased drastically from around 2000 to 3600 as the holding time increased from 0 min to 10 and 15 min [26]. It is known that the formation of O-containing structures in the presence of H_2O is the main reason enhancing Raman peak intensity.

During the pyrolysis in N_2 from room temperature to 420°C, the total Raman areas of all three chars decreased significantly. The decomposition of O-containing structures or the condensation of aromatic ring systems might lead to the reduction in the total Raman area. Considering that the temperature is relatively low (<420°C), it is unlikely for the aromatic ring condensation to occur. Thus the decrease in the total Raman area is possibly as a result of the loss of unstable O-containing structures connected to aromatic rings.

Once the pyrolysed char contacted with O_2, the gasification initiated. During the gasification in air, the total Raman area raised as the char conversion proceeded. The total Raman areas of all the chars at final conversion levels in air were higher than the starting points. The data indicate that the oxygenation of the char is more favourable in air at low temperature than in 15% H_2O-CO_2 at high temperature. For the growth in the total Raman area, it is primarily owing to the enhanced resonance effect between O-containing structures and the connecting aromatic ring or due to the reduced light absorptivity. As shown in Fig. 3-2 below, the ratio between small and large aromatic rings reduced during the gasification in air, implying that the condensation of ring systems led to increasing the light absorptivity. Thus the formation of O-containing structures is the main reason causing the enhancement of the total Raman area during the gasification in air. Furthermore, it is worth noting that the total Raman area of the 0 min char increased more significantly (from around 1500 to 3500) than the chars with

longer holding time. It is known from Ref. 26 and also Fig. 3-2 below (the data for gasified char) that the ratio between small and large rings dropped with increasing holding time in 15% H_2O-CO_2, indicating that the aromatic rings became more condensed as gasification proceeded. The data in Fig. 3-1 thus indicate that the O-containing species were more readily present in the less ordered char than in the more ordered one during the gasification in air.

3.3.2.2 Changes in aromatic ring systems

Figure 3-2a displays the changes in the ratio between small and large rings as a function of char conversion. In the band assignment of Raman spectrum, the three bands Gr+Vl+Vr together stand for the small rings with <6 rings. D band primarily stands for the larger rings with not less than six rings. The area ratio between (Gr+Vl+Vr) and D band is an important parameter reflecting the evolution of aromatic ring systems in the char. Tracing the changes in the relative amount of small and large rings during gasification is important for the determination of reaction pathways.

As seen from Fig. 3-2a, the selected three char samples with different ratios between small and large aromatic rings (different char structure) underwent different reaction pathways. Where the ratios were similar for the starting char samples (the 10 min char and the 15 min char), the reaction pathways were closer to each other. For individual char sample, the ratio firstly increased during the pyrolysis of the chars in N_2 from room temperature to 420°C. It is implied that the large rings were consumed and/or transformed into smaller ones during reheating. In the subsequent gasification in air, the ratio decreased with increasing char conversion level. It is assumed that the small rings were consumed and/or transformed into larger ones during gasification in air. In order to gain further insights into the changes in aromatic ring systems, the percentage of small rings and large rings in the total Raman intensity were plotted separately in Figs. 3-2b and 3-2c.

In Fig. 3-2b, the concentration of small rings in the char remained almost unchanged, excluding a slight increase during the pyrolysis of the 15 min char. It is assumed that

the decomposition and formation of small rings reaches a dynamic balance during the pyrolysis and gasification in air. For the large aromatic ring systems (shown in Fig. 3-2c), it firstly decreased during pyrolysis and then increased significantly during gasification. It is indicated that the structure of the char obtained from 15% H_2O-CO_2 was unstable, the breakage of aromatic ring systems occurred during reheating in N_2 at low temperature. It is believed that in the aged char that is rich in large aromatic rings, the large aromatic ring systems would be consumed less quickly and enriched in the char during further gasification in air. When taking ratio of the small and large rings peak intensity, as seen in Fig. 3-2a, it is clear that relatively more large rings were left during the gasification in air.

As mentioned in Section 3-1, in a parallel study, a nascent char obtained from the pyrolysis of Loy Yang brown coal in a wire-mesh reactor with 0 s holding at 600°C was pyrolysed to 370°C and gasified in air at 370°C in TGA [25]. Comparing the nascent char in Ref. 25 with the aged char used in this study, it is noticed that the changes in the ratio between small and large rings show opposite trends in the pyrolysis in N_2 and gasification in air. For the nascent char that is abundant in small ring systems ($I_{(Gr+Vl+Vr)}/I_D$ >3), the ratio between small and large rings firstly decreased in N_2 and then increased in air. In Li's study [25], the pyrolysed chars obtained from the pyrolysis of Loy Yang brown coal in a two-stage fluidised-bed/fixed-bed reactor (operated as a fixed-bed reactor) between 600 and 900°C were gasified in air at 400°C in TGA. For the pyrolysed chars, the ratios between small and large rings ($I_{(Gr+Vl+Vr)}/I_D$) were between 1.4 and 2.6 (calculated by the data in Fig. 3-8 in Ref. 25). Once experiencing the gasification in air, the ratio decreased (lower ratio for starting char) or remained unchanged (higher ratio for starting char) in the progress of gasification. Taking the results from Li [25], Zhang [26] and this study, it is thus fair to conclude that the exact pathway for the small/large rings depends on the structure of the starting char.

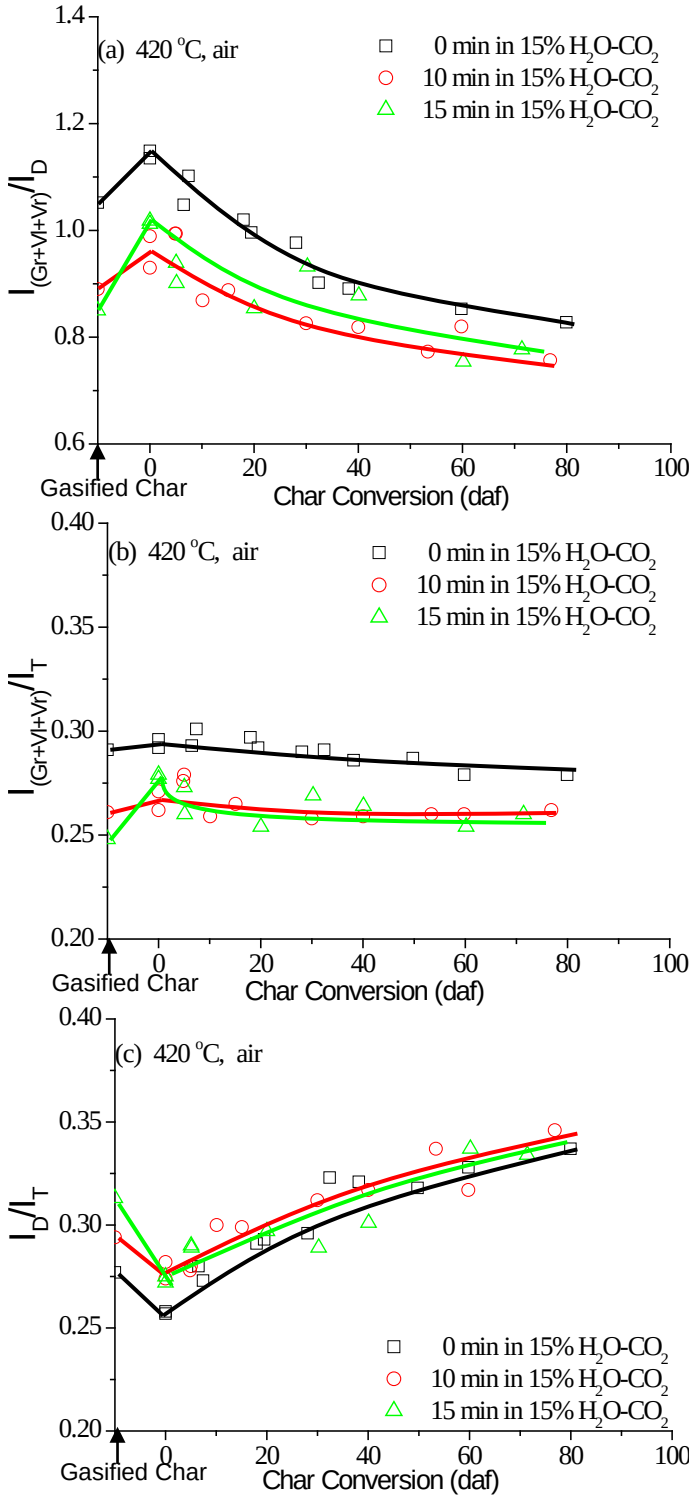

Fig. 3-2 Changes in (a) the band intensity ratio between small and large rings, (b) the percentage of small rings intensity in the total Raman area and (c) the percentage of large rings intensity in the total Raman area during the pyrolysis and gasification in air in TGA at 420°C. The data for the gasified char were plotted based on the results from Ref. 26.

3.3.2.3 Changes in S band

Figure 3-3 displays the changes in the fraction of S band peak intensity in the total Raman area as a function of char conversion during the pyrolysis in N_2 and gasification in air. In the band assignment, S band is mainly due to the cross-linking structures [6]. As can be seen from Fig. 3-3, the fractions of S band were almost the same for chars with different holding time immediately after the gasification at 850°C (around 0.18). During pyrolysis, the fraction of S band increased sharply from 0.18 to 0.21. As discussed in earlier section, the total Raman area decreased during pyrolysis owing to the decomposition of O-containing structures. It is assumed that the decomposition of O-containing structures resulted in the formation of additional cross-linking structures. The newly formed C-C bond between aryl and alkyl caused the increase in the fraction of S band. Once the char contacted with air, the fraction of S decreased steadily with increasing char conversion level. It is in good agreement with the previous work done by Li [25] and Zhang [26].

As discussed above, it is clearly seen that, during the gasification in air, the relative ratio of small aromatic ring systems remained unchanged, the large aromatic ring systems increased and the fraction of S band dropped with increasing conversion level. In another word, the structure of the char remaining becomes more enriched with large aromatic ring systems and less cross-linked. This clearly indicates that cross-linking structures were preferentially consumed together with the small aromatic ring systems.

In order to investigate the correlation between the cross-linking structures and large rings, the band area ratio between S band and D band is plotted as a function of char conversion level in Fig. 3-4. As seen in Fig. 3-4, the relative ratio between S and D band firstly increased during pyrolysis and then decreased remarkably with increasing char conversion level for all the chars. The data indicate that the large aromatic ring systems appear to have more cross-linking structures per carbon during pyrolysis and have less during the gasification in air.

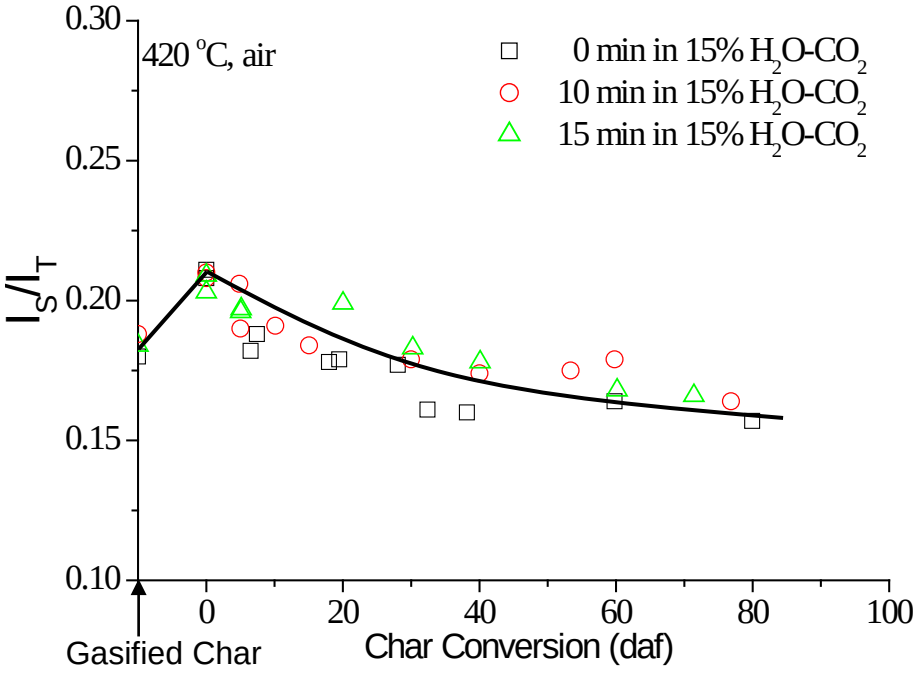

Fig. 3-3 Changes in the fraction of S band intensity in the total Raman area during the pyrolysis and gasification in air in TGA at 420°C. The data for the gasified char were plotted based on the results from Ref. 26.

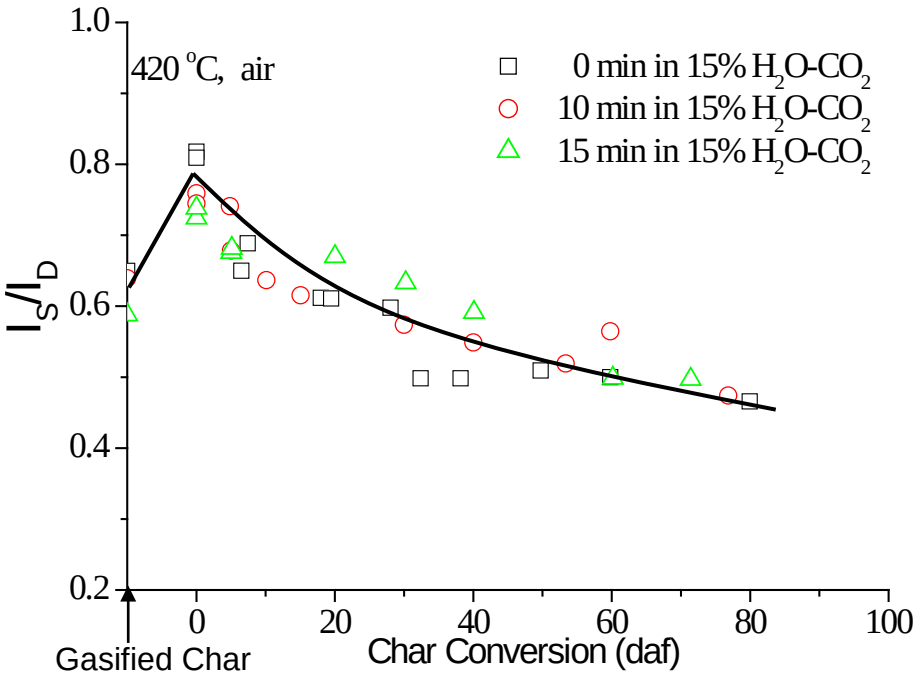

Fig. 3-4 Changes in the band intensity ratio of S band and D band during the pyrolysis and gasification in air in TGA at 420°C. The data for the gasified char were plotted based on the results from Ref. 26.

3.3.3 Char-O_2 specific reactivity

Figure 3-5 shows the char-O_2 specific reactivity of the gasified char obtained from the fluidised-bed/fixed-bed reactor at 850°C. The reactivity measurement was conducted in air at 420°C. For all three chars, an obvious peak was observed within 20% char conversion level. For the 0 min char, the peak arose even before 5% char conversion level, followed by a gradual decrease. After 15% conversion level, the char-O_2 specific reactivity gradually went up with increasing char conversion level. For the two chars with longer holding time at 850°C, the peak value appeared at around 10% conversion level and then decreased steadily to around 50% conversion level. Afterwards, the char specific reactivity increased as char gasification proceeded. It is noticed that the specific reactivity of all three chars came to close to each other after reaching 50% char conversion level.

It is known that the char reactivity is mainly affected by the char structure and the properties of AAEM species left in char. Moreover, according to previous study [34], the AAEM species would not volatilise during the slow gasification in air at temperature lower than 600°C. In other words, the AAEM species would accumulate in the char during char conversion in TGA. If the AAEM concentration is the only factor affecting the char reactivity, a monotonous increase of specific reactivity should be observed due to the monotonous accumulation of AAEM species in char. While the initial peaks followed by a reduction in the char reactivity were observed in all three chars, it is clearly that the effect of char structure cannot be overlooked. Moreover, for the three chars obtained at different conversion levels in 15% H_2O-CO_2 at 850°C, the magnitude of the peaks increased significantly with increasing holding time. The initial peaks indicated that the chars prepared in 15% H_2O-CO_2 were very heterogeneous and that the char gasification in 15% H_2O-CO_2 created structures that were highly reactive in air at 420°C. Once contacted with O_2, these reactive structures were consumed quickly, leading to a high specific reactivity peak at initial stage. With the consumption of these reactive structures, the char reactivity decreased gradually. After reaching about 17% char conversion of the 0 min char and 50% char conversion

of the 10 min char and the 15 min char, the specific reactivities of three chars all increased as reaction proceeded.

When the char conversion level was higher than 50%, the specific reactivities of three chars almost overlapped together. Considering the different carbon skeleton structures of the chars and the accumulation of AAEM species in the chars, it is concluded that the increasing concentrations of AAEM species in the chars were the primary factor affecting the specific reactivity after 50% char conversion level.

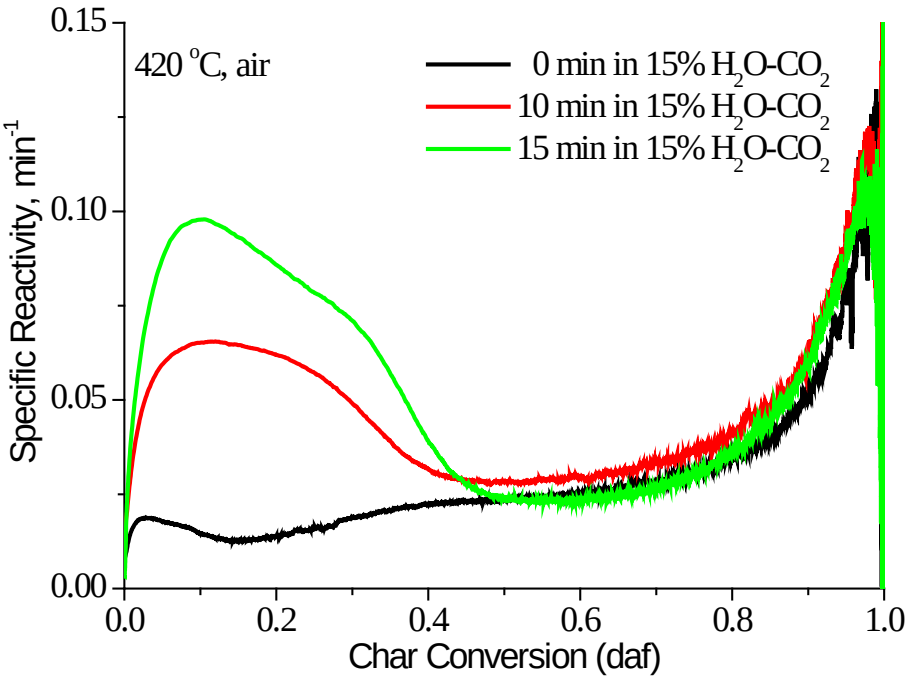

Fig. 3-5 Specific char-O_2 reactivity of the chars produced from the gasification of Loy Yang brown coal in 15% H_2O-CO_2 at 850°C [26]. The reactivity measurement was done at 420°C in air in TGA.

3.4 Conclusions

The char structural changes during the pyrolysis and gasification in air of Loy Yang brown coal char were investigated in this study. The results revealed that the structure of the original char obtained at high temperature determines the exact reaction pathway for the small/large aromatic rings during the pyrolysis and gasification in air at low temperature. The loss of the O-containing structures and the breakage of aromatic rings during pyrolysis show that the char structure is very unstable after gasification in 15% H_2O-CO_2. In comparison with the mixture of CO_2 and H_2O at high temperature, the oxygen at low temperature is more effective in the oxygenation of the char. Furthermore, the oxygen was more easily introduced into the char with less condensed structures than the more condensed one.

3.5 References

[1] Li C-Z. Special issue-gasification: A route to clean energy. Process Safety and Environmental Protection 2006;84:407-8.

[2] Hayashi J-i, Kudo S, Kim H-S, Norinaga K, Matsuoka K, Hosokai S. Low-temperature gasification of biomass and lignite: consideration of key thermochemical phenomena, rearrangement of reactions, and reactor configuration. Energy Fuels 2014;28:4-21.

[3] Tomita A, Ohtsuka Y. Chapter 5 Gasification and combustion of brown coal. In: C.-Z. Li, editor. Advances in the Science of Victorian Brown Coal: Elsevier; 2004. p. 223-85.

[4] Miura K, Hashimoto L, Silveston PL. Factors affecting the reactivity of coal chars during gasification, and indices representing reactivity. Fuel 1989;68:1461-75.

[5] Li C-Z. Some recent advances in the understanding of the pyrolysis and gasification behaviour of Victorian brown coal. Fuel 2007;86:1664-83.

[6] Li X, Hayashi J-i, Li C-Z. FT-Raman spectroscopic study of the evolution of char structure during the pyrolysis of a Victorian brown coal. Fuel 2006;85:1700-7.

[7] Tay HL, Kajitani S, Wang S, Li C-Z. A preliminary Raman spectroscopic perspective for the roles of catalysts during char gasification. Fuel 2014;121:165-72.

[8] Moulijn JA, Kapteijn F. Towards a unified theory of reactions of carbon with oxygen-containing molecules. Carbon 1995;33:1155-65.

[9] Livneh T, Bar-Ziv E, Sennec O, Salatino P. Evolution of reactivity of highly porous char s from Raman microscopy. Combustion Science and Technology 2000;153:65-82.

[10] Bar-Ziv E, Kantorovich II. Mutual effects of porosity and reactivity in char oxidation. Progress in Energy and Combustion Science 2007;27:667-97.

[11] Zhao Y, Feng D, Zhang Y, Huang Y, Sun S. Effect of pyrolysis temperature on char structure and chemical speciation of alkali and alkaline earth metallic species in biochar. Fuel Processing Technology 2016;141:54-60.

[12] Liu L, Cao Y, Liu Q. Kinetics studies and structure characteristics of coal char under pressurised CO_2 gasification conditions. Fuel 2015;146:103-10.

[13] Russell NV, Gibbins JR, Williamson J. Structural ordering in high temperature coal chars and the effect on reactivity. Fuel 1999:78;803-7.

[14] Tay HL, Li C-Z. Changes in char reactivity and structure during the gasification of a Victorian brown coal: Comparison between gasification in O_2 and CO_2. Fuel Processing Technology 2010;91:800-4.

[15] Zhang S, Min Z, Tay HL, Asadullah M, Li C-Z. Effects of volatile-char interactions on the evolution of char structure during the gasification of Victorian brown coal in steam. Fuel 2011;90:1529-35.

[16] Li C-Z. Importance of volatile-char interactions during the pyrolysis and gasification of low-rank fuels – A review. Fuel 2013;112:609-23.

[17] Bai Y, Wang Y, Zhu S, Li F, Xie X. Structural features and gasification reactivity of coal chars formed in Ar and CO_2 atmospheres at elevated pressures. Energy 2014;74;464-70.

[18] Li T, Zhang L, Dong L, Li C-Z. Effects of gasification atmosphere and temperature on char structural evolution during the gasification of Collie sub-bituminous coal. Fuel 2014;117:1990-5.

[19] Meng H, Wang S, Chen L, Wu Z, Zhao J. Thermal behavior and the evolution of char structure during co-pyrolysis of platanus wood blends with different rank coals from northern China. Fuel 2015;158:602-11.

[20] Liu X, Zheng Y, Liu Z, Ding H, Huang X, Zheng C. Study on the evolution of the char structure during hydrogasification process using Raman spectroscopy. Fuel 2015;157:97-106.

[21] Wang S, Li T, Wu L, Zhang L, Dong L, Hu X, Li C-Z. Second-order Raman spectroscopy of char during gasification, Fuel Processing Technology 2015;135:105-11.

[22] Zhang L, Li T, Quyn DM, Dong L, Qiu P, Li C-Z. Formation of nascent char structure during the fast pyrolysis of mallee wood and low-rank coals. Fuel 2015;150:486-92.

[23] Zhang L, Li T, Quyn DM, Dong L, Qiu P, Li C-Z. Structural transformation of nascent char during the fast pyrolysis of mallee wood and low-rank coals. Fuel Processing Technology 2015;138:390-6.

[24] Li X, Hayashi J-i, Li C-Z. Volatilisation and catalytic effects of alkali and alkaline earth metallic species during the pyrolysis and gasification of Victorian brown coal. Part VII. Raman spectroscopic study on the changes in char structure during the catalytic gasification in air. Fuel 2006;85:1509-17.

[25] Zhang L, Li T, Wang S, Song Y, Dong L, Zhang S, Li C-Z. Changes in char structure during the thermal treatment of nascent chars in N_2 and the in-situ gasification in O_2. Submitted.

[26] Li T, Zhang T, Dong L, Li C-Z. Effects of gasification temperature on char structural evolution and AAEM retention during the gasification of Loy Yang brown. Submitted.

Chapter 4

Effects of gasification atmosphere and temperature on char structural evolution during the gasification of Collie sub-bituminous coal

4.1 Introduction

Gasification is a clean and efficient way to convert solid coal to gaseous products [1-2]. As char gasification is the rate-limiting step, high char reactivity is important for achieving high conversion levels [3]. Many factors can influence char reactivity [3-7], among which the importance of char structure is not particularly well understood [8]. The char structure could not only directly determine which carbon atoms are gasified first during gasification but also affect the interaction between char and catalysts, hence influencing the activity of catalysts [9-10]. So tracing the changes in char structure during gasification is really essential for a better understanding of gasification mechanism.

Char-CO_2 reaction and char-H_2O reaction are both fundamentally important reactions. The mechanisms of the carbon-CO_2 reaction and the carbon-H_2O reaction have been studied extensively [11-14]. Many researchers have worked on the char gasification mechanism in CO_2 or H_2O separately. A few papers focus on the char gasification in the mixture of CO_2 and H_2O. In these papers, there is a debate arguing whether there is an interaction between CO_2 and H_2O during the gasification in the mixture. Some show that char-CO_2 and char-H_2O reactions take place separately on different active sites on the char and the gasification rate in the mixture is equal to the sum of the gasification rates in each gasification atmosphere respectively [15-16]. On the other hand, some indicate that during the gasification in the mixture, the char-CO_2 and char-H_2O reactions are not independent. There are interactions such as competition or inhibition between CO_2 and H_2O. CO_2 and H_2O compete or share some active sites on the char [17-18].

According to the previous work in our group [4,6-8,19-23], FT-Raman spectroscopy is shown to be a powerful tool to investigate the structural features of highly disordered char. It is indicated that the changes of char structure take place not only on the char surface but also inside the char matrix. It introduces an effective method to study the bulk properties of the char.

As investigated in previous study for Loy Yang brown (Chapter 2), it is known that both CO_2 and H_2O can affect the evolution of char structure and their effects are not the same. CO_2 plays an increasingly important role in the char structural evolution with temperature increasing from 800 to 900°C. As a higher-rank coal, a sub-bituminous coal is different from a brown coal in its chemical forms. The effects of gasification atmosphere and temperature on the changes in char structure for a sub-bituminous coal are still unclear. This study aims to investigate the effects of gasification atmosphere and temperature on char structural evolution during the gasification of Collie sub-bituminous coal. Three gasification atmospheres were used: pure CO_2, 15% H_2O balanced with Ar (15% H_2O-Ar) and 15% H_2O balanced with CO_2 (15% H_2O-CO_2). Chars produced from the gasification at 800-900°C in three gasification atmospheres were characterised by FT-Raman spectroscopy. The changes in char structure were traced by the evolution of the oxygenation of the char and the aromatic ring systems in the char. The results show that the reaction pathways for char-CO_2 reaction and char-H_2O reaction are different while the reaction pathway in each gasification atmosphere does not change with temperature between 800 and 900°C.

4.2 Experimental

4.2.1 Coal sample preparation

Collie sub-bituminous coal was used in this study, which was obtained from Muja Power Station, Western Australia. The sample was partially dried at low temperature (<35°C) and then ground and sieved to obtain a sample of particle sizes between 106 and 150 μm. The properties of the coal sample are presented in Table 4-1.

Table 4-1 Properties of Collie coal in weight percentage (dry and ash free basis).

Ash (db)	Volatile matter	C	H	N	S	O (by diff.)
5.7	38.8	75.7	4.5	1.4	0.5	17.9

4.2.2 Gasification

The gasification experiments were carried out in a fluidised-bed/fixed-bed reactor. The details of the reactor can be found in Ref. 9. Silica sand (300-355 μm) placed on the lower frit acted as the fluidised bed and was fluidised by the fluidising gas. An external furnace was used to heat up the reactor. Two thermocouples were used for monitoring the temperature distribution inside the reactor before and during the experiments. After the temperature inside the reactor was stabilised at the required temperature (e.g. 800, 850 or 900°C) for at least 15 minutes, the feeding of coal started. About 1.5 g coal was fed into the reactor (at a rate of 75 mg/min) through a water-cooled probe, keeping the particles at room temperature before entering the reaction area. After rapid pyrolysis, the chars flowing out from the sand bed would form a char bed underneath the upper frit, which featured as a fixed bed. The top frit in the free board would stop the chars coming out from the reactor. The volatiles generated at a later stage would go through the char bed and experience volatile-char interaction. When the coal feeding or a pre-set holding time was achieved, the reactor would be lifted out of the furnace immediately to quench the gasification reaction. In order to minimise the air pollution (oxidation) of the char collected after the experiments, the char samples were well sealed and stored in the fridge. Before carrying out further analysis, the samples would be well mixed to ensure a good reproducibility of the analysis results. The char yields were determined by the weight difference of the reactor before and after each experiment. The moisture content of coal/char was determined by a Perkin-Elmer Pyris 1 thermogravimetric analyser (TGA) and considered in the calculation of char yields.

4.2.3 Char characterisation

The key purpose of char characterisation was to obtain information about the chemical structural feature of chars, especially their carbon skeleton. The true graphitic structure does not exist in chars from brown coal prepared at low temperature such as the chars in this study [4, 6-8,19]. Furthermore, the key focus should be the reactive structure. For this reason, techniques such as X-ray diffraction would not be suitable for this

purpose as it would focus more on ordered and thus less reactive structures in the chars. FT-Raman spectroscopy [4,6-8,19] appears to be most suitable for this task.

The FT-Raman spectra of chars were acquired using a Perkin-Elmer Spectrum GX FT-IR/Raman spectrometer according to the procedures outlined in Ref. 19. The char sample was mixed and ground with KBr which served as heat-dissipating medium. In order to eliminate the influence of concentration of char-KBr mixture on the comparison of total Raman area, a concentration of 0.25 wt% char in the mixture of char and KBr was selected after careful examination. Each sample was scanned 200 times with a laser power of 150 mW. The Raman spectrum in the range between 800 and 1800 cm^{-1} was firstly baseline-corrected and then curve-fitted using 10 Gaussian bands which was developed in our group [19]. One example of spectral deconvolution is shown in Fig. 4-1. As the band assignment has been well discussed in the previous work [19], only Gr, Vl, Vr and D bands will be briefly described in the later sections.

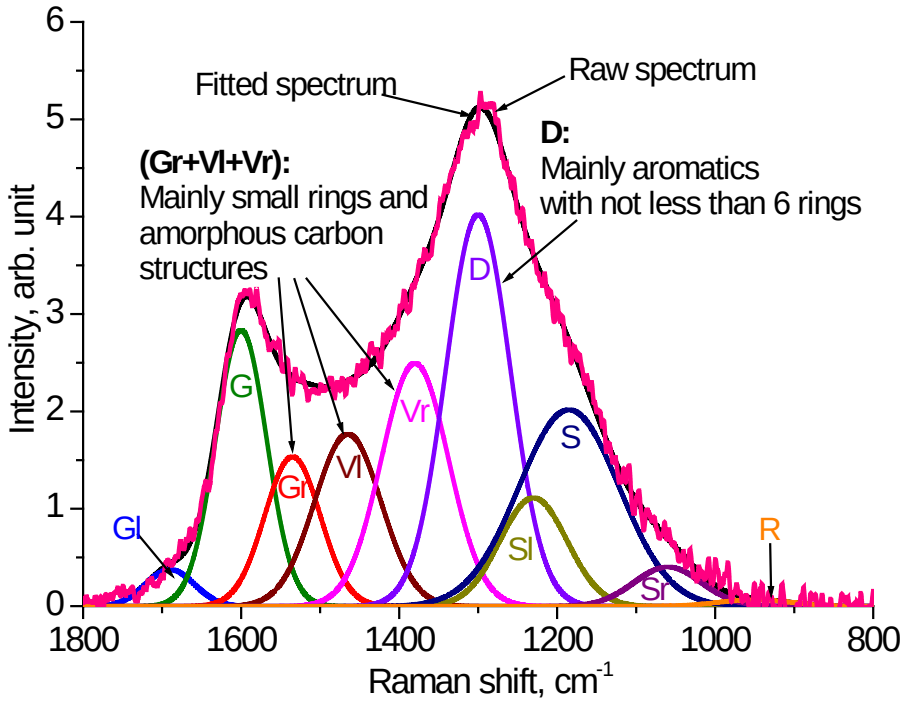

Fig. 4-1 A curve-fitted Raman spectrum of the char prepared from the gasification of Collie sub-bituminous coal in pure CO_2 at 800°C.

4.3 Results and discussion

4.3.1 Char yields

The gasification of Collie sub-bituminous coal was carried out in the fluidised-bed/fixed-bed reactor in three atmospheres (pure CO_2, 15% H_2O-Ar, 15%H_2O-CO_2) in the temperature range of 800-900°C. The main purpose of this study is to investigate if the pathways for char-CO_2 and char-H_2O gasification would be the same. A steam concentration of 15% was chosen, which is within the range of steam concentrations in a typical gasifier. The CO_2 concentration was chosen so that the char-H_2O and char-CO_2 reaction rates were of similar magnitudes and comparable. Figure 4-2 shows the char yields as a function of holding time during the gasification. Each point corresponded to one gasification experiment. The "0" min holding time means the time when coal feeding was completed.

It can be seen that, at each temperature, the gasification in pure CO_2 proceeded slowest among the three atmospheres used in this study. The conversion of char proceeded fastest during the gasification in the mixture of H_2O and CO_2 (15% H_2O-CO_2). However, the char conversion during the gasification in the mixture was lower than the sum of the char conversion during the gasification in pure CO_2 and 15% H_2O-Ar separately (The addition of the char conversions is described as the dashed line in Fig. 4-2). Clearly, the reactions of char-CO_2 and char-H_2O are not independent during gasification. CO_2 and H_2O compete for active sites on the char. Gasification also takes place inside the matrix of char, which will be discussed later based on the FT-Raman spectroscopy data.

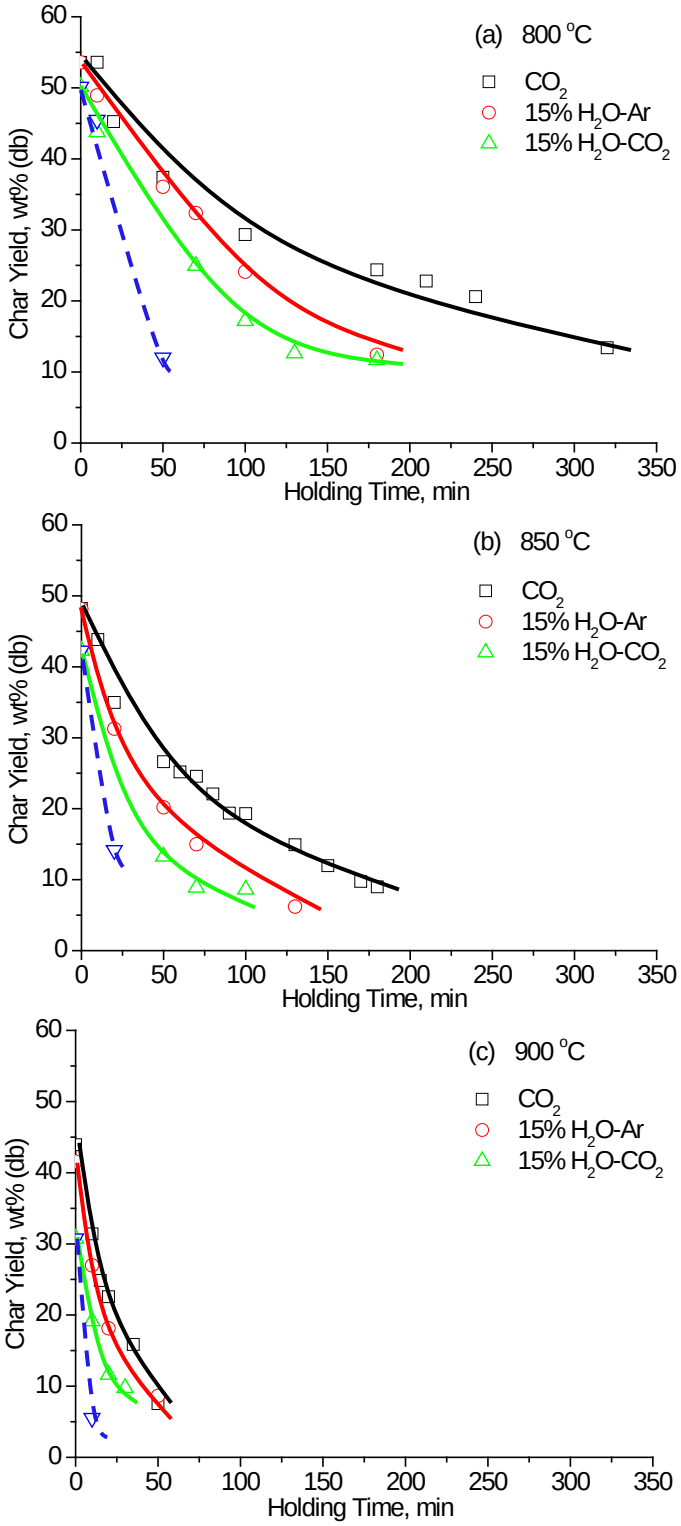

Fig. 4-2 Char yields (dry base) from the gasification of Collie sub-bituminous coal in pure CO_2, 15% H_2O balanced with Ar and 15% H_2O balanced with CO_2 as a function of holding time at (a) 800°C; (b) 850°C; (c) 900°C. The dashed lines show the predicted char yields based on those in 15% H_2O balanced with CO_2.

4.3.2 Char structural changes

4.3.2.1 Oxygenation of the char

The total Raman area was taken as the total peak area between 800 and 1800 cm^{-1} of the Raman spectrum. It is known to be affected by the Raman scattering ability and the light absorptivity of the char [19]. The presence of O-containing structures would increase the Raman intensity mainly due to the resonance effect between O and the aromatic ring structure it is connected to. Along with the condensation of the aromatic ring systems in the char, the light absorption of the char would increase, hence decreasing the observed Raman intensity.

The data in Fig. 4-3 describe the total Raman areas as a function of char yield for the chars produced from the gasification of Collie sub-bituminous coal. At each temperature, the data can be classified into two groups. For the chars produced from the gasification in steam-containing atmospheres (15% H_2O-Ar and 15%H_2O-CO_2), the total Raman area increased drastically with descending char yield. For the chars produced from the gasification in CO_2, the total Raman area did not change much with the char conversion. Comparing the total Raman area of the chars produced from the gasification in 15% H_2O-CO_2 with that from the gasification in 15% H_2O-Ar, the increasing trend of total Raman area in the two gasification atmospheres were quite similar and no significant change can be seen due to the presence of CO_2. Comparing the total Raman area of the chars produced from the gasification in 15% H_2O-CO_2 with that from the gasification in pure CO_2, a remarkable contrast was shown. Clearly, in the presence of H_2O, the total Raman area of the chars behaved quite differently from that in the gasification in CO_2 alone. It is believed that more O-containing species connected with the aromatic ring systems structure were formed in the presence of H_2O to increase the total Raman area; while in the gasification in CO_2, the amount of such structure remained almost constant, resulting in the almost constant total Raman area.

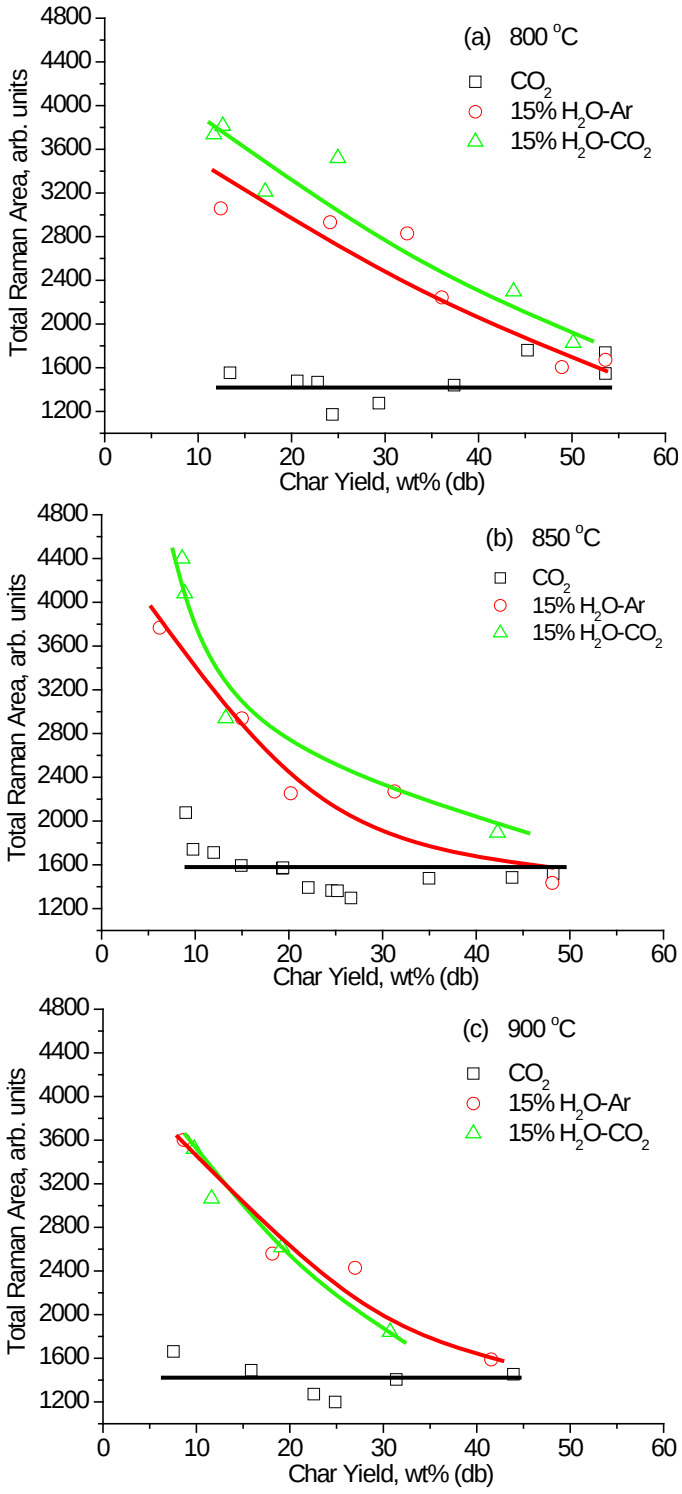

Fig. 4-3 Total Raman areas as a function of char yield for the chars produced in the gasification of Collie sub-bituminous coal in pure CO_2, 15% H_2O balanced with Ar and 15% H_2O balanced with CO_2 at (a) 800°C; (b) 850°C; (c) 900°C.

When char was gasified with CO_2 or H_2O, CO_2 or H_2O could firstly dissociate on the char surface to form intermediates, most likely as CO, O-containing species and H radical, as shown in the following reactions [11-14, 20].

$$C \xrightarrow{CO_2} C(CO) + C(O) \qquad (4-1)$$

$$C \xrightarrow{H_2O} C(OH) + C(H) \qquad (4-2)$$

These intermediates would activate aromatic ring systems for further reactions, possibly by the following steps [11-14, 20].

$$C(CO) = C + C(O) \qquad (4-3)$$

$$C(OH) + C = C(O) + C(H) \qquad (4-4)$$

$$2C(H) = 2C + H_2 \qquad (4-5)$$

$$C(O) = CO \qquad (4-6)$$

It is believed that the oxygen derived from CO_2 and H_2O contributed to the oxygenation of the aromatic ring systems. Since the char gasification by CO_2 is much slower than that by H_2O, it is believed that the concentration of O-containing species connected with the aromatic ring systems structure from CO_2 must be lower than that from H_2O, partly explaining the lower Raman intensity for the former than for the latter.

4.3.2.2 Changes in the aromatic ring systems in the char

In order to acquire more information about the char structure, each Raman spectrum between 800 and 1800 cm^{-1} was deconvoluted into 10 Gaussian bands [19]. The ratio between some major bands was used as an important parameter to investigate the char structure. Figure 4-4 shows the band area ratio $I_{(Gr+Vl+Vr)}/I_D$ during the gasification of Collie sub-bituminous coal in three atmospheres at 800-900°C. $I_{(Gr+Vl+Vr)}$ is the total Raman area of (Gr+Vl+Vr) representing typical structures in amorphous carbon, mainly due to small aromatic ring systems (less than 6 fused rings). I_D is the Raman

area of D band mainly represents the large aromatic ring systems with no less than 6 fused rings [19]. Hence the relative ratio $I_{(Gr+Vl+Vr)}/I_D$ could reflect the ratio of the amounts of small and large aromatic ring systems in the char.

As presented in Fig. 4-4, the ratio decreased with decreasing char yield for the chars produced from all three gasification atmospheres at different gasification temperature. It is indicated that, small aromatic rings were consumed and/or converted into large ones during gasification, while large ones were left and/or formed during gasification. Based on the same char conversion level, the relative amount of small aromatic rings in the chars produced from the gasification in pure CO_2 was much higher than that in the chars produced from the gasification in the steam-containing atmospheres during the whole gasification process. In the steam-containing gasification atmospheres, H radicals generated by H_2O would penetrate into the char matrix and induce the ring condensation [2,7,11,21-23]. Therefore, small aromatic ring systems were converted into large ones. Meanwhile, small ring systems were more selectively consumed during the gasification in steam-containing atmospheres [2,11,21-23], which also contributed to the decrease of the band area ratio in the gasification of Collie sub-bituminous coal in the steam-containing atmospheres.

Judging from the different band area ratio among the chars produced from the gasification in three atmospheres at each char conversion level, it can be seen that the char structures were different, which was most likely caused by the different reaction pathways in three gasification atmospheres.

Figure 4-5 shows the band area ratio $I_{(Gr+Vl+Vr)}/I_D$ as a function of char yield and gasification temperature for the chars produced from the gasification of Collie sub-bituminous coal in three atmospheres at 800-900°C. It can be seen that, within one gasification atmosphere, the band area ratio was quite similar and followed the same trend line with decreasing char yield for different gasification temperature, indicating that the char structures were the same at the same char conversion levels. Thereby the reaction pathway remained unchanged within the temperature investigated in this study.

As stated in the result of char yields during the gasification, CO_2 and H_2O compete for active sites on the char. For the chars produced from the gasification in 15% H_2O-CO_2, the total Raman area and the band area ratio $I_{(Gr+Vl+Vr)}/I_D$ have quite similar trends as chars prepared from the gasification in 15% H_2O-Ar with the char conversion. As the FT-Raman technique measures the bulk properties of the char, surface reaction alone cannot be detected. Thus it can be concluded that the competition between CO_2 and H_2O during the gasification most likely took place on the char surface.

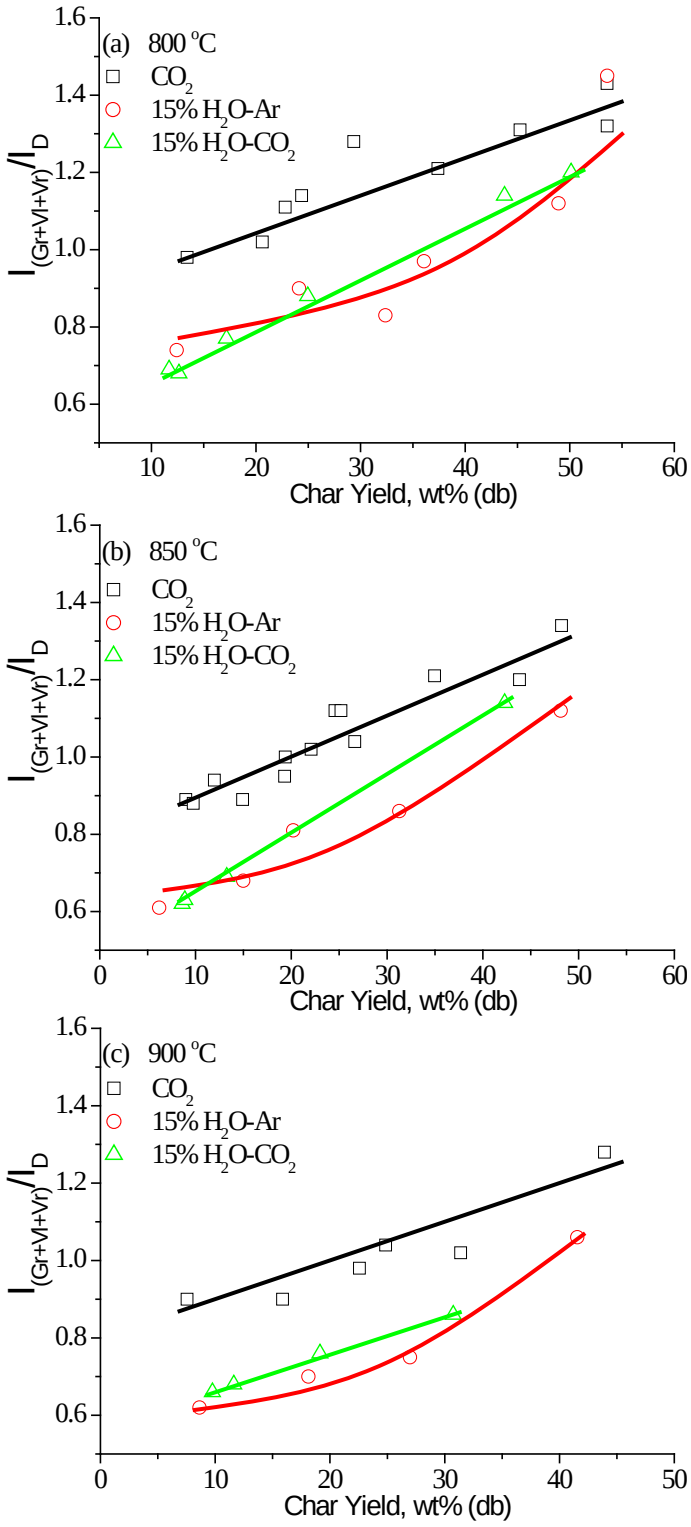

Fig. 4-4 Raman band ratios Gr+Vl+Vr/D as a function of char yield for the chars produced in the gasification of Collie sub-bituminous coal in pure CO_2, 15% H_2O balanced with Ar and 15% H_2O balanced with CO_2 at (a) 800°C; (b) 850°C; (c) 900°C.

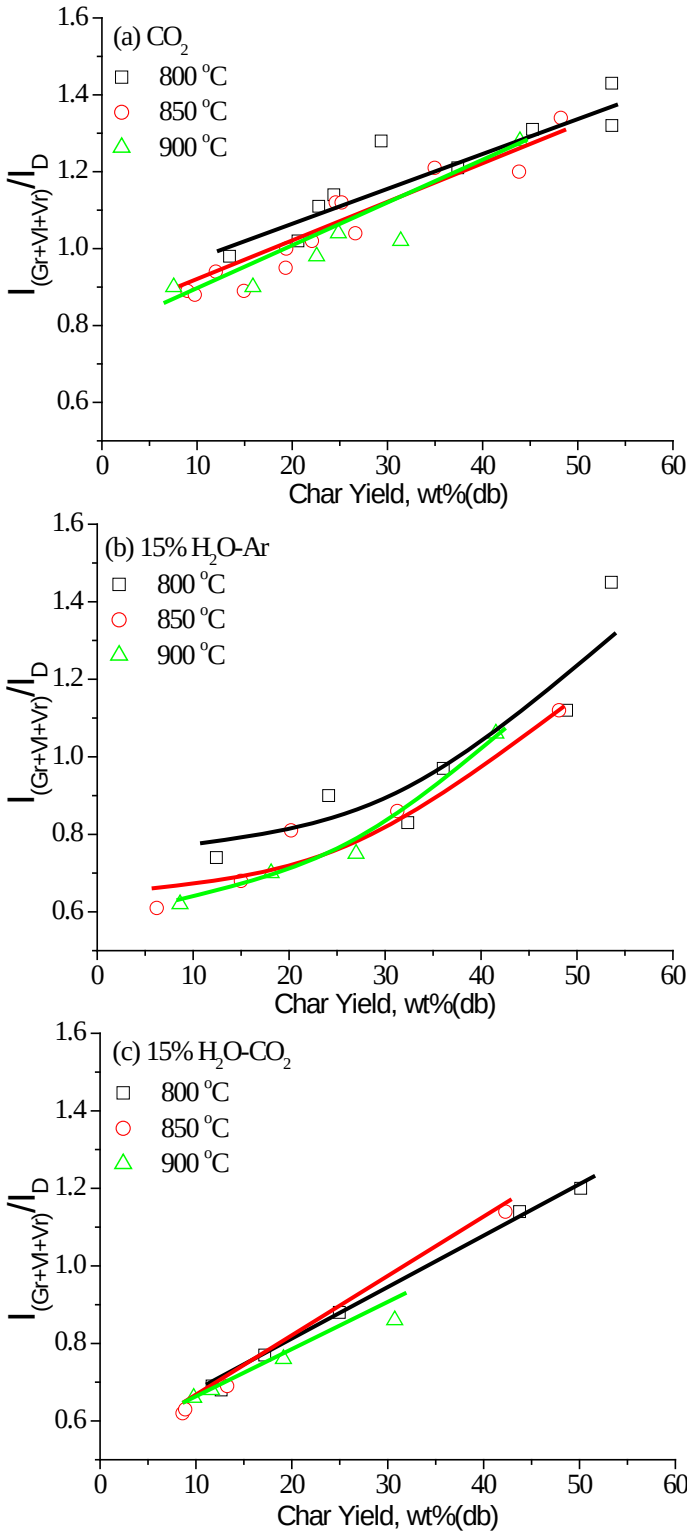

Fig. 4-5 Raman band ratios Gr+Vl+Vr/D as a function of char yield for the chars produced in the gasification of Collie sub-bituminous coal at 800-900°C in (a) pure CO_2, (b) 15% H_2O balanced with Ar; (c) 15% H_2O balanced with CO_2.

4.4 Conclusions

Chars produced from the gasification of Collie sub-bituminous coal in three atmospheres at 800-900°C in a fludised-bed/fixed-bed reactor were characterised by FT-Raman spectrometer. It shows that the gasifying agents CO_2 and H_2O compete for active sites most likely on the char surface during gasification. H_2O plays a decisive role in the evolution of char structure in H_2O-containing atmospheres. The char-CO_2 reaction and char-H_2O reaction do not follow the same reaction pathway. Within one gasification atmosphere, the reaction pathway does not change between 800 and 900°C.

4.5 References

[1] Tomita A, Ohtsuka Y. Chapter 5 gasification and combustion of brown coal. In: Li C-Z, editor. Advances in the science of Victoria brown coal. Oxford: Elsevier; 2004. p. 223-85.

[2] Li C-Z. Special issue-gasification: a route to clean energy. Process safety and environmental protection 2006;84:407-8.

[3] Miura K, Hashimoto K, Silveston PL. Factors affecting the reactivity of coal chars during gasification, and indices representing reactivity. Fuel 1989;68:1461-75.

[4] Li C-Z. Some recent advances in the understanding of the pyrolysis and gasification behaviour of Victorian brown coal. Fuel 2007;86:1664-83.

[5] Li X, Wu H, Hayashi J-I, Li C-Z. Volatilisation and catalytic effects of alkali and alkaline earth metallic species during the pyrolysis and gasification of Victorian brown coal. Part VI. Further investigation into the effects of volatile-char interactions. Fuel 2004;83:1273-9.

[6] Li X, Hayashi J-I, Li C-Z. Volatilisation and catalytic effects of alkali and alkaline earth metallic species during the pyrolysis and gasification of Victorian brown coal. Part VII. Raman spectroscopic study on the changes in char structure during the catalytic gasification in air. Fuel 2006;85:1509-17.

[7] Li X, Li C-Z. Volatilisation and catalytic effects of alkali and alkaline earth metallic species during the pyrolysis and gasification of Victorian brown coal. Part VIII. Catalysis and changes in char structure during gasification in steam. Fuel 2006;85:1518-25.

[8] Zhang S, Min ZH, Tay HL, Asadullah M, Li C-Z. Effects of volatile-char interactions on the evolution of char structure during the gasification of Victorian brown coal in steam. Fuel 2011;90:1529-35.

[9] Quyn DM, Wu H, Hayashi J-I, Li C-Z. Volatilisation and catalytic effects of alkali and alkaline earth metallic species during the pyrolysis and gasification of Victorian brown coal. Part IV. Catalytic effects of NaCl and ion-exchangeable Na in coal on char reactivity. Fuel 2003;2:587-93.

[10] Takarada T, Tamai Y, Tomita A. Reactivities of 34 coals under steam gasification. Fuel 1985;64:1438-42.

[11] Blackwood JD, Ingeme AJ. The reaction of carbon with carbon dioxide at high pressure. Australian Journal of Chemistry 1960;13:194-9.

[12] Gadsby J, Long FJ, Sleightholm P, Sykes KW. The mechanism of the carbon dioxide-carbon reaction. Proceedings of the Royal Society of London. Series A, Mathematical and Physical Sciences 1948;193:357-76.

[13] Long FJ, Sykes KW. The mechanism of the steam-carbon reaction. Proceedings of the Royal Society of London. Series A, Mathematical and Physical Sciences 1948;193:377-99.

[14] Hermann G, Hüttinger KJ. Mechanism of water vapour gasification of carbon—a new model. Carbon 1986;24:705-13.

[15] Tay HL, Kajitani S, Zhang S, Li C-Z. Effects of gasifying agent on the evolution of char structure during the gasification of Victorian brown coal. Fuel 2013;103:22-8.

[16] Nilsson S, Gomez-Barea A, Ollero P. Gasification of char from dried sewage sludge in fluidized bed: Reaction rate in mixtures of CO_2 and H_2O. Fuel 2013;105:764-8.

[17] Roberts DG, Harris DJ. Char gasification in mixtures of CO_2 and H_2O: Competition and inhibition. Fuel 2007;86:2672-8.

[18] Umemoto S, Kajitani S, Hara S. Modeling of coal char gasification in coexistence of CO_2 and H_2O considering sharing of active sites. Fuel 2013;103:14-21.

[19] Li X, Hayashi J-I, Li C-Z. FT-Raman spectroscopic study of the evolution of char structure during the pyrolysis of a Victorian brown coal. Fuel 2006;85:1700-7.

[20] Tay HL, Li C-Z. Changes in char reactivity and structure during the gasification of a Victorian brown coal: Comparison between gasification in O_2 and CO_2. Fuel Processing Technology 2010;91:800-4.

[21] Keown DM, Hayashi J-I, Li C-Z. Drastic changes in biomass char structure and reactivity upon contact with steam. Fuel 2008;87:1127-32.

[22] Guo X, Tay HL, Zhang S, Li C-Z. Changes in char structure during the gasification of a Victorian brown coal in steam and oxygen at 800°C. Energy & Fuels 2008;22:4034-8.

[23] Keown DM, Li X, Hayashi J-I, Li C-Z. Evolution of biomass char structure during oxidation in O_2 as revealed with FT-Raman spectroscopy. Fuel Processing Technology 2008;89:1429-35.

Chapter 5

Effects of char structure and AAEM retention in char during the gasification at 900°C on the changes in low-temperature char-O_2 reactivity for Collie sub-bituminous coal

5.1 Introduction

The high efficiency and environmental performance of gasification-based power generation technologies would greatly save the consumption of our limited fossil fuels, such as coal, and reduce the emissions of CO_2 [1-3]. Compared with fast devolatilisation of coal and relatively quick reforming of volatiles, the gasification of char is known to be the rate-limiting step of the whole gasification process [4], thereby attracting great attention and research efforts.

Among several important factors that influence the char reactivity, the evolution of char structure has been extensively studied in recent years [1-3, 5-25]. FT-Raman spectroscopy [5-23] has been used to characterise char structure during gasification/pyrolysis. It has proved to be a useful tool to probe the structure of highly disordered chars from two aspects, the O-containing structures in the char and the carbon skeleton (aromatic rings) structures of the char. Tay and co-workers [10] found that the electron-rich O-containing species formed during gasification could largely enhance the gasification rate. The changes in ring structure would provide insights into the quest if the char conversion processes follow the same reaction pathway.

The finely dispersed alkali and alkaline earth metallic (AAEM) species in char, especially those in the form of ion-exchangeable carboxylates or salts, act as a crucial role in the utilisation of brown coal and biomass [24-31]. The AAEM species can serve as good catalysts to enhance the gasification rate by taking part in the reaction [10] between char and (radicals generated from) the gasifying agent(s). In previous work [18-19,30], the AAEM species in biomass/brown coal also showed a pronounced effect on the char-O_2 reactivity at low temperature. The chemical forms and distribution of AAEM species in char, which are related to those in the coal as well as the structure of char in which AAEM species disperse, are all significant elements affecting the char-O_2 reactivity [3,30]. During gasification, the AAEM species could also gradually move from the inner char structure to the surface of the char [30,32-34]. An increase in the char-O_2 reactivity at higher char conversion level is often observed, owing to the accumulation and catalytic activity of these inorganic species [26].

A sub-bituminous coal would differ from a brown coal both in its organic structure (higher rank) and in its inorganic species. The AAEM species in a sub-bituminous coal may not be as well distributed as those in a brown coal, the latter have a lot more AAEM species dispersed at atomic levels, especially for the ion-exchangeable ones, than the former. The relative importance of char chemical structure (e.g. reflected by FT-Raman spectroscopy) and the catalytic effect of AAEM species for a bituminous coal is still unclear, which forms the motivation of this study as a direct continuation of our previous studies in this area on brown coal. This study mainly focuses on the changes in the char-O_2 reactivity of Collie sub-bituminous coal chars obtained from gasification at 900°C in different atmospheres [11]. The ex situ char-O_2 reactivity will be investigated from both the aspects of char structural features and the concentration of AAEM species. FT-Raman spectroscopy was applied to characterise the structural features of the chars collected at varying gasification conversion levels [11]. The concentration of AAEM species left after the partial gasification of Collie sub-bituminous coal in different atmospheres has been quantified with inductively coupled plasma – optical emission spectroscopy (ICP-OES). The results show that the changes in aromatic ring structure play a more important role in the changes in char-O_2 reactivity than the concentrations of AAEM species in char.

5.2 Experimental

5.2.1 Coal sample preparation and gasification experiments

A Western Australian (Collie) sub-bituminous coal [11] was selected in this study. Before grinding and sieving to the required particle size range (106-150 μm), the coal sample was firstly air dried at < 35°C. The coal contained 75.7, 4.5, 1.4, 0.5 wt% (daf) of C, H, N and S individuallly, with the ash yield being of 5.7 wt% (db) [11]. The chars prepared in pure CO_2, 15% H_2O-Ar and 15% H_2O-CO_2 at 900°C during the gasification of Collie sub-bituminous coal in a fluidised-bed/fixed-bed reactor [30] in the previous study [11] were used in this study. The details of the gasification experiment can be found in reference 11. Briefly, the coal particles (around 1.5 g that

was accurately weighed) were fed into the reactor at a rate of 75 mg/min. After feeding, the reactor was kept in the furnace for different periods of time to obtain chars with varying conversion levels. The deionised water was delivered by A HPLC pump at the desired rate and would immediately turn into steam and be diluted by the carrier gas (Ar, 99.999% ultra high purity) once fed into the reactor. 15% steam concentration was selected that is within the steam concentration range in a typical gasifier. Research grade (99.999%) CO_2 was used in this study.

5.2.2 Characterisation of char structure

The structural features of the char characterised by FT-Raman spectroscopy and reported previously [11], such as the oxygenation of the char and the changes in aromatic ring systems in the char, were used herein for comparison purposes.

5.2.3 Quantification of alkali and alkaline earth metallic (AAEM) species

Crucially, the AAEM species should be fully extracted from the raw coal/chars and fully dissolved with acid in order to quantify the concentrations of AAEM species accurately with ICP-OES. For this purpose, the ashing method previously developed in our group [31] was followed to remove the carbonaceous matter before digesting the resultant ash with acid [31]. Approximately, 6 mg coal/char was placed evenly in a platinum crucible and ashed in a muffle furnace in air. O_2 would bond with AAEM species, thereby minimising the loss of AAEM species. The coal/char samples were heated from room temperature to 300°C at 5°C/min, followed by a temperature increase to 415°C at 1°C/min. During the heating up process, the coal/chars were held for 10 min at 375°C and 415°C respectively. Within the temperature range between 300 and 415°C, the generation of volatiles were very drastic. Thus a very slow heating rate of 1°C/min was selected to avoid any possible ignition, so as to eliminate the loss of AAEM species. Afterwards, the temperature was further increased at a heating rate of 5°C/min to 600°C and then held for 20 min to burn off all the carbonaceous materials.

After cooling down, the ash together with the platinum crucible was put in a Teflon beaker for digestion. Concentrated hydrofluoric acid (47-51%, TraceSELECT) and nitric acid (65%, Suprapur) were used to digest the ash. 3 ml of each acid was injected gently through the beaker wall, making sure that no ash splashed out. Then, the beaker was covered with a lid and put on a hot plate (at 80°C) for at least 16 hours until the ash was completely digested. Afterwards, the lid was taken off and the acid mixture was allowed to evaporate. After evaporation, dilute HNO_3 was used to wash the residue inside the beaker. The solution was kept in a vial and weighed for further analysis. A Perkin-Elmer Optima 7300 DV ICP-OES was used to analyse the solution in order to quantify (calculate) the concentrations of AAEM species in coal/char.

5.2.4 Measurement of char-O_2 reactivity

The chars obtained from the gasification experiments were burned in air in a Perkin-Elmer Pyris 1 thermogravimetric analyser (TGA) for the measurement of their reactivity, following the procedures developed previously [30]. Briefly, around 3 mg char was placed evenly in a platinum crucible. The char was initially heated to 105°C at a heating rate of 20°C/min in nitrogen (ultra high purity, 99.999%) and kept for 20 min to remove the moisture from the char. In the following step, the temperature went up to 400°C/420°C. After stabilising for about 2 min at 400°C or 420°C, the gas supply to the TGA was changed from N_2 to air to start the reactivity measurement. At 420°C, the chars obtained in pure CO_2 ignited when the atmosphere was changed from N_2 to air. The temperature increased to around 440°C and a rapid weight loss was observed. In order to avoid the char sample ignition and to complete the char-O_2 reaction within a limited time range, the final temperature in the TGA was 400°C for the chars obtained in CO_2 or 420°C for the chars obtained in H_2O-containing atmospheres. When the weight loss remained unchanged, the temperature further went up to 600°C to burn off any organic carbonaceous material left. The final weight was taken as the weight of ash and considered in the calculation of specific reactivity, using the following equation:

$$R = -\frac{1}{W}\frac{dW}{dt} \qquad (5-1)$$

W herein is the weight of the char (on the dry and ash free basis) at any given time t.

5.3 Results and discussion

5.3.1 Changes in char structures

Figure 5-1 illustrates the main structural features of the char characterised by FT-Raman spectroscopy based on the data reported previously [11]. As mentioned in Ref. 11, the char structures were quite different for the chars obtained in different gasification atmospheres. In the presence of H_2O, the formation of O-containing structures led to remarkable growth in the observed total Raman peak area as char yield decreased during the gasification in 15% H_2O-Ar and 15% H_2O-CO_2. While in pure CO_2, the amounts of O-containing species, as are reflected by the Raman peak area, remained almost unchanged.

Apart from the oxygenation of the char, the relative amounts of small to large aromatic rings ($I_{(Gr+Vl+Vr)}/I_D$) are another important factor to reflect the carbon skeleton structure. The small aromatic rings were selectively consumed in H_2O-containing atmospheres (15% H_2O balanced with Ar or CO_2). They were richer in the chars obtained in pure CO_2. As represented by the decreasing ratio between small and large rings, the char structure became more condensed and ordered with longer holding time in all three atmospheres. Particularly, sharp decreases were observed within the first 10 min holding in the gasification atmospheres, followed by slight decreases with longer holding time. It is implied that smaller rings consumed/converted into larger ones more quickly during the first 10 min holding in the gasifying agent(s).

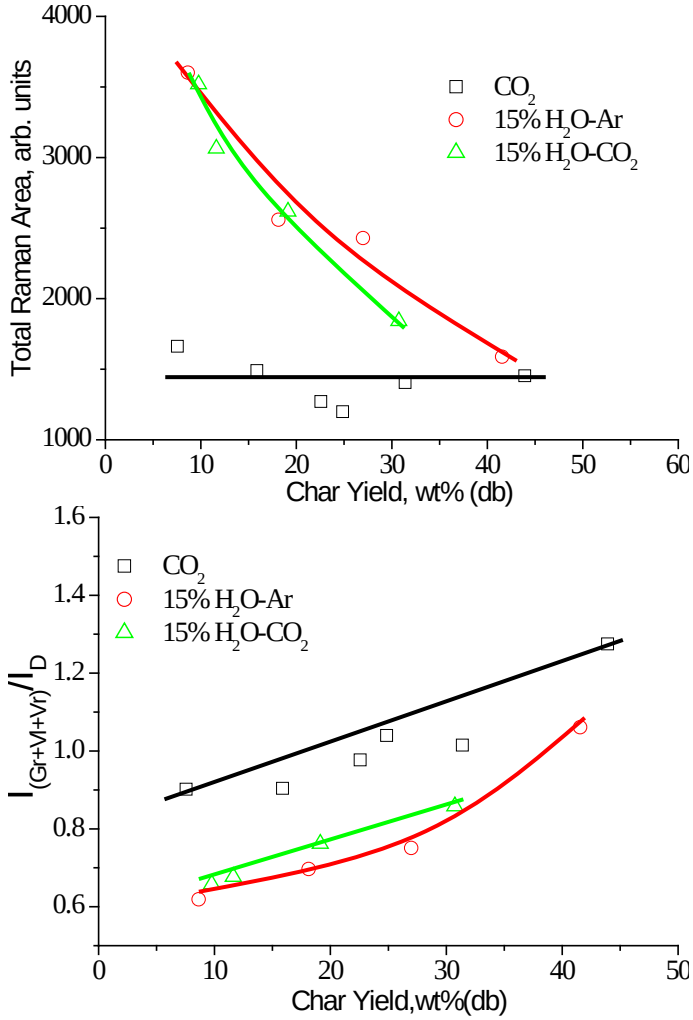

Fig. 5-1 Total Raman area and Raman band ratio of (Gr+Vl+Vr)/D versus char yield for the chars obtained in pure CO_2, 15% H_2O-Ar and 15% H_2O-CO_2 during the gasification of Collie sub-bituminous coal at 900°C. (Replotted from the data in Ref. [11], with permission from Elsevier).

5.3.2 Retention of AAEM species in char during gasification

The concentrations of AAEM species in the raw Collie sub-bituminous coal were 0.020 wt% Na, 0.062 wt% Mg, 0.094 wt% Ca and 0.015 wt% K on dry basis.

Figure 5-2 shows the concentrations of different AAEM species (Na, Mg, Ca and K) in left chars after the gasification of Collie sub-bituminous coal as a function of char yield. Each char sample obtained from the gasification experiment was analysed for four times for the quantification of AAEM species in char. It can be seen in the figures that the concentrations of AAEM species all increased with decreasing char yield as gasification at 900°C proceeded. During gasification, the AAEM species were accumulated in the char. At low conversion level, the AAEM concentrations in char were quite similar for the chars obtained in different gasification atmospheres, but slightly different at higher conversion levels. Lower AAEM concentrations were observed for the chars produced from gasification in pure CO_2.

It is believed [34] that, during the gasification in pure CO_2, the volatilisation of AAEM species was remarkable via the formation of carbonates especially when the char conversion level is higher than 80%. These data indicate that the capacity of char holding AAEM species varied with the gasification atmospheres, which is probably due to the changes in the chemical forms of AAEM species with the gasification atmosphere. As is shown in Fig. 5-1, the observed total Raman peak area, reflecting the concentrations of some O-containing structures in char that can cause resonance [23], tended to be lower for the chars obtained in pure CO_2 than those in H_2O-containing atmospheres. It is obvious that oxygen in char represents much more important sites than carbon or hydrogen for the AAEM species to bond with the char matrix. Taken together, the data in Figs. 5-1 and 5-2 provide some circumstantial evidence that the char's capacity of holding (i.e. chemically bonding) the AAEM species is related to its concentration of O-containing species that can be reflected in the Raman intensity. In other words, the Raman-sensitive O-containing structures are important sites to bond the AAEM species to char during the gasification at 900°C.

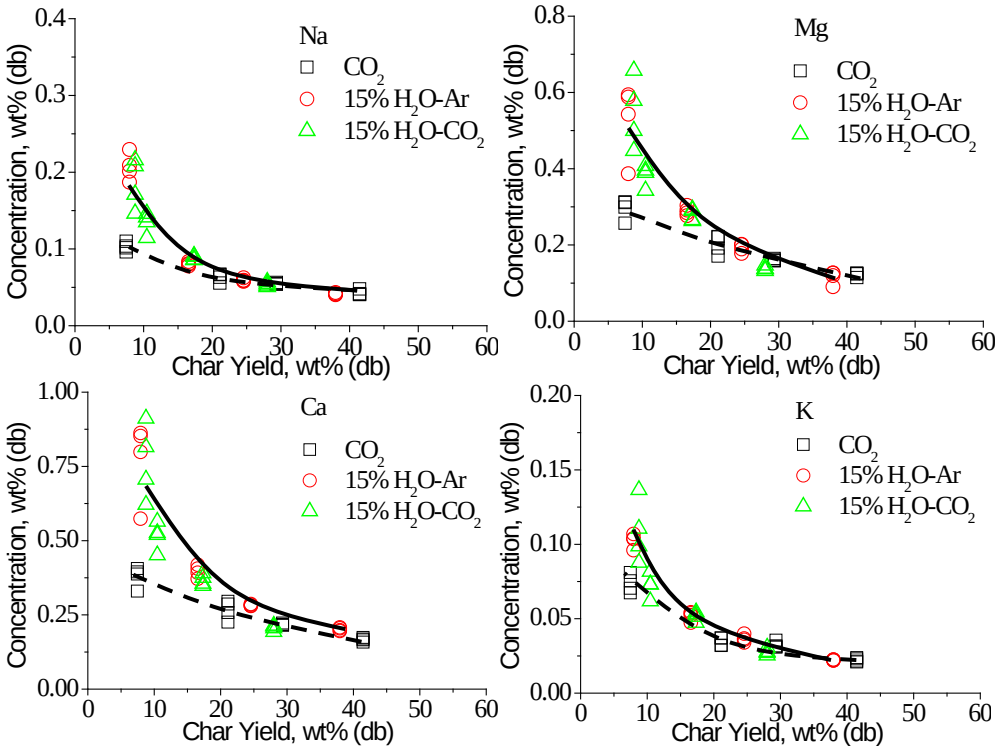

Fig. 5-2 Concentrations of AAEM species in char versus char yield for the chars obtained in pure CO_2, 15% H_2O balanced with Ar and 15% H_2O balanced with CO_2 at 900°C during the gasification of Collie sub-bituminous coal.

5.3.3 Char-O_2 reactivity at low temperature

Effects of char structure on char-O_2 reactivity. Figure 5-3 shows the specific char-O_2 reactivity measured in TGA in air at 400°C for the chars obtained in pure CO_2 or at 420°C for the chars obtained in 15% H_2O-Ar/15% H_2O-CO_2 during the gasification of Collie sub-bituminous coal at 900°C. For each gasification atmosphere, the specific reactivity decreased with increasing holding time, especially quickly in the initial 10 min holding at 900°C in the gasifying agent(s). As was mentioned earlier, the chars obtained in pure CO_2 at 900°C would tend to ignite in air at 420°C. It is obvious that the char-O_2 reactivity has much higher magnitude for the chars produced in pure CO_2 than for chars produced in steam-containing atmospheres.

Taking together the changes in char-O_2 reactivity and the total Raman peak area of the char, it is noticed that the chars with more O-containing species do not necessarily have higher low-temperature char-O_2 reactivity than the chars with less O-containing species inferred from the Raman peak area. The total Raman area increased drastically for the chars prepared in H_2O-containing atmospheres primarily owing to the formation of more O-containing structures in the char, which was initially expected to increase the char-O_2 reactivity. However, when the ex situ char-O_2 reactivity was measured in TGA, the chars produced in the mixture of 15% H_2O and CO_2 were much lower than those produced in pure CO_2 only. No obvious difference can be observed in the char reactivity for the chars obtained in 15% H_2O-CO_2 and H_2O alone. It is then fair to conclude that the presence of H_2O at 900°C during gasification plays an important role in char-O_2 reactivity at low temperature. However, the char-O_2 reactivity is not determined by the oxygenation of the char as is reflected by the Raman peak area.

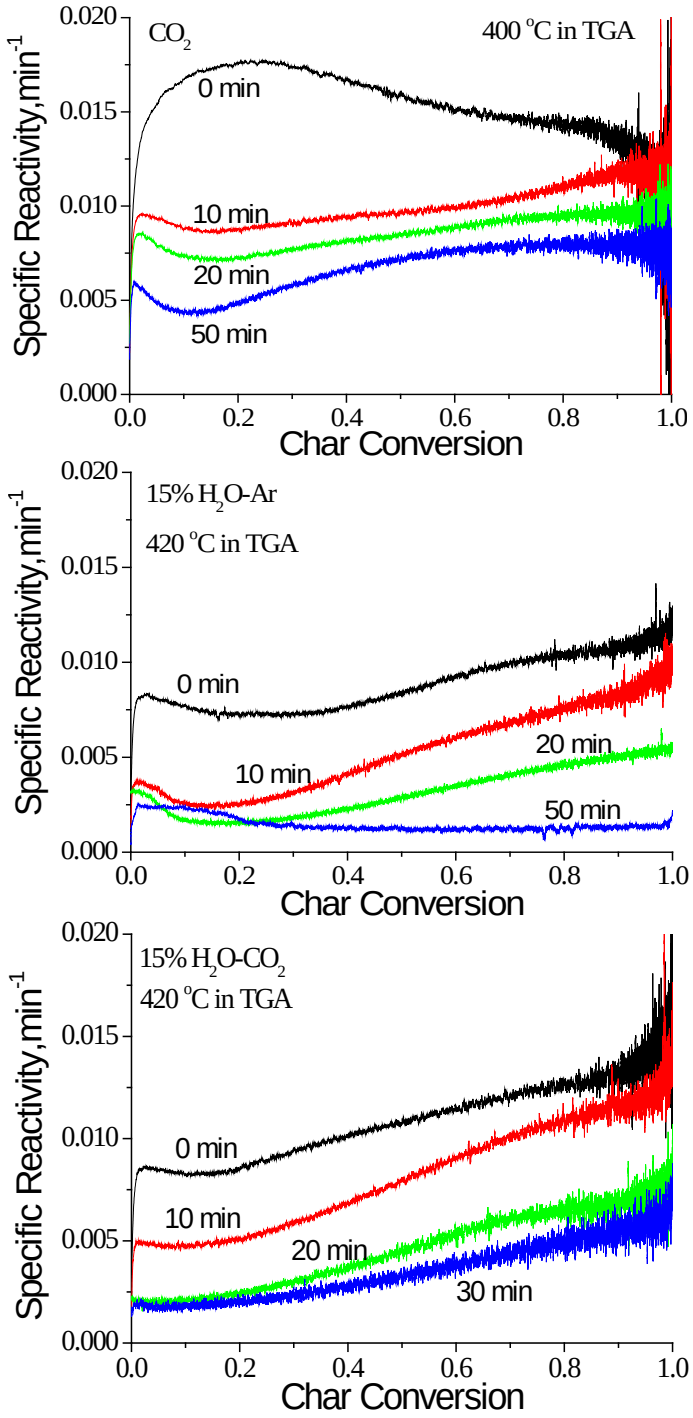

Fig. 5-3 Specific char-O_2 reactivity measured in air in TGA at 400°C/420°C for the chars prepared in pure CO_2, 15% H_2O balanced with Ar and 15% H_2O balanced with CO_2 during the gasification of Collie sub-bituminous coal at 900°C.

In order to further understand the effects of char structure on the changes in char-O_2 reactivity, the small to large ring ratios mentioned in Section 5.3.1 (Fig. 5-1) had to be considered. In each atmosphere, the smaller aromatic rings were consumed preferentially or converted into larger ones with decreasing char yield (i.e. the progress in gasification). These reduction in the small-to-large aromatic ring ratios (Fig. 5-1) coincide with the decreases in the low-temperature char-O_2 reactivity (Fig. 5-3). Furthermore, when there was a big drop in small to large ring ratio from 0 to 10 min holding time in Fig. 5-1, a significant decrease in the char-O_2 reactivity was seen in Fig. 3-3. It is thus fair to state that the chars rich in small aromatic rings would tend to give higher char-O_2 reactivity. With increasing holding time, which means higher gasification conversion level, the char became more condensed and the subsequent char-O_2 reactivity decreased. Among different gasification atmospheres, smaller rings were selectively consumed in the presence of steam. Relative low amounts of smaller rings in the chars produced from steam-containing atmospheres led to lower char-O_2 reactivity.

Effects of AAEM concentrations on char-O_2 reactivity. On examining the char reactivity and the AAEM concentrations in char mentioned in Fig. 5-2, a reverse trend was observed that the overall char-O_2 reactivity decreased while the concentrations of AAEM species increased with increasing holding time in three gasification atmospheres.

In order to further investigate the effects of AAEM species on the char-O_2 reactivity, the specific reactivity of the chars produced in 15% H_2O-Ar is plotted in Fig. 5-4 as a function of Na, Mg, Ca and K concentration in char, respectively. The same char conversion levels of 20%, 40%, 60%, 80% and 90% achieved during the reactivity measurement in TGA are connected with dashed lines for the chars produced with varying gasification holding times at 900°C. As there was no AAEM volatilisation during the reaction of char with O_2 in TGA, the AAEM concentrations in char at any given time was calculated by the initial AAEM concentrations in char and the char conversion level. It is obvious that the trends of the specific reactivity as a function of AAEM species concentration were quite similar, regardless of which element was

used as the x-axis. Similar trends were also observed for the chars obtained in pure CO_2 and 15% H_2O-CO_2. Therefore, the specific reactivity as a function of Na concentration in char was used for further discussion below.

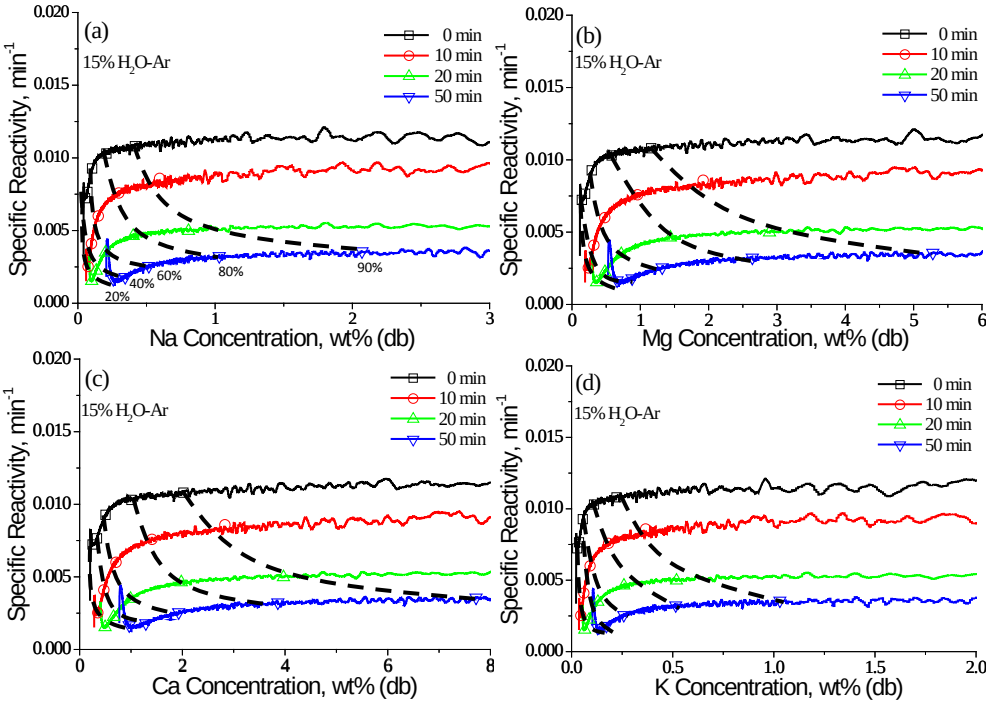

Fig. 5-4 Specific reactivity (measured in air in TGA at 420°C) of char versus the AAEM concentrations in char. The chars were produced in 15% H_2O balanced with Ar during the gasification of Collie sub-bituminous coal at 900°C. The char conversion levels in TGA are labelled with numbers and dashed lines in the figure.

Figure 5-5 displays the specific char-O_2 reactivity of the chars obtained in three gasification atmospheres as a function of Na concentration. The data in Figs. 5-4 and 5-5 indicate that the char-O_2 reactivity does increase, albeit not directly proportional to, with increasing Na concentration in char. This is expected to reflect the catalytic effects of AAEM species in char on the char-O_2 reactivity. Since the coal contained Na, K, Mg and Ca in concentrations of similar magnitudes, the catalytic effects cannot be easily attributed to any specific AAEM species.

For the chars obtained from the gasification in a given gasifying agent but with different gasification times at 900°C, their char-O_2 reactivities did not overlap together

as a single function of Na concentration. In fact, they even showed different trends. For example, the char-O_2 reactivity decreased with increasing Na concentration in char for the char obtained in CO_2 with 0 min holding time, the char-O_2 reactivity showed initial increases and then levelled off for the chars prepared in CO_2 with holding times of 10 min, 20 min and 50 min. Further examination of the data in Fig. 5-5 also indicated that the char-O_2 reactivity versus Na concentration did not fall into the same lines for the chars produced in CO_2, 15% H_2O balanced with Ar or balanced with CO_2 even if the same holding time was used. Similar observations were also made when the char-O_2 reactivity was plotted as a function of K, Mg or Ca concentration in char. All these data clearly indicate that the low-temperature char-O_2 reactivity is not solely determined by the concentration of any AAEM species or all AAEM species combined. Obviously, as was discussed above, the char structure played a crucial role in the char-O_2 reactivity. Indeed, for chars with reactive structure (e.g. the char produced in CO_2 with 0 min holding time in Fig. 5-5a), the preferential consumption of reactive char structures at the beginning of char-O_2 reaction (also corresponding to low Na concentration in Fig. 5-5) dominated the char-O_2 reaction and has resulted in apparent decreases in char-O_2 reactivity with increasing Na concentration.

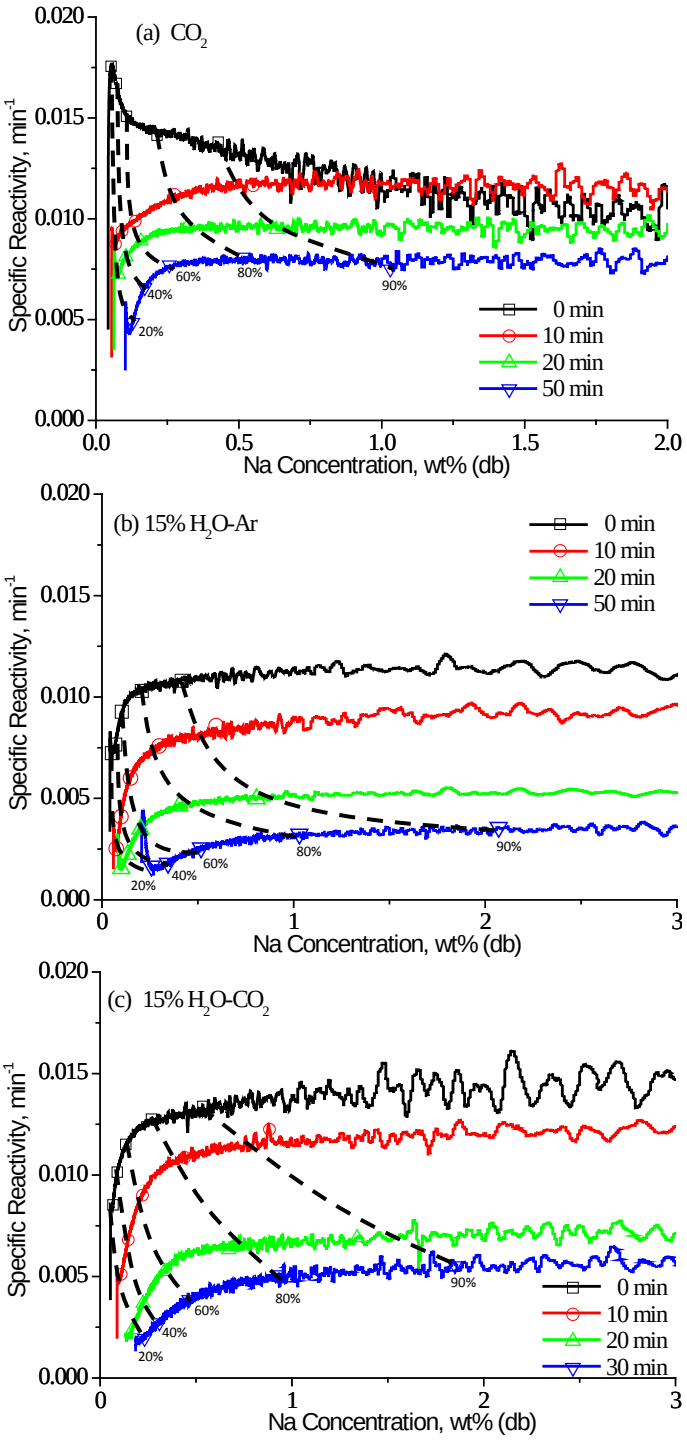

Fig. 5-5 Specific reactivity (measured in air in TGA at 400/420°C) of char versus Na concentration in char. The chars were produced in pure CO_2, 15% H_2O balanced with Ar and 15% H_2O balanced with CO_2 during the gasification of Collie sub-bituminous coal at 900°C. The char conversion levels in TGA are labelled with numbers and dashed lines in the figure.

Our findings on the weaker effects of AAEM species on the char-O_2 reactivity for the Collie sub-bituminous coal differ from our earlier findings [30,35] on the Victorian brown coal. In the cases of Victorian brown coal, direct linear relationships were observed [35] between the char-O_2 reactivity and the concentration of Na in char at least for lower char conversions during the char-O_2 reactions. In this case, the presence of Na catalyst dominated the char-O_2 reactivity. The difference between the sub-bituminous coal and the brown coal stems from the chemical forms of AAEM species in the coal substrates. AAEM species, especially Na, exist in brown coal as ion-exchangeable carboxylates or NaCl salt, which, during the gasification at high temperature (e.g. 900°C in the present study), can transform into active catalysts bonded with the char. On the other hand, a lot less AAEM species in the ion-exchangeable or salt form exist in the sub-bituminous coal, which cannot all be transformed during gasification into the most active form of catalyst to be bonded directly with the char. The chars from the sub-bituminous coal would also be less reactive than those from the brown coal. The weaker catalytic effects of AAEM species and less reactive char structure from the sub-bituminous coal have meant that the AAEM species were not the dominant factor of char-O_2 reactivity even at low char conversion levels during the char-O_2 reaction.

5.4 Conclusions

The gasification of Collie sub-bituminous coal in pure CO_2, 15% H_2O balanced with Ar and 15% H_2O balanced with CO_2 at 900°C produced chars with different chemical structures and concentrations of AAEM species, which in turn influence the intrinsic char-O_2 reactivity at low temperatures (400 or 420°C). The O-containing species in char that can cause resonance effects to give enhanced Raman intensity tend to improve the AAEM species retention in char during the gasification at 900°C. However, these O-containing structures do not necessarily ensue a high char-O_2 reactivity at low temperature. While AAEM species in char would catalyse the char-O_2 reactions, they are not sufficient to determine the char-O_2 reactivity. The relative ratio between small and large rings in char, as reflected by the Raman spectroscopy, greatly influences the char-O_2 reactivity. The sub-bituminous coal used in this study does not behave in the same way as the brown coal used in previous studies in terms of the factors affecting the char-O_2 reactivity.

5.5 References

[1] Li C-Z. Special issue-gasification: a route to clean energy. Process safety and environmental protection 2006;84:407-8.

[2] Li C-Z. Importance of volatile-char interactions during the pyrolysis and gasification of low-rank fuels – A review. Fuel 2013;112:609-23.

[3] Li C-Z. Some recent advances in the understanding of the pyrolysis and gasification behaviour of Victorian brown coal. Fuel 2007;86:1664-83.

[4] Miura K, Hashimoto K, Silveston PL. Factors affecting the reactivity of coal chars during gasification, and indices representing reactivity. Fuel 1989;68:1461-75.

[5] Zhang L, Li T, Quyn DM, Dong L, Qiu P, Li C-Z. Structural transformation of nascent char during the fast pyrolysis of mallee wood and low-rank coals. Fuel Processing Technology 2015;138:390-6.

[6] Zhang L, Shiro K, Satoshi U, Wang S, Quyn DM, Song Y, Li T, Zhang S, Dong L, Li C-Z. Changes in nascent char structure during the gasification of low-rank coals in CO_2. Fuel 2015;158:711-8.

[7] Zhang L, Li T, Quyn DM, Dong L, Qiu P, Li C-Z. Formation of nascent char structure during the fast pyrolysis of mallee wood and low-rank coals. Fuel 2015;150:486-92.

[8] Su S, Song Y, Wang Y, Li T, Hu S, Xiang J, Li C-Z. Effects of CO_2 and heating rate on the characteristics of chars prepared in CO_2 and N_2 atmospheres. Fuel 2015;142:243-9.

[9] Wang S, Li T, Wu L, Zhang L, Dong L, Hu X, Li C-Z. Second-order Raman spectroscopy of char during gasification, Fuel Processing Technology 2015;135:105-11.

[10] Tay HL, Kajitani S, Wang S, Li C-Z. A preliminary Raman spectroscopic perspective for the roles of catalysts during char gasification. Fuel 2014;121:165-72.

[11] Li T, Zhang L, Dong L, Li C-Z. Effects of gasification atmosphere and temperature on char structural evolution during the gasification of Collie sub-bituminous coal. Fuel 2014;117:1990-5.

[12] Tay HL, Kajitani S, Zhang S, Li C-Z. Inhibiting and other effects of hydrogen during gasification: Further insights from FT-Raman spectroscopy. Fuel 2014;116:1-6.
[13] Qi X, Guo X, Xue L, Zheng C. Effect of iron on Shenfu coal char structure and its influence on gasification reactivity. Journal of Analytical and Applied Pyrolysis 2014;110:401-7.
[14] Bai Y, Wang Y, Zhu S, Li F, Xie K. Structural features and gasification reactivity of coal chars formed in Ar and CO_2 atmospheres at elevated pressures. Energy 2014;74:464-70.
[15] Tay HL, Kajitani S, Zhang S, Li C-Z. Effects of gasifying agent on the evolution of char structure during the gasification of Victorian brown coal. Fuel 2013;103:22-8.
[16] Min Z, Zhang S, Yimsiri P, Wang Y, Asadullah M, Li C-Z. Catalytic reforming of tar during gasification. Part IV. Changes in the structure of char in the char-supported iron catalyst during reforming. Fuel 2013;106:858-63.
[17] Zhang S, Min Z, Tay HL, Asadullah M, Li C-Z. Effects of volatile-char interactions on the evolution of char structure during the gasification of Victorian brown coal in steam. Fuel 2011;90:1529-35.
[18] Asadullah M, Zhang S, Min Z, Yimsiri P, Li C-Z. Effects of biomass char structure on its gasification reactivity. Bioresource Technology 2010;101:7935-43.
[19] Tay HL, Li C-Z. Changes in char reactivity and structure during the gasification of a Victorian brown coal: Comparison between gasification in O_2 and CO_2. Fuel Processing Technology 2010;91:800-4.
[20] Keown DM, Li X, Hayashi J-i, Li C-Z. Evolution of biomass char structure during oxidation in O_2 as revealed with FT-Raman spectroscopy. Fuel Processing Technology 2008;89:1429-35.
[21] Keown DM, Hayashi J-i, Li C-Z. Drastic changes in biomass char structure and reactivity upon contact with steam. Fuel 2008;87:1127-32.
[22] Guo X, Tay HL, Zhang S, Li C-Z. Changes in char structure during the gasification of a Victorian brown coal in steam and oxygen at 800 °C. Energy & Fuels 2008;22:4034-8.
[23] Li X, Hayashi J-i, Li C-Z. FT-Raman spectroscopic study of the evolution of char structure during the pyrolysis of a Victorian brown coal. Fuel 2006;85:1700-7.

[24] Li X, Li C-Z. Volatilisation and catalytic effects of alkali and alkaline earth metallic species during the pyrolysis and gasification of Victorian brown coal. Part VIII. Catalysis and changes in char structure during gasification in steam. Fuel 2006;85:1518-25.

[25] Li X, Hayashi J-i, Li C-Z. Volatilisation and catalytic effects of alkali and alkaline earth metallic species during the pyrolysis and gasification of Victorian brown coal. Part VII. Raman spectroscopic study on the changes in char structure during the catalytic gasification in air. Fuel 2006;85:1509-17.

[26] Zhang S, Hayashi J-i, Li C-Z. Volatilisation and catalytic effects of alkali and alkaline earth metallic species during the pyrolysis and gasification of Victorian brown coal. Part IX. Effects of volatile-char interactions on char–H_2O and char–O_2 reactivities. Fuel 2011;90:1655-61.

[27] Keown DM, Hayashi J-i, Li C-Z. Effects of volatile–char interactions on the volatilisation of alkali and alkaline earth metallic species during the pyrolysis of biomass. Feul 2008;87:1187-94.

[28] Keown DM, Favas G, Hayashi J-i, Li C-Z. Volatilisation of alkali and alkaline earth metallic species during the pyrolysis of biomass: differences between sugar cane bagasse and cane trash. Bioresource Technology 2005;96:1570-7.

[29] Li X, Wu H, Hayashi J-i, Li C-Z. Volatilisation and catalytic effects of alkali and alkaline earth metallic species during the pyrolysis and gasification of Victoria brown coal. Part VI. Further investigation into the effects of volatile-char interactions. Fuel 2004;83:1273-9.

[30] Quyn DM, Wu H, Hayashi J-i, Li C-Z. Volatilisation and catalytic effects of alkali and alkaline earth metallic species during the pyrolysis and gasification of Victorian brown coal. Part IV. Catalytic effects of NaCl and ion-exchangeable Na in coal on char reactivity. Fuel 2003;82:587-93.

[31] Li C-Z, Sathe C, Kershaw JR, Pang Y. Fates and roles of alkali and alkaline earth metals during the pyrolysis of a Victorian brown coal. Fuel 2000;79:427-38.

[32] Quyn DM, Wu H, Li C-Z. Volatilisation and catalytic effects of alkali and alkaline earth metallic species during the pyrolysis and gasification of Victorian brown coal. Part I. Volatilisation of Na and Cl from a set of NaCl-loaded samples. Fuel 2002;81:143-9.

[33] Quyn DM, Wu H, Bhattacharya SP, Li C-Z. Volatilisation and catalytic effects of alkali and alkaline earth metallic species during the pyrolysis and gasification of Victorian brown coal. Part II. Effects of chemical form and valence. Fuel 2002;81:151-8.
[34] Quyn DM, Hayashi J-i, Li C-Z. Volatilisation of alkali and alkaline earth metallic species during the gasification of a Victorian brown coal in CO_2. Fuel 2005;86:1241-51.
[35] Zhang S, Hayashi J-i, Li C-Z. Volatilisation and catalytic effects of alkali and alkaline earth metallic species during the pyrolysis and gasification of Victorian brown coal. Part IX. Effects of volatile-char interactions on char–H_2O and char–O_2 reactivities. Fuel 2011;90:1655-61.

Chapter 6

Insights into mechanisms of char-CO_2 and char-H_2O reactions by probing kinetic parameters

6.1 Introduction

Gasification-based technologies have been expected to be one of the promising ways to utilise traditional low-grade fuels, such as low-rank coals, biomass and various solid wastes, owing to their particularly high gasification reactivity [1-2]. Three types of char gasification take place in the typical gasifiers, char-CO_2, char-H_2O and char-O_2 reactions [3]. As the oxygen would be quickly consumed, thereby the reactions between char and CO_2/H_2O are regarded as the rate-limiting steps. Gasification is a complex process, and a better understanding of char-CO_2 and char-H_2O reaction mechanisms may greatly improve the efficiency and performance of gasification-based technologies.

A fierce debate has lasted for long arguing if there is a competition/synergy effect between char-CO_2 and char-H_2O reactions in the gas mixture [4-7], if so whether it is a competition or enhancement effect [3,8-10]. In previous work, the char-CO_2 and char-H_2O reaction pathways during the gasification of Collie sub-bituminous coal have been investigated from the perspective of the changes in char structure using FT-Raman spectroscopy [11]. FT-Raman spectroscopy [1-2, 11-20] is an excellent tool to characterise the evolution of char structure during gasification/pyrolysis. It displays the char structural features from the aspects of the formation of the O-containing structures and the transformation of the aromatic rings in the char. Taking advantage of FT-Raman spectroscopy, the different changes in the formation of O-containing structures and in the ratio of large rings in char-CO_2 and char-H_2O reactions demonstrate the different reaction pathways for two reactions.

Apart from the extensive experimental studies on char-CO_2 and char-H_2O reactions, a lot of kinetic analysis has been done [21-28]. For the heterogeneous gas-solid reaction, the reaction rate constant can be represented by Arrhenius equation [21]. The kinetic parameters, including the apparent activation energy and the apparent pre-exponential factor, can be calculated based on the experimental data. As the composition of char is heterogeneous, the chemical nature and activation energy level of the carbon atoms in

the char are likely to be different [22]. The number of the active sites on the char is changing as gasification proceeded.

In our previous work, the kinetic parameters for the char-O_2 reaction have been determined based on the experimental data to further investigate on the influence of volatile-char interaction on the binding between Na and char [29]. It is found that the changes in the Na catalyst dispersion should be caused by the condensation of ring structures, based on the data of the apparent activation energy for the char measured at varying conversion level. However, due to the lack of a suitable tool to characterise the structural features of the highly disordered char at any conversion level, the effects of char structure on the changes in the activation energy and the pre-exponential factor in the progress of gasification is still unclear.

This study focuses on gaining insights into the char-CO_2 and char-H_2O reaction mechanisms by investigating the kinetic parameters in conjunction with the char structural evolution as reflected by FT-Raman spectroscopy. Owing to the utilisation of FT-Raman spectroscopy, the transformation of char structure can be determined at different gasification conversion levels. The results show that the condensation of char structure due to the selective consumption of small rings would increase the kinetic parameters; the formation of O-containing structures would decrease the kinetic parameters.

6.2 Experimental

6.2.1 Coal sample preparation and gasification

Collie sub-bituminous coal [C, 75.7 wt%; H, 4.5 wt%; N, 1.4 wt%; S, 0.5 wt% (daf) with an ash yield 5.7 wt% (db), see Ref. 11] from Western Australia was used in this study. The coal sample was firstly dried in the open air followed by sampling and grinding. It was then sieved into the required particle size range of 106-150 μm and was well mixed. A fluidised-bed/fixed-bed reactor was used to conduct the gasification of Collie sub-bituminous coal at 800, 850 and 900 °C [11]. Pure CO_2

(99.999% purity), 15% H_2O balanced with Ar (99.999% purity) and a mixture of 15% H_2O and CO_2 (balancing gas) were used as the gasifying agents.

6.2.2 Characterisation of char structure

The structural features of the chars at different conversion levels have been characterised by FT-Raman spectroscopy [11]. Two important parameters, the oxygenation of the char and the changes in aromatic ring systems in the char, were used herein for comparison purposes.

6.2.3 Char conversion and char gasification reactivity

Based on the experimental data that were reported in Ref. 11, the Microcal Origin software was used to interpolate the trend line of char yield at each temperature/in each atmosphere. The weight loss versus holding time thus can be calculated based on the trend lines of char yield and the assumption of 1.5 gram (db) coal that delivered into the reactor. The char conversion (daf) versus holding time can be calculated by Equation 6-1 (Eq. 6-1):

$$x = \frac{W_0 - W_t}{W_0 - W_a} \qquad (6-1)$$

W_0 is the initial coal weight (db, dry basis) fed into the reactor, W_t is the char weight (db) at any given time t and W_a is the ash weight (db).

As the coal/char experienced fast pyrolysis/gasification and volatile-char interactions during feeding period, the char yield at 0 min holding time was different for the chars prepared in different atmospheres at different temperatures. In order to compare the char gasification reactivity at the same coal conversion level, it is necessary to convert the char conversion into the coal conversion versus holding time for the determination of kinetic parameters.

The char gasification reactivity at any carbon conversion level *x*, r_x, is calculated as a differential of the coal conversion versus time, using Eq. 6-2:

$$r_x = \frac{dx}{dt} = -\frac{1}{W_0 - W_a}\frac{dW_t}{dt} \qquad (6-2)$$

For a heterogeneous gas-solid reaction, such as char gasification, the reaction equation can be expressed in Eq. 6-3 [21]:

$$r_x = k(P_g, T)f(x) \qquad (6-3)$$

k is the rate constant at temperature *T* and under partial pressure in the gas phase P_g. *f(x)* contains the information of the changes in the char properties at any coal conversion level *x*. As the concentrations of the gasifying agents in this study were fixed, the partial pressure in the gas phase remained invariable. Thus, the kinetic rate constant can be expressed as a function of the temperature based on the Arrhenius equation [29]:

$$k(T) = Aexp\left(-\frac{E}{RT}\right) \qquad (6-4)$$

Hence the reaction rate of char gasification r_x can be expressed and simplified as [30]:

$$r_x = Aexp\left(-\frac{E}{RT}\right)f(x) = A_{app}\,exp\left(-\frac{E_{app}}{RT}\right) \qquad (6-5)$$

The apparent pre-exponential factor A_{app} contains the conversion-dependent factors that can influence the char gasification rate, such as the amount of active sites and the changes in char structure. E_{app} is the apparent activation energy. *R* is the ideal gas constant and *T* is the absolute temperature. Taking logarithm of both sides of Eq. 6-5 results in Eq. 6-6:

$$ln(r_x) = -\frac{E_{app}}{RT} + ln(A_{app}) \qquad (6-6)$$

Once the results of $ln(r_x)$ are plotted versus $1/T$, the apparent activation energy E_{app} and the apparent pre-exponential factor A_{app} can be determined from the gradient and y-intercept of the trend lines.

6.3 Results and discussion

6.3.1 Coal conversion

Figure 6-1 shows the coal conversion (on dry and ash free basis) versus holding time in different gasification atmospheres, including the experimental data (symbols) and curve-fitting lines (dash lines). The gasification temperatures were selected at 800, 850 and 900°C. The chars were partially gasified up to around 99% (daf). During the period of coal feeding (about 20 min), the coal firstly experienced rapid devolitilisation and then gasified with the gasifying agent(s). Owing to the different gasification temperature, at the starting point of holding (0 min) in each gasification atmosphere, the coal conversion level was different. As expected, the coal conversion level (as shown at 0 min) during feeding was higher and the subsequent conversion rate during holding became faster as gasification temperature increased. In order to make the char gasification reactivities at different temperatures comparable (at the same coal conversion level), the reactivities at 60% coal conversion for CO_2, 65% for 15% H_2O-Ar and 75% for 15% H_2O-CO_2 were selected as the starting comparison points.

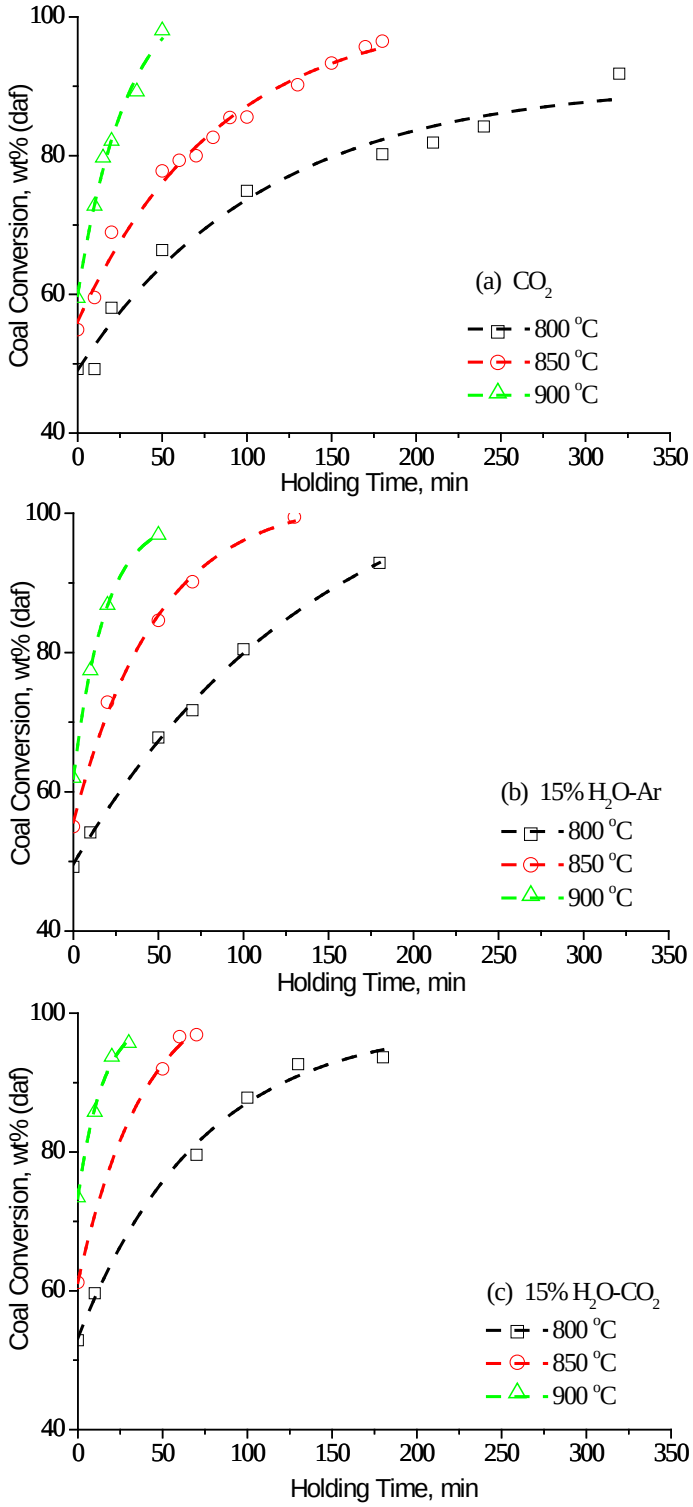

Fig. 6-1 Coal conversion (daf) versus holding time in (a) CO_2, (b) 15% H_2O balanced with Ar and (c) 15% H_2O balanced with CO_2 at 800, 850 and 900°C during the gasification of Collie sub-bituminous coal in a fluidised-bed/fixed-bed reactor. (The experimental data are replotted based on the data in Ref. 11)

6.3.2 Isokinetic temperature

The logarithm of char gasification reactivity r_x versus reciprocal of absolute temperature in three gasification atmospheres is displayed in Fig. 6-2. The values of the char gasification reactivity at different coal conversion levels ranging from 60% to 90% (daf) were calculated by Eq. 6-2 and marked with different symbols in Fig. 6-2. The straight Arrhenius lines demonstrate that Eq. 6-5 is a good approximation of the char gasification reactivity. According to the slopes and the y-intersects, the values of the apparent activation energy E_{app} and the apparent pre-exponential factor A_{app} at different conversion levels during gasification in three gasification atmospheres can be determined and will be further discussed in later section.

As shown in Fig. 6-2a and b, all the Arrhenius plots meeting in one point corresponding to 1130 K and 1160 K for gasification in pure CO_2 and 15% H_2O-Ar respectively. This is traditionally termed as isokinetic temperature, which means that at this point the rates of the reaction are the same. In Fig. 6-2a, for the gasification in pure CO_2, the char gasification reactivity decreased as gasification proceeded (higher conversion level) when the gasification temperature is lower than the isokinetic temperature, while the gasification reactivity increased with increasing conversion level when the gasification temperature is higher than the isokinetic temperature. Fig. 6-2b shows a different trend of the reaction rates versus coal conversion level for the gasification in 15% H_2O-Ar. For the gasification in 15% H_2O-CO_2 (shown in Fig. 6-2c), the Arrhenius plots for different coal conversion level paralleled (almost overlapped) to each other, no obvious isokinetic temperature can be found that lies between the isokinetic temperatures for the gasification in pure CO_2 or 15% H_2O-Ar. It can be concluded that one type of reaction took place in pure CO_2 or 15% H_2O-Ar, yet two different types of reactions took place in 15% H_2O-CO_2 during the gasification of sub-bituminous coal.

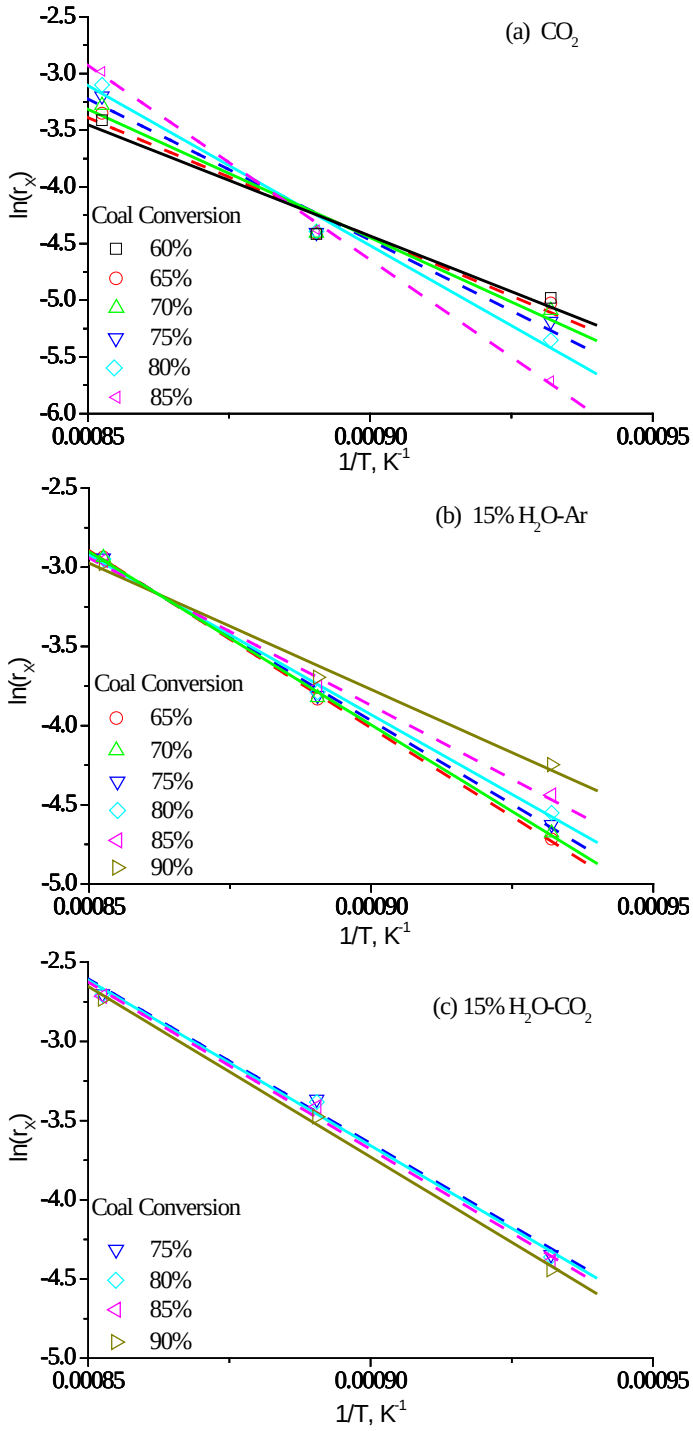

Fig. 6-2 Logarithm of char gasification reactivity as a function of reciprocal of absolute stemperature with different coal conversions (daf) for gasification in (a) pure CO_2, (b) 15% H_2O balanced with Ar and (c) 15% H_2O balanced with CO_2.

6.3.3 Changes in *Eapp* and *Aapp* during gasification

In Fig. 6-3, (a) the apparent activation energy and (b) the logarithm of apparent pre-exponential factor were plotted versus coal conversion level for the chars obtained in three gasification atmospheres. The values of the kinetic parameters were calculated from Fig. 6-2. As is shown in Figs. 6-3a and 6-3b, the apparent activation energy and pre-exponential factor both increased with increasing conversion level for the gasification in pure CO_2. In the gasification in 15% H_2O-Ar, both of the kinetic parameters decreased with increasing conversion level. While for the gasification in the gas mixture of CO_2 and H_2O, both kinetic parameters remained almost constant as gasification proceeded. This simultaneous change in the apparent activation energy and the apparent pre-exponential factor exhibit the so-called kinetic compensation effect [30].

A linear plot between the two kinetic parameters in each atmosphere is shown in Fig. 6-4a. Since the value range of the apparent activation energy for the chars obtained in 15% H_2O balanced with CO_2 is relatively narrow, an enlarged drawing is presented in Fig. 6-4b, showing a good linear plot as well. The kinetic compensation effect has been reported for the gasification in CO_2 and H_2O in previous studies [23,30]. In this study, it will be discussed in conjunction with the char structural evolution as gasification proceeded.

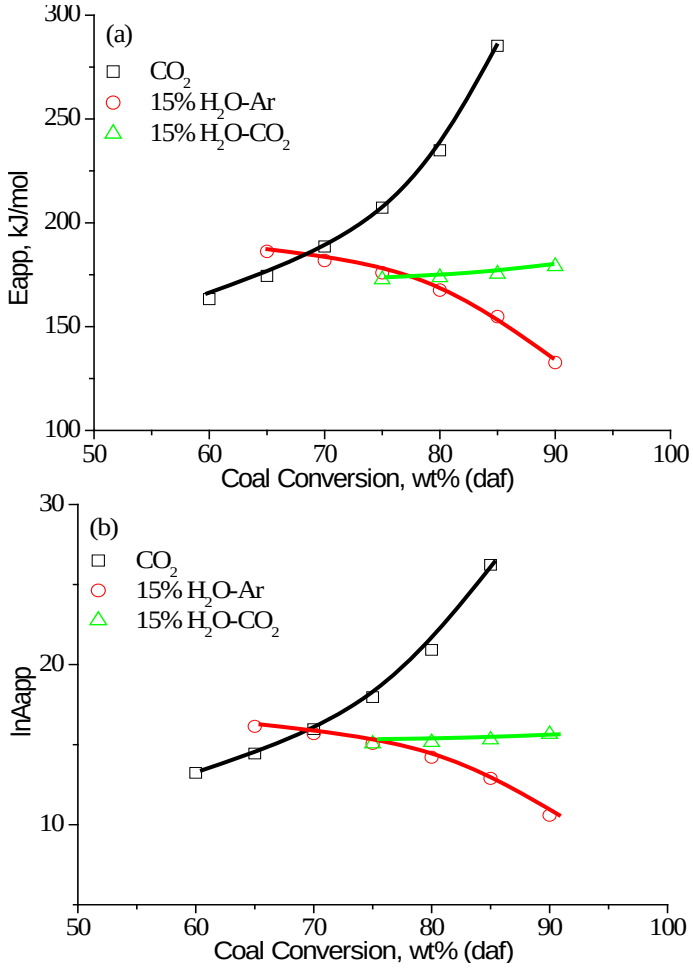

Fig. 6-3 The (a) activation energy and (b) logarithm of pre-exponential factor versus of coal conversion (daf) in pure CO_2, 15% H_2O-Ar and 15% H_2O-CO_2 during the gasification of Collie sub-bituminous coal.

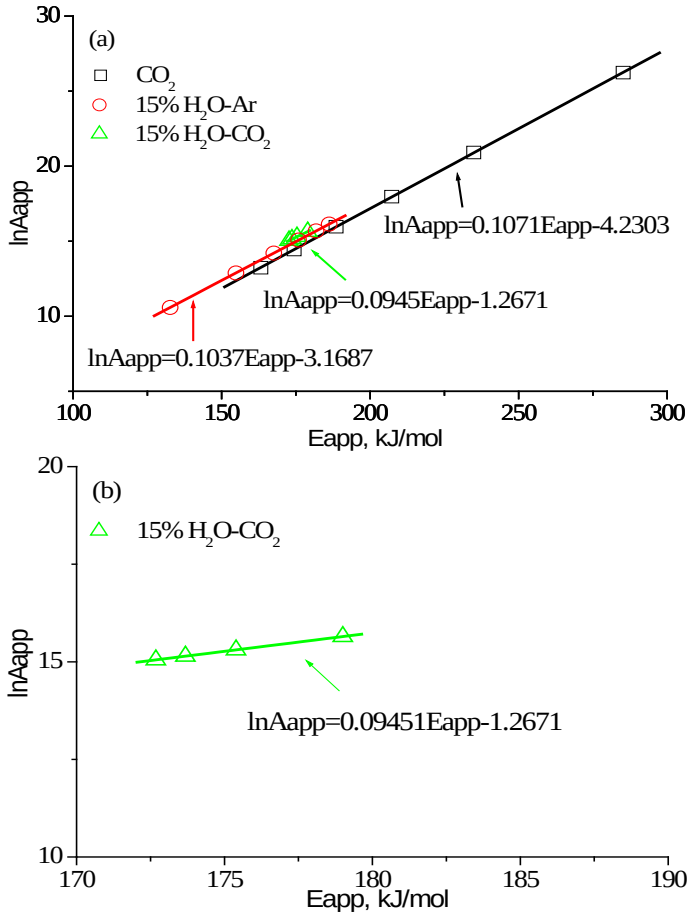

Fig. 6-4 Logarithm of pre-exponential factor versus activation energy for the gasification of Collie sub-bituminous coal (a) in CO_2, 15% H_2O balanced with Ar and 15% H_2O balanced with CO_2 and (b) expansion of the plot for 15% H_2O-CO_2.

6.3.4 Effects of the char oxygenation on the changes in kinetic parameters

In Fig. 6-5, (a) the apparent activation energy and (b) the apparent pre-exponential factor are plotted versus total Raman area for the chars produced in three atmospheres. The peak intensity between 800 and 1800 cm^{-1} of the Raman spectrum is integrated and taken as total Raman area [12]. In Ref. 11, the total Raman area increased significantly with increasing gasification conversion level in 15% H_2O balanced with Ar and balanced with CO_2, due to the formation of O-containing structures. While the total Raman area remained almost unchanged in pure CO_2, indicating a dynamic balance between the formation and decomposition of O-containing structures. As indicated by the arrow direction, the coal conversion processed from lower to higher value of the total Raman area.

Clearly in Figs. 6-5a and 6-5b, with increasing O-containing species formed in the char, the apparent activation energy and the pre-exponential factor both decreased greatly for the gasification in 15% H_2O-Ar and remained almost constant in the gas mixture of CO_2 and H_2O. While for the gasification in pure CO_2, as the total Raman area changed little during gasification, the results are within experimental error. Therefore, no conclusion can be drawn between the kinetic parameters and the total Raman area in pure CO_2.

During gasification in 15% H_2O-Ar, H_2O would dissociate on the char to form intermediates, such as H and OH [31-32]. Once a ring system is broken, the oxygen derived from H_2O would oxygenate the aromatic ring system and the H radicals would stabilise the broken structure and make it less reactive. With the addition of O-containing structures, the aromatic ring system became more reactive, leading to decrease the apparent activation energy. It is in agreement with previous work [33] that the Raman-sensitive O-containing structures are the same as the O-containing structures that are responsible for boosting the char gasification reaction rate [33]. With the stabilisation effect of H radicals, less carbon atoms would be activated at the position where the O-containing structure formed with increasing conversion level,

indicating a decreasing trend of the apparent pre-exponential factor as gasification proceeded in 15% H_2O-Ar.

During gasification in 15% H_2O-CO_2, it is known that CO_2 and H_2O partly compete for some active sites on the char [11]. Taking the nearly constant values of the apparent activation energy and the apparent pre-exponential factor and the significant increasing trend of O-containing structures in 15% H_2O-CO_2, these data indicate that there might be some other factors influencing the gasification reactivity other than the O-containing structures formed in the char.

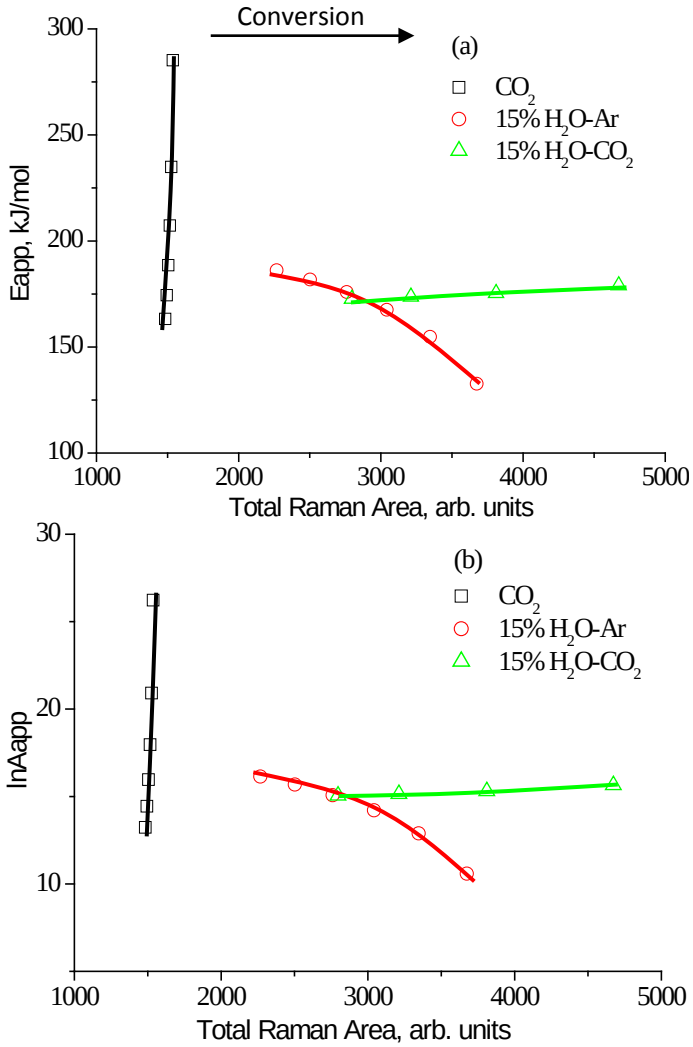

Fig. 6-5 The (a) activation energy and (b) logarithm of pre-exponential factor versus total Raman area for the gasification of Collie sub-bituminous coal in CO_2, 15% H_2O balanced with Ar and 15% H_2O balanced with CO_2. (The total Raman area is plotted based on the data in Ref. [11])

6.3.5 Effects of the relative ratio of small to large rings on the changes in kinetic parameters

Figure 6-6 displays (a) the apparent activation energy and (b) the apparent pre-exponential factor as a function of $I_{(Gr+Vl+Vr)}/I_D$, which represents the relative amount of small (<6 rings) to large (not less than six rings) aromatic rings in the char. As mentioned in Ref. 11, the band area ratio between small and large rings reduced with progress of gasification in all three atmospheres, which means the small rings were preferentially consumed/converted into larger ones. The ratio is relatively lower in 15% H_2O balanced with Ar/CO_2 than that in pure CO_2, which means the smaller rings were more selectively consumed in the presence of H_2O [34]. As indicated by the arrow direction, the coal conversion processed from higher to lower value of the relative ratio.

As shown in Figs. 6-6a and 6-6b, the apparent activation energy and the apparent pre-exponential factor increased with increasing aromatic ring size for the gasification in pure CO_2. For the gasification in 15% H_2O-Ar, the kinetic parameters decreased with increasing aromatic ring size. Both kinetic parameters remained unchanged in the gasification in 15% H_2O-CO_2.

As coal char is heterogeneous material, the activation energy level should be different for different part of active sites. It is assumed that for the gasification in CO_2, the active sites that have lower activation energy values are likely to be on the smaller aromatic rings. While the active sites on the larger aromatic rings tend to have relative higher activation energy values. With increasing conversion level, the chars became more condensed and the activation energy increased as well. However, for the highly condensed char, once one carbon site was activated, a lot of carbon atoms existed on the aromatic ring clusters would be activated, resulting in a larger pre-exponential factor [30].

For the gasification in 15% H_2O-Ar, although the ring size was relatively larger than the chars obtained from CO_2 (indicating by the lower ratio) and the ring condensation

took place during gasification as well, the significant amount of O-containing species formed in the char has greatly changed the char structure, and in turn influence the changes in the apparent activation energy and the apparent pre-exponential factor.

As the apparent activation energy and the pre-exponential factor is a sum of the activation energies and pre-exponential factors for different active sites on the char, and two types of reactions took place in 15% H_2O-CO_2 (mentioned in the discussion for Fig. 6-2), these data indicate that the almost constant kinetic parameters are probably due to the opposite effects from pure CO_2 and 15% H_2O-Ar.

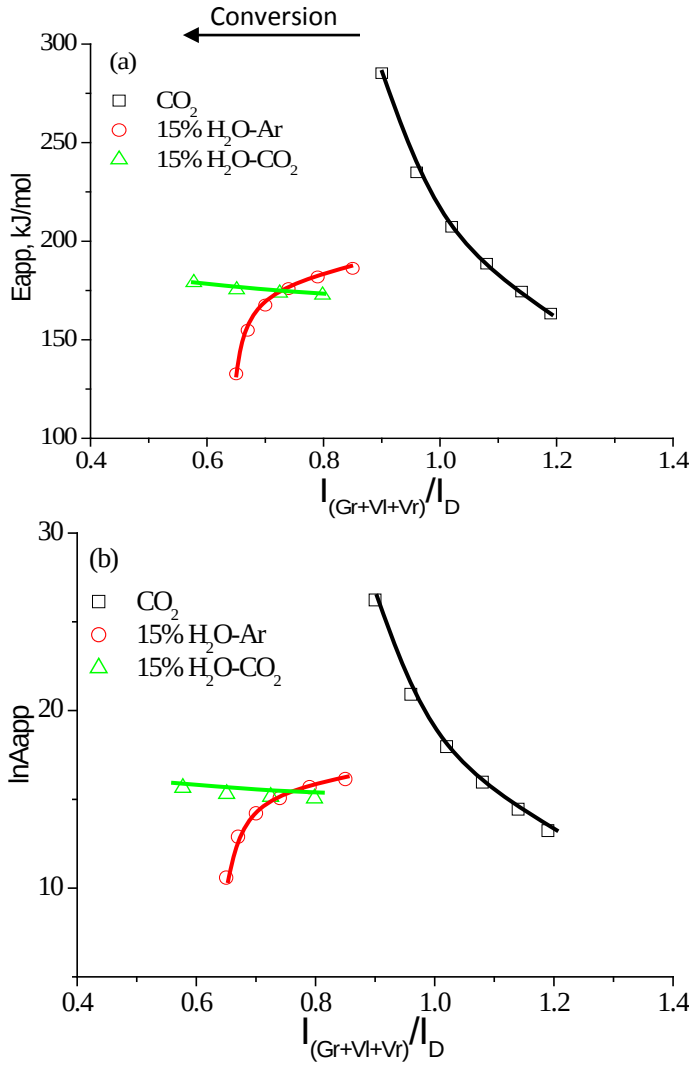

Fig. 6-6 The (a) activation energy and (b) logarithm of pre-exponential factor versus (Gr+Vl+Vr)/D for the gasification of Collie sub-bituminous coal in CO_2, 15% H_2O balanced with Ar and 15% H_2O balanced with CO_2. (The ratio between small and large rings is plotted based on the data in Ref. [11])

6.4 Conclusions

A compensation effect between the apparent activation energy and the apparent pre-exponential factor was observed, yet with entirely different trends, among pure CO_2, 15% H_2O balanced with Ar and 15% H_2O balanced with CO_2. These data confirm the different reaction pathways between char-CO_2 and char-H_2O reactions [11]. With the selective consumption of small rings, the aromatic ring systems become more condensed, leading to increasing apparent activation energy and apparent pre-exponential factor, such as in the gasification in pure CO_2. If accompanied with the aromatic ring systems condensation, significant amount of O-containing species formed in the char would decrease the kinetic parameters, such as the gasification in 15% H_2O-Ar. The opposite effects on the kinetic parameters from pure CO_2 and 15% H_2O-Ar lead to the almost constant kinetic parameters in 15% H_2O-CO_2.

6.5 References

[1] Li C-Z. Some recent advances in the understanding of the pyrolysis and gasification behaviour of Victorian brown coal. Fuel 2007;86:1664-83.

[2] Li C-Z. Importance of volatile-char interactions during the pyrolysis and gasification of low-rank fuels – A review. Fuel 2013;112:609-23.

[3] Umemoto S, Kajitani S, Hara S. Modelling of coal char gasification in coexistence of CO_2 and H_2O considering sharing of active sites. Fuel 2013;103:14-21.

[4] Blackwood JD, Ingeme AJ. The reaction of carbon with carbon dioxide at high pressure. Australian Journal of Chemistry 1960;13:194-9.

[5] Gadsby J, Long FJ, Sleightholm P, Sykes KW. The mechanism of the carbon dioxide-carbon reaction. Proceedings of the Royal Society of London. Series A, Mathematical and Physical Sciences 1948;193:357-76.

[6] Long FJ, Sykes KW. The mechanism of the steam-carbon reaction. Proceedings of the Royal Society of London. Series A, Mathematical and Physical Sciences 1948;193:377-99.

[7] Hermann G, Hüttinger KJ. Mechanism of water vapour gasification of carbon—a new model. Carbon 1986;24:705-13.

[8] Tay HL, Kajitani S, Zhang S, Li C-Z. Effects of gasifying agent on the evolution of char structure during the gasification of Victorian brown coal. Fuel 2013;103:22-8.

[9] Nilsson S, Gomez-Barea A, Ollero P. Gasification of char from dried sewage sludge in fluidized bed: Reaction rate in mixtures of CO_2 and H_2O. Fuel 2013;105:764-8.

[10] Roberts DG, Harris DJ. Char gasification in mixtures of CO_2 and H_2O: Competition and inhibition. Fuel 2007;86:2672-8.

[11] Li T, Zhang L, Dong L, Li C-Z. Effects of gasification atmosphere and temperature on char structural evolution during the gasification of Collie sub-bituminous coal. Fuel 2014;117:1190-5.

[12] Li X, Hayashi Ji, Li C-Z. FT-Raman spectroscopic study of the evolution of char structure during the pyrolysis of a Victorian brown coal. Fuel 2006;85:1700-7.

[13] Tay HL, Li C-Z. Changes in char reactivity and structure during the gasification

of a Victorian brown coal: Comparison between gasification in O_2 and CO_2. Fuel Processing Technology 2010;91:800-4.

[14] Asadullah M, Zhang S, Min Z, Yimsiri P, Li C-Z. Effects of biomass char structure on its gasification reactivity. Bioresource Technology 2010;101:7935-43.

[15] Zhang S, Min Z, Tay H, Asadullah M, Li C-Z. Effects of volatile-char interactions on the evolution of char structure during the gasification of Victorian brown coal in steam. Fuel 2011;90:1529-35.

[16] Bai Y, Wang Y, Zhu S, Li F, Xie K. Structural features and gasification reactivity of coal chars formed in Ar and CO_2 atmospheres at elevated pressures. Energy 2014;74:464-70.

[17] Wang S, Li T, Wu L, Zhang L, Dong L, Hu X, Li C-Z. Second-order Raman spectroscopy of char during gasification, Fuel Processing Technology 2015;135:105-11.

[18] Zhang L, Li T, Quyn DM, Dong L, Qiu P, Li C-Z. Formation of nascent char structure during the fast pyrolysis of mallee wood and low-rank coals. Fuel 2015;150:486-92.

[19] Zhang L, Kajitani S, Umemoto S, Wang S, Quyn DM, Song Y, Li T, Zhang S, Dong L, Li C-Z. Changes in nascent char structure during the gasification of low-rank coals in CO_2. Fuel 2015;158:711-8.

[20] Zhang L, Li T, Quyn DM, Dong L, Qiu P, Li C-Z. Structural transformation of nascent char during the fast pyrolysis of mallee wood and low-rank coals. Fuel Processing Technology 2015;138:390-6.

[21] Skodras G, Nenes G, Zafeiriou G. Low rank coal-CO_2 gasification: Experimental study, analysis of the kinetic parameters by Weibull distribution and compensation effect. Applied Thermal Engineering 2015;74:111-8.

[22] Kandasamy Jayaraman, Iskender Gokalp, Elisa Bonifaci, Nazim Merlo. Kinetics of steam and CO_2 gasification of high ash coal-char produced under various heating rates. Fuel 2015;154:370-9.

[23] Seo DK, Lee SK, Kang MW, Hwang J, Yu TU. Gasification reactivity of biomass chars with CO_2. Biomass Bioenergy 2010;34:1946-53.

[24] Kajitani S, Tay HL, Zhang S, Li C-Z. Mechanisms and kinetic modelling of

steam gasification of brown coal in the presence of volatile-char interactions. Fuel 2013;103:7-13.

[25] Gomez A, Mahinpey N. Kinetic study of coal steam and CO_2 gasification: A new method to reduce interparticle diffusion. Fuel 2015;148:160-7.

[26] Jayaraman K, Gokalp I, Bonifaci E, Merlo N. Kinetics of steam and CO_2 gasification of high ash coal-char produced under various heating rates. Fuel 2015;154:370-9.

[27] Wu X, Tang J, Wang J. A new active site/intermediate kinetic model for K_2CO_3-catalyzed steam gasification of ash-free coal char. Fuel 2016;165:59-67.

[28] Tanner J, Bhattacharya S. Kinetics of CO_2 and steam gasification of Victorian brown coal chars. Chemical Engineering Journal 2016;285:331-40.

[29] Wu H, Li X, Hayashi Ji, Chiba T, Li C-Z. Effects of volatile-char interactions on the reactivity of chars from NaCl-loaded Loy Yang brown coal. Fuel 2005;84:1221-8.

[30] Dhupe AP, Gokarn AN, Doraiswamy LK. Investigations into the compensation effect at catalytic gasification of active charcoal by carbon dioxide. Fuel 1991;70:839-44.

[31] Gadsby J, Long FJ, Sleightholm P, Sykes KW. The mechanism of the carbon dioxide-carbon reaction. Proceedings of the Royal Society of London. Series A, Mathematical and Physical Sciences 1948;193:357-76.

[32] Long FJ, Sykes KW. The mechanism of the steam-carbon reaction. Proceedings of the Royal Society of London. Series A, Mathematical and Physical Sciences 1948;193:377-99.

[33] Tay HL, Kajitani S, Wang S, Li C-Z. A preliminary Raman spectroscopic perspective for the roles of catalysts during char gasification. Fuel 2014;121:165-72.

[34] Li X, Li C-Z. Volatilisation and catalytic effects of alkali and alkaline earth metallic species during the pyrolysis and gasification of Victorian brown coal. Part VIII. Catalysis and changes in char structure during gasification in steam. Fuel 2006;85:1518-25.

Every reasonable effort has been made to acknowledge the owners of copyright material. I would be pleased to hear from any copyright owner who has been omitted or incorrectly acknowledged.

Chapter 7

Conclusions and Recommendations for Future Work

7.1 Introduction

The purpose of this study was to gain fundamental knowledge about the effects of gasification atmosphere and temperature on the evolution of char structure and its reactivity during the gasification of Loy Yang brown coal and Collie sub-bituminous coal. Moreover, the measurements of the AAEM retention in char and the kinetic parameters provide further insights into the gasification mechanisms. The main conclusions of each chapter of this thesis are summarised in the following sections.

7.2 Conclusions

7.2.1 Effects of gasification temperature on char structural evolution and AAEM retention during the gasification of Loy Yang brown coal

1. The gasification rate in the gas mixture of CO_2 and steam is quicker than that in either individual gasification atmosphere, but slower than the sum of the two, indicating the existence of competition between char-CO_2 and char-H_2O reactions.

2. Increasing total Raman area with increasing gasification temperature caused by the formation of O-containing structures in char is responsible for the increases in gasification rate in CO_2, which provide further evidence to previous findings. However, while the char was continuously oxygenated in steam-containing atmospheres, the formation of O-containing structures in char does not appear to be the only factor determining the gasification rate in H_2O-containing atmospheres.

3. In the gas mixture of CO_2 and steam, steam acts as a dominating role in the char structural evolution during gasification at 800°C, reflected by similar total Raman areas and ratios between small and large rings of the chars produced from 15% balanced with Ar/CO_2. However, CO_2 plays an increasingly more important role with increasing temperature between 800 and 900°C, reflected by the approaching

ratio between small and large rings for the char produced in the gas mixture to that for the char produced in pure CO_2.

7.2.2 Changes in char structure during low-temperature pyrolysis in N_2 and gasification in air of Loy Yang brown coal char

1. The structure of the original char obtained at high temperature determines the exact reaction pathway for the small/large aromatic ring systems during the pyrolysis and gasification in air at low temperature. For instance, three chars obtained from the partial gasification in 15% H_2O-CO_2 at 850°C, of which the relative amounts of small and large aromatic rings were different, followed different reaction pathways in low-temperature pyrolysis in N_2 and gasification in air. Furthermore, comparing the char structural evolution of the gasified char used in this study with those of the nascent char and pyrolysed char from previous studies in our group, it is noticed that the reaction pathways in the gasification in air for the small/large aromatic ring systems in char showed completely different trends.

2. The char structure is very unstable after the partial gasification in the mixture of 15% H_2O and CO_2 at 850°C. Before reaching gasification temperature in air, the gasified char was heated up in N_2. The decreases in the total Raman area and the increases in the ratio of small to large rings revealed the loss of the O-containing structures and the breakage of aromatic rings during pyrolysis at low temperature.

3. In comparison with the mixture of CO_2 and steam at high temperature, the oxygen at low temperature is more effective in the oxygenation of the char, reflected by the relatively higher total Raman area at the final conversion in air than that at the starting point.

4. The oxygen was more easily introduced into the char with less condensed structure than into the more condensed one in air. With increasing holding time in 15% H_2O-CO_2 at 850°C, from 0 min to 10 or 15 min holding time, the char structure

became more condensed as reflected by the decreasing ratio between small and large rings. The increases in the total Raman area of the 0 min char were more significant than those of the 10 min char and 15 min char during the gasification in air.

7.2.3 Effects of gasification atmosphere and temperature on char structural evolution during the gasification of Collie sub-bituminous coal

1. The lower char conversion during the gasification in the mixture of CO_2 and H_2O than the sum of the individual char conversion in pure CO_2 and 15% H_2O-Ar reveals that the reactions of char-CO_2 and char-H_2O are not independent during gasification. CO_2 and H_2O compete for active sites on the char.

2. The structural features of the char obtained in pure CO_2 behaved much differently from the chars produced from H_2O-containing atmospheres. H_2O plays a dominating role in the evolution of char structure during the gasification of Collie sub-bituminous coal between 800 and 900°C. In the presence of H_2O, a significant increase of total Raman area was observed due to the formation of O-containing functional groups as gasification proceeded. Small aromatic ring systems were selectively consumed in H_2O-containing atmospheres, resulting in a much lower ratio between small and large rings left in the char.

3. The same decreasing trend line of band area ratio for the chars obtained in the same atmosphere at temperature between 800 and 900°C indicating that the char-CO_2 and char-H_2O reaction pathways remain unchanged within the temperature range of 800 to 900°C.

7.2.4 Effects of char structure and AAEM retention in char during the gasification at 900°C on the changes in low-temperature char-O_2 reactivity for Collie sub-bituminous coal

1. The O-containing structures in char formed during the gasification at 900°C tend to improve the retention of AAEM species in char. The AAEM species in char left after the gasification at 900°C is relatively low in the chars produced from the gasification in pure CO_2 than those from H_2O-containing atmospheres. Meanwhile, the increases in the concentration of O-containing structures were significant in H_2O-containing atmospheres and almost constant in pure CO_2.

2. In the measurement of char-O_2 specific reactivity at low temperature, the magnitude of the reactivity for the char obtained from H_2O-containing atmospheres was lower than that from pure CO_2. These data reveal that the O-containing structures formed in the char in the presence of H_2O at 900°C do not ensue a high char-O_2 reactivity at low temperature. The retention of AAEM species in char would catalyse the char-O_2 reactions, but not the main factor to determine the char-O_2 reactivity.

3. Taking the char-O_2 reactivities among the chars from three atmospheres together with the decreasing reactivity accompanied by decreasing ratio of small to large aromatic ring systems of each char sample, it is concluded that the relative ratio between small and large aromatic ring systems in char greatly influences the char-O_2 reactivity. The more amounts of smaller aromatic ring systems in char left after gasification at 900°C leads to a higher char-O_2 reactivity at low temperature.

7.2.5 Insights into mechanisms of char-CO_2 and char-H_2O reactions by probing kinetic parameters

1. A kinetic compensation effect between the apparent activation energy and pre-exponential factor was observed, yet with entirely different trends, among the gasification of Collie sub-bituminous coal in pure CO_2, 15% H_2O-Ar and 15%

H_2O-CO_2. The changes in the kinetic parameters with atmosphere confirm the different reaction pathways between char-CO_2 and char-H_2O reactions in Chapter 4.

2. As gasification proceeded, the aromatic ring systems became more condensed, due to the preferentially consumption of small aromatic ring systems in all atmospheres. The condensation of aromatic ring systems leads to increasing apparent activation energy and pre-exponential factor for the gasification in pure CO_2. Accompanied with the formation of significant amounts of O-containing structures in char, these kinetic parameters tend to decrease with increasing char conversion level during the gasification of Collie sub-bituminous coal in 15% H_2O-Ar. The opposite effects of the char structure on the kinetic parameters in pure CO_2 and 15% H_2O-Ar leads to an unchanged apparent activation energy and pre-exponential factor during the gasification in 15% H_2O-CO_2.

7.2.6. General concluding remarks

In general, achieving high char reactivity is essential for improving the overall gasification efficiency. As the char structure is paramount factor in determining the char reactivity, this study mainly focuses on the char structural evolution during gasification of two low-rank coals. With the development of FT-Raman spectroscopy in our group, the char structural changes can be characterised semi-quantitatively.

Firstly, looking at the relative ratio between small and large rings in char, the reaction pathway in a given gasification atmosphere remain unchanged within temperature ranging from 800 to 900°C for both Loy Yang brown coal and Collie sub-bituminous coal.

Secondly, competitions on the char exist between CO_2 and steam for both Loy Yang brown coal and Collie sub-bituminous coal and the relative importance of CO_2 and steam is different for the two coals. For the sub-bituminous coal, the changes in the total Raman area and the ratio between small and large rings for the chars produced

from 15% H_2O-CO_2 were quite similar with those from 15% H_2O-Ar. H_2O was the dominating factor in the gas mixture for sub-bituminous coal. For the brown coal, the ratio between small and large rings for the char obtained in 15% H_2O-CO_2 was firstly overlapped with that from 15% H_2O-Ar at 800°C and then increasingly approached to that from pure CO_2 with temperature increasing to 900°C. CO_2 plays an increasingly important role in the char structural changes for Loy Yang brown coal.

Other than the evolution of char structure, the AAEM species in char is also an crucial factor affecting the char reactivity. Comparing the relative importance of char structure and AAEM retention in char on the char-O_2 reactivity, it is different between Loy Yang brown coal and Collie sub-bituminous coal. For brown coal, the highly dispersed AAEM species, especially Na plays a key role in the changes in char-O_2 reactivity. The relative ratio between small and large rings in char greatly influences the char-O_2 reactivity for sub-bituminous coal. It is speculated that the differences originate from the chemical form of AAEM species in the coal substrates. The AAEM species, especially Na, are well dispersed in brown coal in the form of salts or ion-exchangeable carboxylates. During gasification at high temperature, the AAEM species can transformed into active catalysts bonded with char. However, a lot less AAEM species in the salts or ion-exchangeable carboxylates form in the sub-bituminous coal and cannot be all transformed into active catalysts to be bonded with char during gasification. Thus, a weaker catalytic effect of AAEM species has been observed for sub-bituminous coal.

As it is known that char structural evolution is relatively important for Collie sub-bituminous coal than Loy Yang brown coal from previous chapters, a further investigation on the gasification mechanisms has carried out for Collie coal by combining the char structure and the kinetic parameters. From the investigation in Chapter 6, the different changes in the apparent activation energy and pre-exponential factor with atmosphere confirm the different reaction pathway in a given atmosphere. The increasing condensation of char structure tends to increase the kinetic parameters in pure CO_2. While accompanied with the formation of O-containing structures, the kinetic parameters tend to decrease as gasification proceeded in steam only. In the gas

mixture of CO_2 and steam, the kinetic parameters remain unchanged due to the opposite effects of char structure in individual atmosphere.

7.3 Future work

1. Under the experimental conditions investigated in this study, the total Raman area increased drastically in the presence of H_2O (15% H_2O balanced with Ar or 15% H_2O balanced with CO_2) and remained almost unchanged in pure CO_2 during the gasification of Loy Yang brown coal and Collie sub-bituminous coal. In order to gain a better understanding on the competition effect between H_2O and CO_2 on the char, it is recommended to investigate the changes in the total Raman area with the relative concentration of CO_2 and/or H_2O (i.e. many more concentrations, such as 100%, 80%, 60%, 40%, 20%, 0%).

2. Renewable sources such as biomass are suitable for gasification-based technologies as well as low-rank coals and are increasingly popular in energy generation. It is recommended to extend our findings from brown coal and sub-bituminous coal to biomass from the aspects of the effects of gasification atmosphere and temperature on the evolution of char structure and the relative importance of char structure and AAEM retention in char on the char-O_2 reactivity.

3. Within the limits of the char gasification kinetics in chemical reaction controlled regime, an ultimate goal of char gasification study should include quantifying/determining real amount of active sites, classifying types of active sites and developing elementary reaction models at each active sites. Based on the understanding of the nature of active sites in char and their evolutional changes during gasification, further efforts could be made toward getting more quantitative information and classification of the active sites for gasification.

Appendix I

Publications

1. **Li T**, Zhang L, Dong L, Li C-Z. Effects of gasification atmosphere and temperature on char structural evolution during the gasification of Collie sub-bituminous coal. Fuel 2014;117:1990-5.
2. Wang S, **Li T**, Wu L, Zhang L, Dong L, Hu X, Li C-Z. Second-order Raman spectroscopy of char during gasification, Fuel Processing Technology 2015;135:105-11.
3. Zhang L, **Li T**, Quyn DM, Dong L, Qiu P, Li C-Z. Formation of nascent char structure during the fast pyrolysis of mallee wood and low-rank coals. Fuel 2015;150:486-92.
4. Zhang L, **Li T**, Quyn DM, Dong L, Qiu P, Li C-Z. Structural transformation of nascent char during the fast pyrolysis of mallee wood and low-rank coals. Fuel Processing Technology 2015;138:390-6.
5. Su S, Song Y, Wang Y, **Li T**, Hu S, Xiang J, Li C-Z. Effects of CO_2 and heating rate on the characteristics of chars prepared in CO_2 and N_2 atmospheres. Fuel 2015;142:243-9.
6. Zhang L, Kajitani S, Umemotob S, Wang S, **Li T**, Zhang S, Dong L, Li C-Z. Changes in nascent char structure during the gasification of low-rank coals in CO_2. Fuel 2015;158:711-8.
7. Zhang, S, Song Y, Yi Q, Dong L, **Li T**, Zhang L, Feng J, Li W, Li C-Z. An advanced biomass gasification technology with integrated catalytic hot gas cleaning. Part III: Effects of inorganic species in char on the reforming of tars from wood and agricultural wastes. Fuel 2016;183:177-84.
8. Wang Y, Hu X, Song Y, Min Z, Mourant D, **Li T**, Gunawan R, Li C-Z. Catalytic steam reforming of cellulose-derived compounds using a char-supported iron catalyst. Fuel Processing Technology 2013;116:234-40.
9. Wu L, Hu X, Wang S, Mourant D, Song Y, **Li T**, Li C-Z. Formation of coke during the esterification of pyrolysis bio-oil. RSC Advances 2016;89: 86485-93.
10. Song Y, Wang Y, Hu X, Xiang J, Hu S, Mourant D, **Li T**, Wu L, Li C-Z. Effects of volatile–char interactions on in-situ destruction of nascent tar during the pyrolysis and gasification of biomass. Part II. Roles of steam. Fuel 2015;143:555-62.

Appendix II

Permission of Reproduction from the Copyright Owner

Copyright Clearance Center RightsLink®

Home | Account Info | Help | Live Chat

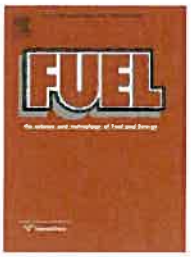

Title: Volatilisation and catalytic effects of alkali and alkaline earth metallic species during the pyrolysis and gasification of Victorian brown coal. Part I. Volatilisation of Na and Cl from a set of NaCl-loaded samples

Author: Dimple Mody Quyn,Hongwei Wu,Chun-Zhu Li

Publication: Fuel

Publisher: Elsevier

Date: January 2002

Logged in as:
tingting li
Account #:
3000932476

LOGOUT

Order Completed

Thank you very much for your order.

This is a License Agreement between tingting li ("You") and Elsevier ("Elsevier"). The license consists of your order details, the terms and conditions provided by Elsevier, and the payment terms and conditions.

Get the printable license.

License Number	3864181235728
License date	May 08, 2016
Licensed content publisher	Elsevier
Licensed content publication	Fuel
Licensed content title	Volatilisation and catalytic effects of alkali and alkaline earth metallic species during the pyrolysis and gasification of Victorian brown coal. Part I. Volatilisation of Na and Cl from a set of NaCl-loaded samples
Licensed content author	Dimple Mody Quyn,Hongwei Wu,Chun-Zhu Li
Licensed content date	January 2002
Licensed content volume number	81
Licensed content issue number	2
Number of pages	7
Type of Use	reuse in a thesis/dissertation
Portion	figures/tables/illustrations
Number of figures/tables /illustrations	1
Format	both print and electronic
Are you the author of this Elsevier article?	No
Will you be translating?	No
Title of your thesis/dissertation	Changes in char structure and reactivity during the gasification of low-rank fuels
Expected completion date	May 2016
Estimated size (number of pages)	140
Elsevier VAT number	GB 494 6272 12
Permissions price	0.00 AUD
VAT/Local Sales Tax	0.00 AUD / 0.00 GBP
Total	0.00 AUD

ORDER MORE... CLOSE WINDOW

Copyright Clearance Center RightsLink®

Home | Account Info | Help | Live Chat

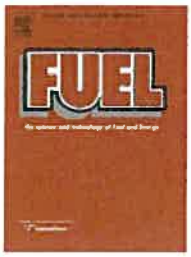

Title: FT-Raman spectroscopic study of the evolution of char structure during the pyrolysis of a Victorian brown coal

Author: Xiaojiang Li,Jun-ichiro Hayashi,Chun-Zhu Li

Publication: Fuel

Publisher: Elsevier

Date: September 2006

Logged in as:
tingting li
Account #:
3000932476

LOGOUT

Order Completed

Thank you very much for your order.

This is a License Agreement between tingting li ("You") and Elsevier ("Elsevier"). The license consists of your order details, the terms and conditions provided by Elsevier, and the payment terms and conditions.

Get the printable license.

License Number	3864181124415
License date	May 08, 2016
Licensed content publisher	Elsevier
Licensed content publication	Fuel
Licensed content title	FT-Raman spectroscopic study of the evolution of char structure during the pyrolysis of a Victorian brown coal
Licensed content author	Xiaojiang Li,Jun-ichiro Hayashi,Chun-Zhu Li
Licensed content date	September 2006
Licensed content volume number	85
Licensed content issue number	12-13
Number of pages	8
Type of Use	reuse in a thesis/dissertation
Portion	figures/tables/illustrations
Number of figures/tables /illustrations	1
Format	both print and electronic
Are you the author of this Elsevier article?	No
Will you be translating?	No
Title of your thesis/dissertation	Changes in char structure and reactivity during the gasification of low-rank fuels
Expected completion date	May 2016
Estimated size (number of pages)	140
Elsevier VAT number	GB 494 6272 12
Permissions price	0.00 AUD
VAT/Local Sales Tax	0.00 AUD / 0.00 GBP
Total	0.00 AUD

ORDER MORE... CLOSE WINDOW

Copyright Clearance Center RightsLink®

Home | Account Info | Help | Live Chat

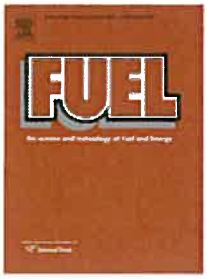

Title: Effects of gasification atmosphere and temperature on char structural evolution during the gasification of Collie sub-bituminous coal

Author: Tingting Li,Lei Zhang,Li Dong,Chun-Zhu Li

Publication: Fuel

Publisher: Elsevier

Date: 30 January 2014

Logged in as:
tingting li
Account #:
3000932476

LOGOUT

Order Completed

Thank you very much for your order.

This is a License Agreement between tingting li ("You") and Elsevier ("Elsevier"). The license consists of your order details, the terms and conditions provided by Elsevier, and the payment terms and conditions.

Get the printable license.

License Number	3862300740544
License date	May 05, 2016
Licensed content publisher	Elsevier
Licensed content publication	Fuel
Licensed content title	Effects of gasification atmosphere and temperature on char structural evolution during the gasification of Collie sub-bituminous coal
Licensed content author	Tingting Li,Lei Zhang,Li Dong,Chun-Zhu Li
Licensed content date	30 January 2014
Licensed content volume number	117
Licensed content issue number	n/a
Number of pages	6
Type of Use	reuse in a thesis/dissertation
Portion	full article
Format	both print and electronic
Are you the author of this Elsevier article?	Yes
Will you be translating?	No
Title of your thesis/dissertation	Changes in char structure and reactivity during the gasification of low-rank fuels
Expected completion date	May 2016
Estimated size (number of pages)	140
Elsevier VAT number	GB 494 6272 12
Permissions price	0.00 AUD
VAT/Local Sales Tax	0.00 AUD / 0.00 GBP
Total	0.00 AUD

ORDER MORE... CLOSE WINDOW